FINAL SUMMARY REPORT

on

EXPERIMENTAL AND RESEARCH WORK IN NEUTRON DOSIMETRY

to

U. S. ARMY SIGNAL RESEARCH AND
DEVELOPMENT LABORATORY
Belmar, New Jersey

June 15, 1960

by

H. C. Gorton, O. J. Mengali, A. R. Zacaroli,
R. K. Crooks, J. M. Swartz, and C. S. Peet

Contract No. DA 36-039 SC-78924
File No. 18685-PM-59-91-91(2203)

For the Period May 15, 1959, to June 15, 1960

BATTELLE MEMORIAL INSTITUTE
505 King Avenue
Columbus 1, Ohio

DISCLAIMER

Battelle Memorial Institute

505 KING AVENUE COLUMBUS 1, OHIO

June 17, 1960

Activity Supply Officer, USASRDL
Building No. 2504
Charles Wood Area
Fort Monmouth, New Jersey

For Applied Physics Division
Inspect at Destination
File No. 18685-PM-59-91-91(2203)

Attention Messrs. William Lonnie and
Abraham Cohen
Atomics Branch
Applied Physics Division

Gentlemen:

This is the Final Summary Report under Contract No. DA 36-039 SC-78924 on the project, "Experimental and Research Work in Neutron Dosimetry". The report covers the period from May 15, 1959, to June 15, 1960.

This report reviews the accomplishments of the year's research efforts. The program has been an interesting and rewarding one, in that a tactical fast neutron dosimeter has been developed, along with a convenient and accurate means of registering accumulated dose, and new insight into the effects of radiation damage in silicon p-n junctions has been gained. The outstanding problems remaining in the development of a practical operating unit are those of optimization and reproducibility of the pertinent device characteristics.

We were happy to have the opportunity to have six .020-inch base width p-n junction dosimeters irradiated in the Godiva reactor. These samples were mailed to Mr. Louis Browne on May 16. Also, in accordance with our phone conversation of May 30, we have prepared six additional dosimeters for delivery to Mr. W. L. Weiss, Air Nuclear Propulsion Department, General Electric Company. It is understood that he will perform irradiation and annealing studies on these samples and will inform us of his results.

A read-out instrument, calibrated in per cent of pre-irradiation current, has been constructed, which we will hold for delivery to you during your proposed visit, June 23, together with about 50 experimental dosimeters.

Very truly yours,

H. C. Gorton

HCG/mmk
In triplicate

H. C. Gorton
Project Leader

TABLE OF CONTENTS

TABLE OF CONTENTS
(Continued)

LIST OF TABLES

LIST OF TABLES
(Continued)

LIST OF FIGURES

LIST OF FIGURES
(Continued)

EXPERIMENTAL AND RESEARCH WORK IN NEUTRON DOSIMETRY

by

H. C. Gorton, O. J. Mengali, A. R. Zacaroli,
R. K. Crooks, J. M. Swartz, and C. S. Peet

INTRODUCTION

There has long been a need for a tactical fast neutron dosimeter, sensitive in the same range as human tissue. Such a dosimeter should be small, lightweight, and provide a continuously observable indication of accumulated dose. Recent advances in semiconductor technology have shown that certain electronic properties of semiconductors, specifically the charge-carrier lifetime, are extremely sensitive to radiation damage resulting from fast neutron irradiation. Under Contract No. DA36-039-SC-73174 with the Signal Corps, Battelle demonstrated the feasibility of utilizing the radiation-induced change in the injected charge-carrier lifetime in a silicon p-n junction rectifier as an effective measure of fast neutron irradiation in the low dose range of interest in tissue damage. The primary objective of the present contract has been to develop a prototype fast neutron dosimeter with the required sensitivity for tactical use utilizing the principles alluded to above. The specific objectives of the research program are listed below:

(1) Using modifications of standard techniques for making diffused-silicon conductivity-modulated rectifiers, prepare devices in which several parameters are varied. These parameters would involve base width, initial lifetime, and preparation techniques. Since the previous work, silicon of higher quality is now available and offers the potential of using higher lifetime initially in the device.

(2) Evaluate sensitivity of the device with fast neutrons representing a fission spectrum. The sensitivity for two or three energy spectra would be determined to evaluate the spectral sensitivity. These would be fission, resonance, and thermal energies. The Battelle weasel tube would be used for the fission spectrum irradiations while the reactor is run at reduced power.

(3) Evaluate the sensitivity of the device to gamma radiation, using $Cobalt^{60}$ as a source. A total dose of 1000 rads would be used, the average energy of gammas in this case being 1.25 mev. If appreciable damage is noted, then the sensitivity to dose rate at dose rates of up to 1,000,000 rads per hour would be investigated.

(4) Investigate effects of annealing on both single-crystal bulk silicon and on devices. The maximum temperature of anneal would be at least 160°F. If any annealing is found, the temperature dependence would be studied in order to evaluate the amount of correction needed.

(5) Investigate the effect of neutron dose rate to as high a rate as possible. Battelle's reactor can provide approximately 5 x 10^{12} neutrons cm^{-2} sec^{-1}. There is a possibility that other reactors with neutron fluxes of 10^{15} cm^{-2} sec^{-1} can be used. However, this is subject to investigation and cannot be considered as a commitment at this time. A burst of fast neutrons would be preferable at the high rates.

(6) Investigate the accuracy of the device in order to evaluate whether or not the electrical circuit or the device will be a major problem. Drift or nonreproducibility would be noted. Also, the possibility of building devices for several different ranges would be determined.

(7) Investigate methods of calibrating the devices. These would include compensation for temperature-dependent components in the electrical circuits, temperature dependences of the silicon-rectifier characteristics, and the effect of ambient atmosphere. The effects of bombardment and annealing prior to use to allow a standard calibration would be investigated. The possibility of recovering devices which have been bombarded would be studied.

(8) Since any finished device should be evaluated under tactical conditions, field tests would be desirable. Such tests, as time and finance permit, would be arranged in conjunction with the Sponsor's technical people.

(9) Study properties of semiconductors or other mechanisms which are sensitive to neutron irradiation. This would include a determination of the possible use of an n-alpha and/or n-p reaction with the semiconductor in its present form as the sensitive element. If these prove to be more sensitive than the present mechanisms of neutron damage in silicon itself, experiments would be devised in an effort to determine the increase in sensitivity.

(10) Submit to the Signal Corps for inspection and evaluation experimental devices which are representative of the state-of-the art. It is expected that several would be available. No set number of devices would be guaranteed.

To carry out this program, the research effort has been divided into four phases:

(1) Theoretical investigations of the physical and electronic phenomena involved in the operation of the silicon p-n junction dosimeter

(2) Determination of the response of the experimental dosimeter to radiation

(3) Design and development of a practical read-out facility

(4) Development of processing techniques for the fabrication of the silicon p-n junction dosimeters.

This final Summary Report covers the period from May 15, 1959, to June 15, 1960, and reviews all the research activities on the project.

SUMMARY

A description of the fundamental electronic properties of the silicon p-n junction fast neutron dosimeter is given, in which the concepts of damage constant and charge carrier lifetime are developed in relation to their effect on the operation of the dosimeter. A theoretical description of the various effects of radiation damage in silicon is given. From these considerations, it is concluded that changes in the lifetime and the current-voltage characteristics of the experimental dosimeters resulting from the gamma and thermal neutron components of a uranium fission reactor are negligible with respect to the damage from fast reactor neutrons. The methods used to measure the dose to which the experimental dosimeters were exposed in the Battelle gamma facility, the Battelle Research Reactor, and the TRIGA Reactor are discussed in detail. Measurements of the voltage profile between the two contacts of the device have shown that essentially all of the change in the current-voltage characteristic with fast neutron irradiation results from the introduction of recombination centers into the base region of the device, and that radiation effects at the p-n^+ junction are relatively unimportant.

Experimental work in the program has been associated with studies related to the sensitivity of the p-n junction dosimeter, and to the uniformity and reproducibility of device characteristics. The sensitivity of the response to fast neutron irradiation has been shown to increase with increasing base width. In devices with base widths of .030 inch (the maximum base width studied), the forward currents at constant voltage decrease by about 75% after exposure to a fast neutron dose of 600 rads.

Experiments to investigate the sensitivity of the experimental dosimeters to gamma radiation have revealed that no appreciable change in lifetime resulted from gamma exposures in excess of 20 times that which would be received from the uranium fission gammas corresponding to a fast neutron flux of 600 rads. However, a small ($\lesssim 4$ per cent) increase in forward current at constant voltage was observed at the equivalent gamma exposure for a fast neutron uranium fission flux of 600 rads. This anomalous increase in current is attributed to reasons other than radiation damage in the base region of the device, and may be associated with an increase in a series resistance, perhaps at the ohmic contact-silicon interface.

The effect of the rate of fast neutron flux on the response of the devices has been investigated between 6 rads sec^{-1} and 2.5×10^4 rads sec^{-1}, and the response of the dosimeters has been shown to be independent of dose rate between these extremes. However, a rather strong temperature dependence of the forward current at constant voltage has been observed, being about 3 per cent per centigrade degree at room temperature for unirradiated devices. This temperature dependence evidently becomes less strong with increasing irradiation, being about half that value after exposure to a fast neutron flux of 600 rads. Such a temperature dependence of the forward current may impose rather stringent conditions on the ambient read-out environment.

No significant changes in device characteristics were observed after heating the irradiated dosimeters for 5 minutes to temperatures up to 100°C. However, annealing of between 50 and 75 per cent of irradiation-induced damage occurred within 60 minutes at 250°C. Continued heating of the samples at 250°C produced no additional recovery of initial characteristics. It appears, therefore, that complete annealing of all the radiation-induced defects below the maximum temperature to which the device can be heated without irreversibly changing its physical or electrical properties may not be feasible.

A high degree of reproducibility in the radiation response has not been observed in the dosimeters produced and tested up to the present time. The nonuniformity of the device characteristics is attributed to uncontrolled variables in the bulk silicon from which the devices are fabricated, and in the fabrication procedure. It is felt that the uniformity of device characteristics may be greatly improved through further research.

A discussion is given of the principles involved in the development of read-out circuits which utilize either forward current at constant voltage or charge carrier lifetime as read-out parameters. A laboratory model of a read-out instrument utilizing the radiation-induced change in forward current at constant voltage has been constructed for delivery to the Signal Corps. The reader is designed to register per cent of preirradiation current through the dosimeter at a fixed voltage. In the operation of this reader, the ability to utilize the forward current at constant voltage as a read-out parameter to the desired degree of accuracy has been demonstrated.

Detailed steps of the production procedure for the fabrication of the experimental silicon p-n junction dosimeters are outlined. This process involves a "modified" standard procedure for the production of wide-base, diffuse junction rectifiers. Commentaries on the production procedure are made whenever necessary to clarify or explain a given step in the procedure. Studies of the effects of variables in the bulk silicon and in the production procedure on the quality of the experimental p-n junction dosimeters indicated that the highest yield and the greatest uniformity of electrical properties of the devices were achieved from Czochralski-pulled material (low etch pit density and high oxygen content) produced by the "nickel slow-cooled" process. The scatter observed in the initial device characteristics is attributed to material and processing variables such as charge carrier lifetime, oxygen content, and dislocation density.

In conclusion, it may be stated that as a result of the research under this contract a practical, prototype silicon p-n junction fast neutron dosimeter, sensitive in the same range as human tissue, has been developed; together with an associated read-out circuit to facilitate the accurate measurement of accumulated dose. From both theoretical and experimental considerations, it has been demonstrated that the dosimeter is essentially insensitive to the gamma and thermal components of a uranium fission spectrum. It has been shown that accumulated damage effects appear to be environmentally stable up to an ambient temperature of 100°C. However, a rather marked reversible temperature dependence of the read-out parameters will require either control of the read-out temperature or temperature compensation in the read-out device. A high degree of reproducibility of dosimeter characteristics from one device to another has not been achieved. The lack of reproducibility is attributed to uncontrolled variables in the bulk silicon from which the devices are fabricated, and in the production procedure. Optimization of device characteristics and control of variables effecting reproducibility remain as outstanding problems in the continued development of the silicon p-n junction fast neutron dosimeter.

PHASE I. THEORETICAL INVESTIGATION OF THE PHYSICAL AND ELECTRONIC PHENOMENA INVOLVED IN THE OPERATION OF THE SILICON P-N JUNCTION DOSIMETER

CONSIDERATIONS OF THE FUNDAMENTAL ELECTRONIC PROPERTIES OF THE EXPERIMENTAL SILICON P-N JUNCTION DOSIMETER

by

A. R. Zacaroli

The property of silicon which is extremely sensitive to neutron damage and which is utilized in the silicon rectifier dosimeter is the excess charge carrier lifetime. When the current is passed in the forward direction through a p-n junction, charge carriers are injected into the material on both sides of the junction. These carriers, being in excess of the normal charge carrier density, decay or become annihilated at a rate which is proportional to their density and reciprocally proportional to a constant, τ. This constant is termed the excess charge carrier lifetime because it represents the average time a carrier exists before annihilation. Excess carrier lifetime may be different in various silicon crystals and can be altered by treatment of the silicon, including neutron irradiation.

The process through which excess carriers decay depends primarily upon the existence of a class of localized crystal defects which are termed recombination centers. A charge carrier, either an electron or a hole, is trapped in a recombination center and remains there until a charge of opposite polarity is also captured by the recombination center. The hole entering the electron-occupied center causes annihilation of both carriers. Electrons and holes also recombine by direct collision, but this is a comparatively infrequent process. Recombination centers act almost independently of each other. Thus, the rate of recombination of electrons and holes is proportional to the density of recombination centers. If recombination centers are introduced by neutron damage, then the recombination rate should be proportional to the amount of neutron damage. Since lifetime is reciprocally related to the recombination rate, it follows that reciprocal lifetime is proportional to neutron damage. Assuming that neutron damage is proportional to the integrated neutron flux, the following equation results:

$$\frac{1}{\tau_f} = \frac{1}{\tau_o} + \alpha \, nvt \quad , \tag{1}$$

where τ_o is the lifetime before irradiation, τ_f is lifetime after irradiation, and α is a constant or proportionality referred to as the damage constant.

There are several assumptions implicit in Equation (1). The first is that a constant, τ, actually exists which linearly relates recombination rate with excess carrier density. In reality, τ varies somewhat with injection level, and therefore can be defined only when the excess carrier density is specified. Fortunately, when the excess carrier density exceeds the normal carrier density, τ reaches a maximum value and

remains constant for a wide range of carrier densities. This is termed high-level lifetime. Because the silicon p-n junction dosimeter is operated under conditions of high-level injection, the lifetime determining its operation is high-level lifetime, and therefore, is both a definitive and a maximum lifetime. The second implicit assumption is that the density of recombination centers introduced into the material is proportional to neutron irradiation, thus allowing α to be defined. While it is possible that neutron irradiation initially creates the same amount of damage in all silicon crystals, it does not follow that the damage remaining after a period of time has elapsed will be a constant fraction of the initial damage for all silicon crystals. As a matter of fact, partial annealing of defects does occur between liquid nitrogen temperature and room temperature.[1] The percentage of annealing depends on the condition of the silicon before irradiation, such as its dislocation density and oxygen content, as well as on the annealing conditions to which it is subjected after irradiation. Whereas the first assumption is practically satisfied in the silicon p-n junction dosimeter, it is apparent that the second assumption which is primarily a material problem is not satisfied, and thus constitutes the major problem in this dosimetery.

The silicon p-n junction dosimeter allows either a direct or an indirect measurement of lifetime. Therefore, if the value of α is known for a given device or a group of devices, a determination of initial lifetime, τ_o, and lifetime after irradiation, τ_f, will allow a determination of the integrated neutron flux. The value of the damage constant can only be determined by previously subjecting other identical devices to known amounts of radiation. Hence, the need for devices having the same α becomes apparent.

A brief description of the physical mechanism of the dosimeter will demonstrate how this device directly or implicitly measures lifetime. Basically, the device is an n^+-p-p^+ junction structure, as shown in Figure 1. The + signs indicate heavy doping exceeding 10^{18} impurity atoms cm^{-3}. The middle p region, which is referred to as the base, contains approximately 10^{14} acceptors cm^{-3}. The n^+ and p^+ regions are about .001 inch to .002 inch thick, and because of their low resistivity, do not contribute any appreciable resistance to the device. The base, however, is purposely made thick so that it introduces considerable resistance to the device. When sufficient current is passed in the forward direction of the device, electrons and holes will be injected into the base from the n^+-p junction and the p-p^+ junction, respectively, increasing the carrier density in the base by a factor of 100 or more and thereby reducing the base resistance. Due to the annihilation or decay of excess carriers, the concentration of the injected carriers will be greatest at the junction boundaries of the base and will be reduced to a minimum near the center of the base. The minimum value is established by the base thickness and the lifetime. The wider the base or the shorter the lifetime, the smaller will be the minimum. Since most of the base resistance is contained in a region about the minimum, the resistance of the base is very sensitive to lifetime changes. The maximum sensitivity of the base resistance to lifetime change results from a proper choice of base width commensurate with the lifetime. In general, the sensitivity of the base resistance to lifetime changes will increase with increasing initial lifetime and, up to a certain limit, with increasing base widths. There is no analytical expression available at the present time which adequately describes the current-voltage characteristic of the base as a function of lifetime and base width, thus the relationship between lifetime and the current-voltage characteristic of a device can only be ascertained empirically.

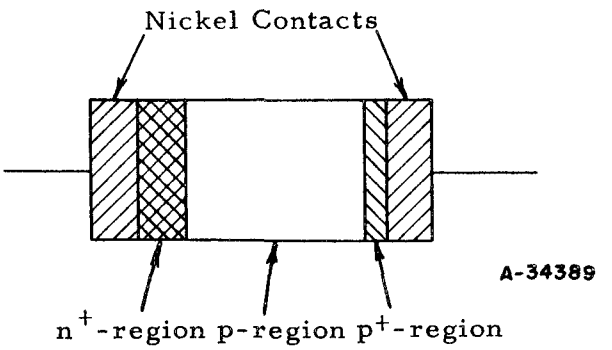

FIGURE 1. SCHEMATIC DIAGRAM OF P-N JUNCTION DOSIMETER

A direct measure of lifetime in the base is possible because the carrier density in the base next to the n^+-p junction is uniquely related to the junction voltage. If the current through the junction is interrupted by open-circuiting the device, and the voltage across the junction is measured as a function of time, the decay of voltage will be related to the decay of excess carriers and hence, to the lifetime. Since no current is flowing in the device, the measured voltage is the sum of the n^+-p and p-p^+ junction voltages. The p-p^+ junction voltage decays to zero very shortly after the current is stopped leaving the n^+-p junction as the only source of voltage in the device. This voltage, which incidentally decays linearly with time, yields the lifetime.

DAMAGE-INTRODUCTION RATES IN SILICON

by

H. C. Gorton

It has been shown that pile irradiation of silicon conductivity-modulated rectifiers results in significant changes in forward-current characteristics at the same levels of irradiation that produce damage to human tissue. As discussed in the preceding section, radiation damage is related to forward current through radiation-induced changes in the lifetime of charge carriers in the base region of the device. Specifically, the charge carrier lifetime in silicon is reduced by the introduction of recombination centers associated with vacant lattice sites and interstitial atoms resulting from nuclear bombardment. Atomic displacements are produced by separate mechanisms associated with fast neutrons, thermal neutrons, and gamma rays.

Fast Neutrons

Damage due to fast-neutron irradiation is a complicated process involving an interaction of a neutron with an atom of the material being irradiated, and subsequent interactions between the "primary knock-on" and other atoms of the lattice. The primary knock-on generally acquires many times its lattice threshold energy, and is displaced from its lattice site in an ionized state. It loses energy to the lattice principally

by inelastic collisions until it has regained its planetary electrons. It then continues to lose its energy by elastic collisions, which are effective in displacing subsequent atoms from their lattice sites. It has been shown by Kinchen and Pease[2] and by others that an atom moving in a lattice with an energy greater than twice the threshold energy, but less than a limiting energy for ionization, E_i, will lose just half its energy, on the average, in producing subsequent displacements, and half in subthreshold collisions. A rough approximation for the limiting energy for ionization is given by Dienes and Vineyard[3] as that energy in kev equal to the atomic weight of the moving atom, regardless of the medium in which it is moving. Atoms moving with higher energies will lose energy principally in inelastic collisions in the process of becoming deionized; i. e., the differential cross section for displacement-producing collisions in this energy range is inversely proportional to the square of the kinetic energy of the moving atom.

The rate of displacement-producing interactions of fast neutrons with silicon is given by

$$f = nv\, n_o\, \sigma_d \quad , \tag{2}$$

where nv is the neutron flux density in neutrons/cm^2 sec, n_o is the atomic density of silicon, and σ_d is the displacement cross section for fast neutrons. The displacement cross section in silicon fluctuates between 1.5 and 5.5 barns across the Watt spectrum, with a value near 3 barns for 2-mev neutrons – the mean energy, $\overline{E}$, of the Watt spectrum being near 2 mev. The rate of production of primary knock-ons per incident neutron from 2-mev neutrons, therefore, is

$$n_p = f/nv = n_o\, \sigma_d = 0.15 \text{ primary events/cm}^3\text{/fast neutron/cm}^2 \quad .$$

The mean energy transferred to the primary knock-ons is related to the neutron energy by the expression[3]

$$\overline{T} = F\left[\frac{2A}{(1+A)^2}\right]\overline{E} \quad , \tag{3}$$

where A is the atomic number of silicon, and F is a correction factor for anisotropy and inelasticity in fast-neutron scattering, taken to be about 2/3 for most reactor neutron bombardments. Since just half the energy of a primary knock-on below the value E_i is available for displacement-producing collisions, the number of secondary knock-ons produced per primary would be

$$N_d = \frac{\overline{T}'}{2E_d} \quad , \tag{4}$$

where E_d is the displacement threshold energy for silicon and $\overline{T}'$ has a maximum value of E_i. The threshold energy for most materials is taken to be about 25 ev. However, Loferski and Rappaport[4] have obtained a value of 12.9 ev for silicon (utilizing electron bombardment and sensitive lifetime measurements). It is probable that a unique value for the threshold energy does not exist, and it is possible that such low values as that reported above may be associated with directional effects, thermal energies, or crystal imperfections. It is felt at the present time that a value of about 20 ev may more nearly represent a typical threshold energy for silicon.

The energy transferred to primary knock-ons in silicon by 2-mev neutrons is, according to Equation (3), $\overline{T}$ = 89 kev. E_i, however, and therefore $\overline{T}'$, is roughly equal to 28 kev, such that N_d, from Equation (4), would be about 700 vacancy-interstitial pairs created per primary knock-on. Since the number of primary events per incident neutron is 0.15 cm^{-1}, the total calculated number of V-I pairs/cm^3/fast neutron/cm^2 produced in silicon would be $n_f = n_o \sigma_d N_d \approx 100\ cm^{-1}$. This value is about an order of magnitude higher than the values that are observed experimentally. For instance, Wertheim[5] quotes an experimental value of 9.1 V-I pairs/cm^3/fast neutron/cm^2. At least two conditions are considered to be effective in decreasing the number of V-I pairs observed. First, annealing effects could appreciably decrease the number of V-I pairs created. Although damaged silicon anneals very slowly at room temperature, certain defect states could well have an annealing rate comparable to the damage-introduction rate at room temperature. For instance, Koehler has indicated that there may be an immediate annealing effect, at least for closely spaced V-I pairs, due to energy imparted to displaced atoms by lattice vibrations resulting from subthreshold collisions of the primary knock-ons[6], and Wertheim has observed that silicon irradiated at 77°K undergoes some annealing between 77°K and room temperature[7]. The annealing processes in silicon are very complicated, and much work remains to be done before a definitive picture will be obtained of the extent and nature of the processes involved.

A second effect that may decrease the effective number of damage defects is associated with the clustering of secondary knock-ons. As the primary knock-on slows down in its transit through matter, the distance between collisions approaches the interatomic distance, resulting in a localized area with an extremely high density of defects. A certain percentage of these will be ionized, depending on the position of the Fermi level and the energy states associated with the defects. The localized areas of high charge density will tend to have a screening effect on charge carriers moving through the medium. This situation is further complicated by the possibility of the generation of "thermal spikes" near the end of the path of a primary knock-on. In such a situation, the primary knock-on may transmit energy to the lattice at a high enough rate for localized melting to occur. The amount of damage introduced in such a situation would depend on the energy-dissipation rate and on the relaxation time of the lattice.

Thermal Neutrons

The reaction of thermal neutrons with matter is different from that of fast neutrons in that the thermal neutron is captured by the nucleus of the interacting atom, with, in the case of silicon, the emission of a gamma ray. Damage occurs as a result of the kinetic energy of recoil imparted to the atom upon the emission of the gamma ray. The energies of the capture gamma rays from the three stable isotopes of silicon are well known, and are in the energy range where essentially every neutron capture results in the displacement of a silicon atom from its lattice site. According to Schweinler[8], the recoil energies vary from 380 ev to 1330 ev, with a mean energy of 780 ev.

Table 1 shows the capture cross sections, σ, for thermal neutrons by the three stable isotopes of silicon, the relative densities, ρ, of the three isotopes, and the relative absorptions, obtained from the product of the cross section and the relative density. Thermal-neutron capture by Si^{30} produces Si^{31}, which is radioactive and decays to P^{31}, with a half-life of 2.6 hours. Thus, 4.1 per cent of all thermal-neutron absorptions result in the creation of phosphorus atoms.

TABLE 1. CROSS SECTION, DENSITY, AND RELATIVE ABSORPTION OF THERMAL NEUTRONS IN SILICON[8]

Isotope	Capture Cross Section, σ, barns	Relative Density, ρ, per cent	Relative Absorption, per cent
Si^{28}	0.08	92.28	81.9
Si^{29}	0.27	4.67	14.0
Si^{30}	0.12	3.05	4.1

Since the mean free path of thermal neutrons in silicon is several centimeters, their capture probability may be considered constant throughout samples as small as the rectifiers under study. The rate of production of primary events from thermal-neutron capture is

$$n_o \Sigma \sigma_i \rho_i = 4 \times 10^{-3} \text{ primary event/cm}^3\text{/thermal neutron/cm}^2 .$$

The energetic nucleus again disposes of half its energy in subthreshold collisions and half in producing additional displacements. So, utilizing a threshold energy of 20 ev, and a mean energy of primary displacements of 780 ev, about 20 secondary knock-ons are produced per primary. The total number of V-I pairs produced per incident thermal neutron, thus, would be ~ 0.08 cm^{-1}. Although annealing processes would be expected to decrease this value somewhat, it is obvious that clustering and its shielding effect would be much less prominent than in the case of fast neutrons. It is also seen that the increase in conductivity by the creation of phosphorus is negligible, being on the order of 10^6 atoms/cm^3 sec.

Gamma Rays

Damage from gamma rays in the energy range of interest consists entirely of a multiple process in which the gammas impart energy to electrons, and these, in turn, produce atomic displacements. Gamma-electron interactions that produce electrons energetic enough to create atomic displacements may occur in three ways: (1) the photoelectric effect, (2) the Compton effect, and (3) pair production. The mean energy of the gamma rays associated with the subject irradiation has recently been measured at 0.7 mev. This value is well below the minimum energy for pair production, such that the photoelectric and Compton effects account for essentially all energetic electrons produced. The photoelectrons have a discrete energy that is equal to the incident photon energy less the appropriate electron-binding energy. A broad spectrum of electron energies, however, may be produced by the Compton effect. Both the partial and total atomic displacement cross sections for both of these effects in silicon down to photon energies of 1 mev have been calculated by Cahn[9], assuming threshold energies of 15 and 30 ev. A small extrapolation of the total displacement cross section σ_T, to 0.7 mev for a threshold energy of 15 ev gives a value near 0.18 barn/atom. The damage-introduction rate in silicon due to reactor gammas, then, is $n_o \sigma_T = 9 \times 10^{-3}$ V-I pair/cm^3/photon/cm^2.

Comparison of Damage-Introduction Rates

The relative amount of damage introduced into a material from fast neutrons, thermal neutrons, and gamma rays depends, of course, on the relative flux density of the incident radiation, as well as its efficiency in producing damage. As an example, in Table 2 are shown the flux densities in the Battelle Research Reactor, at a reactor power level of 10 kw and in core Position 83, as well as the rate of defect production in silicon by each of the three sources of damage under consideration. Considering that the calculated damage from fast neutrons is about an order of magnitude higher than that observed experimentally, it can be seen from Table 2 that damage from fast reactor neutrons would still be roughly three orders of magnitude greater than damage from thermals and two orders of magnitude greater than damage from gamma rays. Reactor gamma rays, therefore, could be expected to account for a few per cent of the total damage, and thermal neutrons for only a few tenths of a per cent.

TABLE 2. DAMAGE-INTRODUCTION RATES IN SILICON FOR FAST NEUTRONS, THERMAL NEUTRONS, AND GAMMA RAYS

Irradiation	Flux Density, $cm^{-2}\ sec^{-1}$	Primary Events per Incident Particle, cm^{-1}	Total V-I Pairs per Primary Event, cm^{-1}	Damage-Introduction Rate, $cm^{-3}\ sec^{-1}$
Fast neutrons	1.5×10^{9}	0.15	100	1.5×10^{11}
Thermal neutrons	3.5×10^{8}	4×10^{-3}	8×10^{-2}	3×10^{7}
Photons	4.5×10^{10}	--	9×10^{-3}	4×10^{8}

Carrier-Removal Rates

Carrier-removal rates in damaged silicon are a strong function of the position of the Fermi level. For instance, donor states introduced into p-type silicon will contribute their electrons for recombination with holes only if the energy of the donor states is greater than the Fermi energy. Likewise, acceptor states will trap electrons from the conduction band in n-type material only if their energy is less than the Fermi energy. Therefore, as the Fermi energy moves away from the band edges; i. e., as higher purity material is considered, carrier-removal rates drop rapidly. In boron-doped silicon with a carrier concentration on the order of $10^{14}\ cm^{-3}$, the Fermi level lies about 0.31 ev above the valence band. The only states contributing appreciably to carrier removal in such material would be donor states lying at energies greater than 0.31 ev above the valence band. As reported earlier, Wertheim has quoted an experimental value for the introduction rate of neutron damage in silicon as $9.1\ cm^{-1}$. If one assumed that all the centers introduced by neutron damage were donors lying above the Fermi level, a total fast neutron flux of 4×10^{11} neutrons/cm^2 (which corresponds to about 600 tissue rads) would result only in the removal of less than 4×10^{12} carriers. Such a situation would affect the conductivity of 10^{14}-cm^{-3} material by only 4 per cent. Since the actual number of centers that would contribute to carrier removal is much less than the total number of defects introduced into the material, the removal of majority carriers from

silicon by neutron damage is not considered to be a significant effect for the purity of material and the radiation doses of interest in neutron dosimetry.

Damage From the Transmutation of Boron

Since boron-doped silicon is used in the diodes under study, it may be pertinent, in consideration of the relatively high cross section of boron for thermal neutrons, to investigate the introduction of damage from the transmutation of boron. Of particular interest in this regard is the fact that the reaction $B^{10} + n \rightarrow Li^7 + \alpha$ releases an α particle with an energy of 2.3 mev in 93 per cent of the reactions and 2.79 mev in the other 7 per cent.[10] Although detailed information is not available on the displacement cross section for α particles in silicon, an estimate of the order of magnitude of the effect may be inferred from Gobeli's work on the irradiation of degenerate germanium with 5-mev alphas.[11] He obtained carrier-removal rates of the order of 3×10^4 carriers/α cm. Since the material was degenerate, one could reasonably expect two carriers removed per V-I pair, giving a damage-introduction rate of the order of 10^4 V-I pairs/α cm. The capture cross section of B^{10} for thermal neutrons at room temperature is near 4000 barns,[12] and the isotopic concentration of B^{10} is about 18 per cent. (The cross section of B^{11} for thermal neutrons is negligible.) Therefore, the atomic density of B^{10} in silicon containing 10^{14} cm^{-3} boron would be $\sim 2 \times 10^{13}$ cm^{-3}. The rate of α-producing events then would be $n_o \sigma \approx 8 \times 10^{-8}$ alpha/cm^3/thermal neutron/cm^2. Using the value of the damage due to alphas in germanium as a rough approximation to the damage produced in silicon, we obtain a total number of V-I pairs per primary event of 8×10^{-4} cm^{-1}. Comparing this value with the figures in Table 2, we see that thermal-neutron capture by the boron dopant accounts for roughly 1 per cent of the V-I pairs produced by thermal neutrons. However, in silicon doped with boron to the order of 10^{18} cm^{-3}, as is the case in the p^+ region adjacent to the base contact of the rectifier, thermal-neutron damage from the boron dopant will be 100 times greater than that from the silicon. Even under these conditions, the thermal-neutron damage would account for only 20 to 40 per cent of the damage from fast neutrons. The question is raised, however, of the effect of damage from the high concentration of boron at the surface of the p^+ region on the contact resistance of the rectifier.

Transient Ionization Effects

As indicated in the section under "Fast Neutrons", a nucleus moving through matter with an energy greater than the limiting energy, E_i, will dissipate its energy principally to the electrons of the atoms near which it passes. Such an effect could be a factor in decreasing the resistivity of a material while in a radiation field. To calculate the extreme case, assume that the moving nucleus loses all of its energy in the range from $\overline{T}$ to E_i in exciting electrons from the top of the valence band to the bottom of the conduction band. The energy loss for a silicon nucleus would be $\overline{T} - E_i = 61$ kev, with 1.1 ev imparted to each excited electron, and 5.5×10^4 carriers added per primary event. Using the values of 0.15 primary event/cm^3/fast neutron/cm^2, $\sim 8.2 \times 10^3$ carriers/cm^3/fast neutron/cm^2 would be added to the material. At a fast-neutron flux density of 1.5×10^9 cm^{-2} sec^{-1}, as given in Table 2, current carriers would be created at a rate of 10^{13} cm^{-3} sec^{-1}. Since the carrier density in the forward direction of the silicon rectifiers under operating conditions is on the order of 10^{16} cm^{-3}, the contribution of the ionization current would be negligible.

DOSIMETRY OF RADIATION SOURCES

by

H. C. Gorton

During the course of the current investigation, experimental rectifier dosimeters were exposed to three different sources of radiation. The sensitivity of the devices to gamma radiation was determined by exposing a number of the experimental units to the Battelle Cobalt 60 facility. The sensitivity of the devices to fast neutron irradiation was determined in the Battelle Research Reactor. The rate dependence of the sensitivity of the devices was studied by exposing them to radiation from the General Atomic TRIGA Reactor. This section of the report will describe the experimental arrangement and the methods used to determine the radiation dose to which the experimental rectifier dosimeters were exposed.

Battelle Gamma Facility

The Battelle gamma facility comprises a 2000-Curie radio cobalt source composed of 60 rods of cobalt 8 inches long by 1/8 inch in diameter, encased in 1/4 inch diameter stainless steel tubes. The tubes were packed in a cylindrical configuration with a mean diameter of about 2 inches, and the p-n junction dosimeters were placed at the center of the cylinder. The activity of the cobalt source was monitored with a ferris sulfate (Fricke) dosimeter, calibrated in ergs gm^{-1} energy absorbed in water to an accuracy of about ±5 per cent. Conversion to reps is made on the basis of 93.8 ergs gm^{-1} = 1 rep.

Two groups of experimental p-n junction dosimeters were exposed to the cobalt facility. In the first irradiation, seven devices were exposed to a gamma dose rate of 8.5×10^5 rep hr^{-1} for 26 hours. Measurements of the forward current-voltage characteristics of the devices were obtained periodically during the irradiation. In the second irradiation, six devices were exposed to a gamma dose rate of 7×10^5 rep hr^{-1} for 2.5 hours. Again, the forward current-voltage characteristics of the devices were obtained periodically during the irradiation and, in addition, the lifetimes of injected charge carriers were obtained before and after irradiation.

Battelle Research Reactor

The Battelle Research Reactor is a 4 megawatt swimming-pool-type reactor using enriched uranium fuel elements. During the course of the experimental program four different sets of devices were exposed to radiation in the reactor. Between the third and fourth irradiations, the fuel elements in the reactor were replaced, and the maximum reactor power level was increased from 2 to 4 megawatts. In order to achieve the relatively low total doses of fast neutrons desired at reasonable exposure times, the reactor was operated during irradiation of the experimental dosimeters at a reduced power of 10 kw for the first three runs and 500 w for the fourth run. Different levels of irradiation were achieved by exposing the devices at a given position near the reactor

core for different periods of time. Samples to be irradiated were placed in a polyethylene exposure tube and were lowered to the reactor core in the Weasel Irradiation Conveyer. Transit times from the surface of the water shield to the reactor core and from the core to the surface were about 15 seconds each way.

In each experiment the fast neutron flux density was determined in the reactor core position used at a reactor power level of 200 kw, using one or more of the threshold detectors listed in Table 3. Table 3 also lists the effective threshold energies of the radio activants, their cross sections for fast neutrons, and the decay particles used to detect the reaction products. The reaction products were counted over several half lives on the RIDL 100-channel analyzer

TABLE 3. THRESHOLD DETECTORS USED FOR FAST NEUTRON FLUX MEASUREMENTS

Reaction	Threshold Energy, Mev	Cross Section (Saturation), 10^{-24} cm^2	Detection
Ni^{58} (n, p) Co^{58}	5	?>	α (0.81 Mev)
S^{32} (n, p) P^{32}	2.9	0.300	β (1.712 Mev)
Al^{27} (n, α) Na^{24}	8.1	0.111	α (1.37 Mev)

The integrated neutron flux above the effective threshold energies is calculated from the equation

$$\phi_F = \frac{NA}{N_o \sigma M (1 - e^{-\lambda t})} , \qquad (5)$$

where

N = disintegration rads, dps

A = atomic weight, amu

N_o = Avagadro's number, atoms/gm-mole

σ = cross section, cm^2

M = mass of foil, gm

λ = decay constant, sec^{-1}

t = activation time, sec.

Since neutron flux is proportional to power, the value of calculated flux from Equation (5) can be extrapolated to the lower power levels used to irradiate the experimental silicon p-n junction dosimeters. The first three irradiations were made in core position 83 which is located 22 cm from the reactor core face, whereas the fourth irradiation was

made in core position 64 which is located at the core face. Measurements of the flux density in core position 64 have shown it to closely approximate a Watt fission spectrum, and it is assumed that the spectrum in core position 83 is not significantly different.

Figure 2 shows graphically the fast neutron flux above threshold energy at 500 watts reactor power versus threshold energy. The smooth curve is the Watt fission spectrum normalized to the S^{32} (n, p) P^{32} data point. As may be seen from this curve, the total fast neutron flux between 0 and 10 Mev is approximately 1.0×10^{9} cm^{-2} sec^{-1} at 500 watts.

Since the threshold detectors referred to above are not sufficiently sensitive at the low doses used to irradiate the experimental devices, gold foils were irradiated along with each of the threshold detectors. Assuming that the ratio of the activities of the threshold detectors to that of the gold foil did not vary with reactor power in a given core position, only gold foils, thus calibrated, were irradiated with the experimental devices. The gold is a more desirable dosimeter at the low neutron dosages to which the samples were exposed because of its much higher activation sensitivity compared to the threshold detectors. The total dose to which the devices were exposed in each irradiation was derived from the known relationship of the fast neutron flux to the gold-foil activity.

General Atomics TRIGA Reactor

Forty-eight p-n junction dosimeters, comprising four different base widths and two processing procedures, were exposed to a burst of neutron irradiation from the TRIGA reactor to study the rate dependence of the device sensitivity. The p-n junction dosimeters were divided into 6 groups of eight devices each, and arranged in a Lucite exposure tube, as shown in Figure 3. As may be seen in the figure, each of three pairs of packages were separated by water columns, and the two packages in each pair were separated by large sulfur pellet dosimeters 8 mm thick. Smaller sulfur pellet dosimeters were included in each of the six packages. The activity of each of the six small sulfur dosimeters was evaluated by Harry M. Murphy, Jr., Institute for Exploratory Research, USASRDL. The activity of the three large sulfur dosimeters was evaluated by Dr. I. N. Wimenitz, Research Supervisor, Nuclear Vulnerability Branch, Diamond Ordinance Fuze Laboratories. Figure 4 is a graph of the conversion of fast neutron dose to rads, as evaluated by Murphy. The Wimenitz data did not include a conversion factor to rads and is superimposed on the curve of Murphy's data. The measured data from the sulfur pellets is shown, of course, on the 2.5 Mev threshold curve. Although Wimenitz used a threshold of 3 Mev in his evaluation, the difference in activity between that and a 2.5 Mev threshold would be less than 4 per cent. The 0.63 Mev threshold data are calculated values corresponding to the neptunium threshold, and are given because of its proximity to the REIC definition of fast neutron dose as being the number of neutrons cm^{-2} whose energy is above 0.5 Mev. As may be observed in Figure 4, there is some discrepancy between the measured flux from the two sets of sulfur pellets, the difference increasing with increasing distance from the reactor core. Wimenitz' data should fall between the three pairs of points in the curve. Taking into account the differences in threshold energy used in the two cases, the activity of the large pellets is greater than the average of that of the corresponding two smaller pellets by about 15 per cent, 30 per cent, and 45 per cent, the difference increasing with distance from the core. The correlation of the data from the two sources is much better on the calculated curve

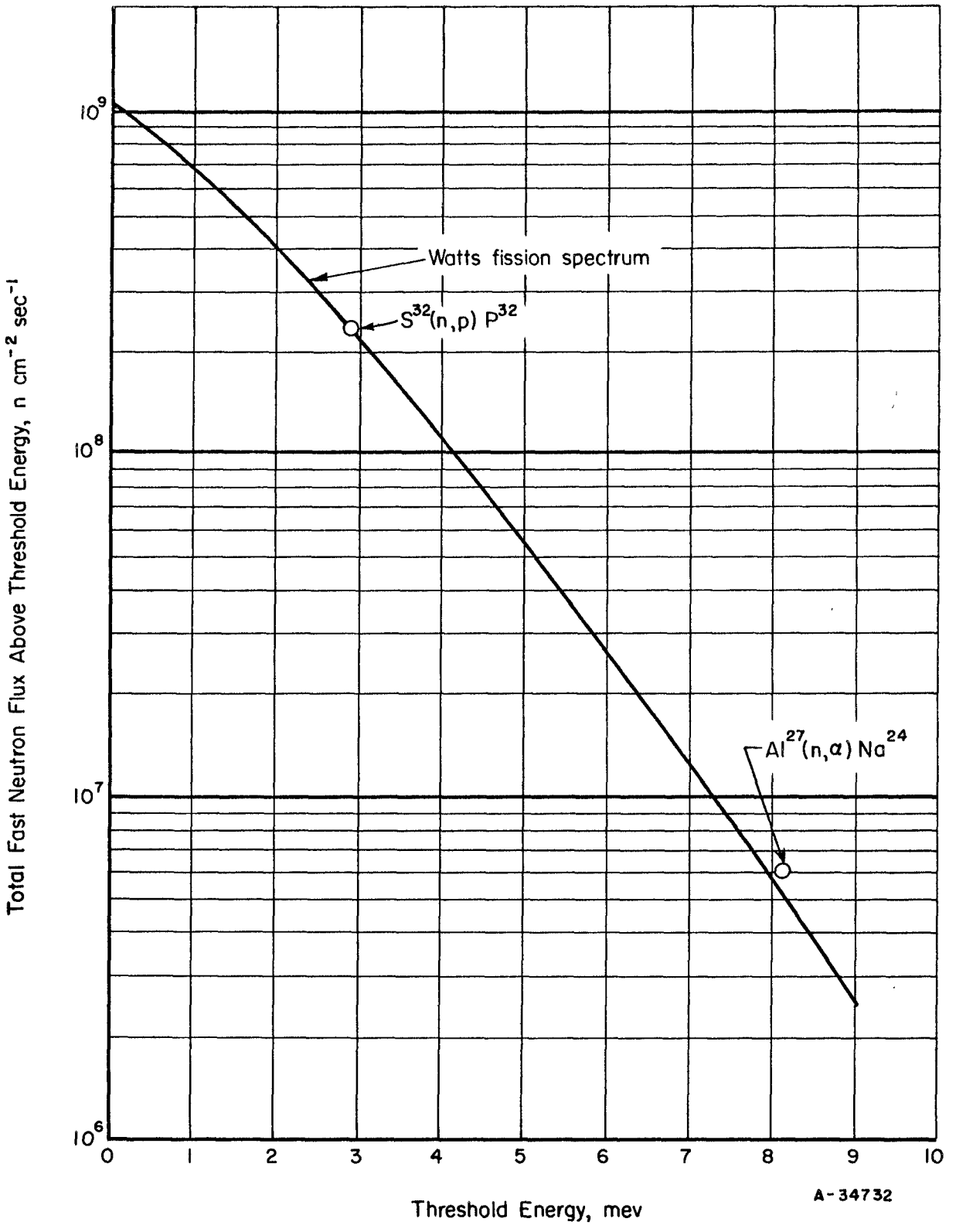

FIGURE 2. INTEGRATED FAST NEUTRON FLUX ABOVE THRESHOLD ENERGY VERSUS THRESHOLD ENERGY, 500-WATT REACTOR POWER

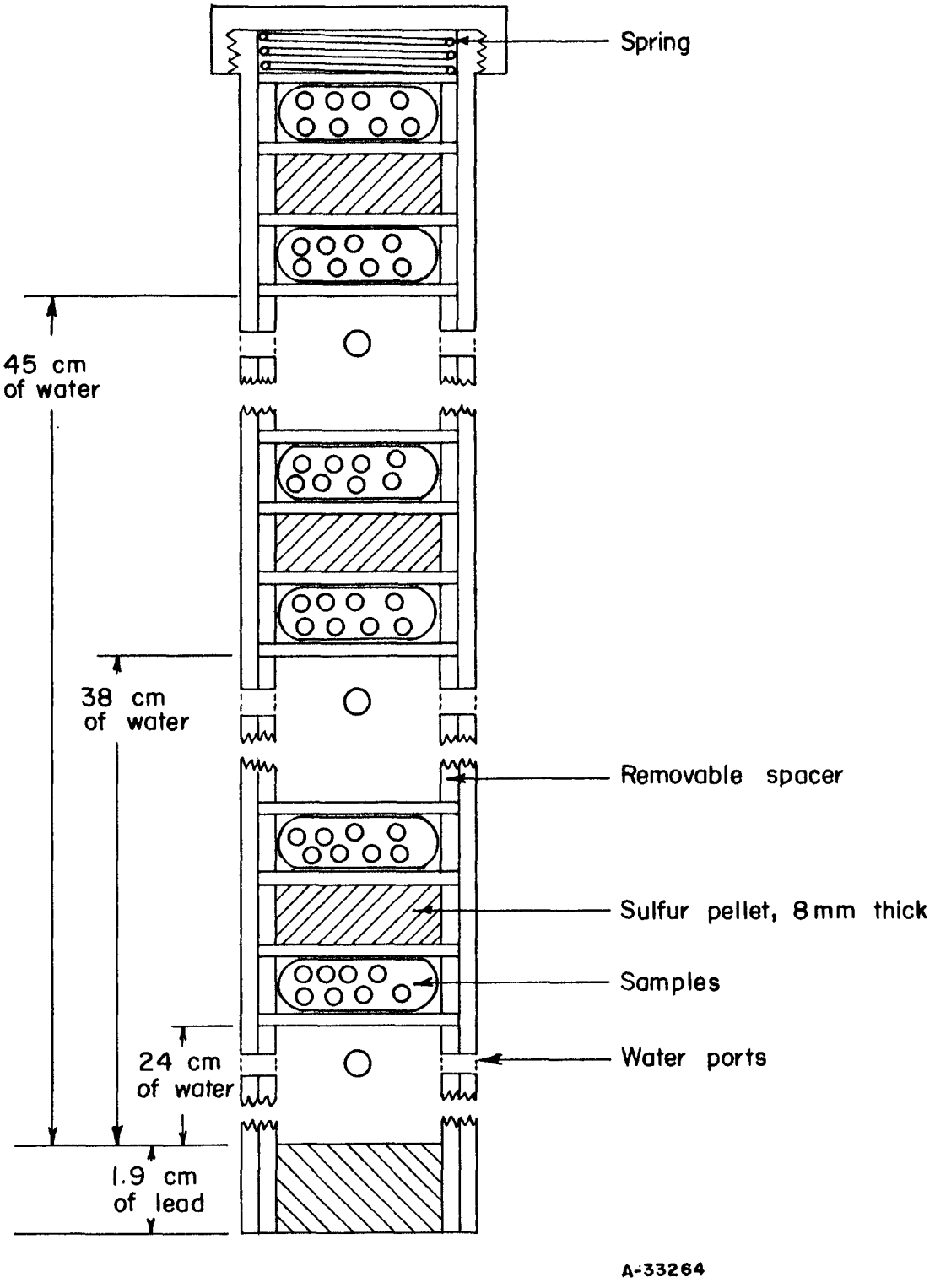

FIGURE 3. LUCITE EXPOSURE TUBE USED IN TRIGA TRANSIENT 1048

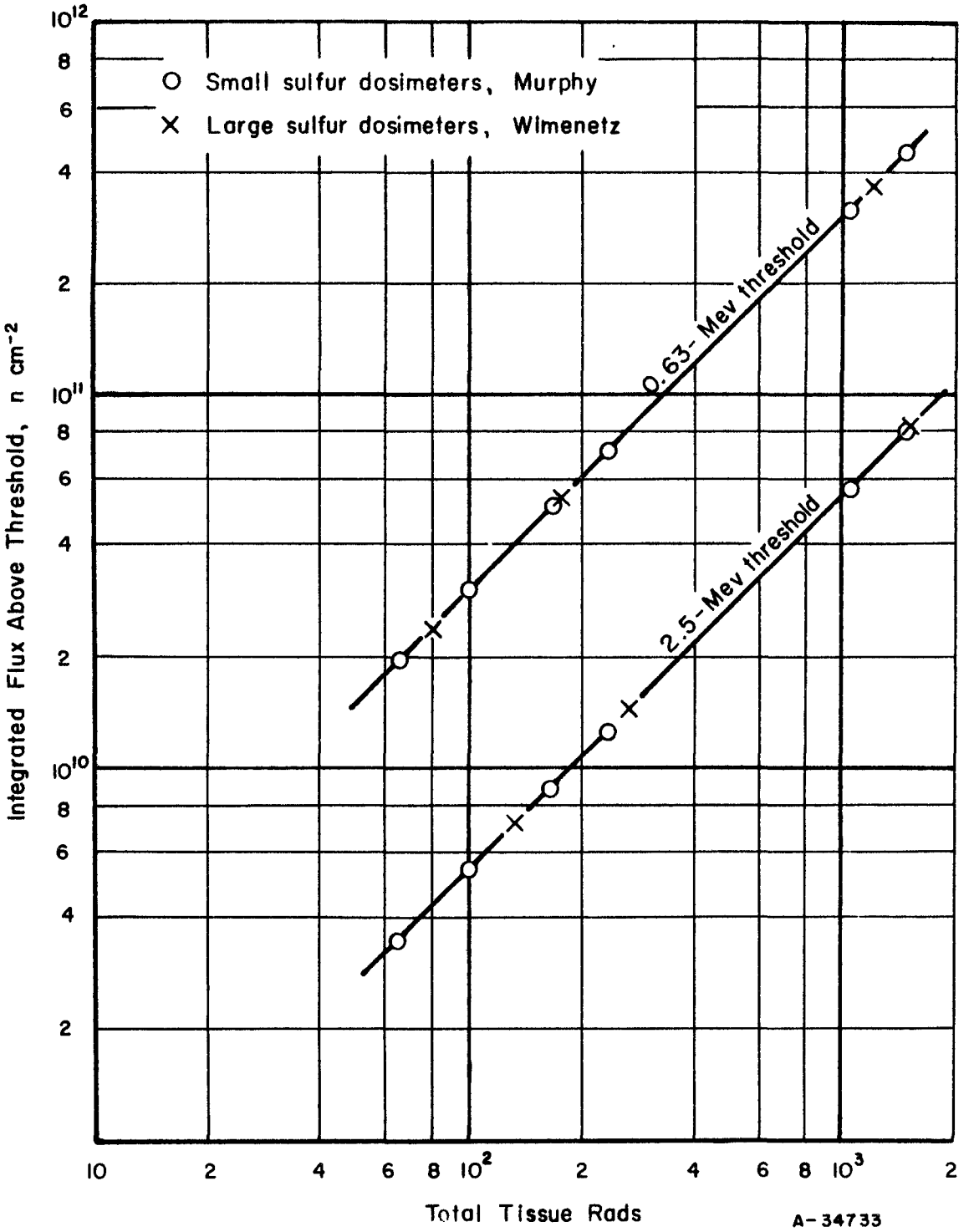

FIGURE 4. CONVERSION OF INTEGRATED FAST NEUTRON DOSE ABOVE INDICATED THRESHOLDS TO TOTAL TISSUE RADS FOR THE GENERAL ATOMICS TRIGA REACTOR

corresponding to a threshold energy of 0.63 Mev. However, it is less meaningful since it was arrived at by two different methods. Murphy used a constant factor of 7.16 to convert from the integrated flux above 2.5 Mev to the integrated flux above 0.63 Mev. This value was obtained from the average activity of a number of sulfur and neptunium dosimeters exposed at 5 different distances from a TRIGA burst. Dr. Wimenitz used conversion factors of 4.37, 3.55, and 3.35 at the 24, 38, and 45 cm positions from the reactor core, respectively.

VOLTAGE PROFILE OF FORWARD BIASED SILICON P-N JUNCTION DOSIMETERS

by

J. M. Swartz

Neutron damage in a silicon rectifier increases the dynamic resistance of the device under a forward applied bias. This increased resistance is credited to a decrease of the minority carrier lifetime in the base region.

In order to determine if the junction region and electrical contacts contribute to an appreciable extent to the increase in resistance from fast neutron radiation, a voltage profile was taken before and after exposing three 0.030-inch base-width silicon p-n junction dosimeters to a fast neutron dose of 1240 rads.

Three of the 0.030-inch p-n junction dosimeters processed from Czochralski-pulled material, prepared by the "standard process" as described in the Second Quarterly Report, November 15, 1959, were used for this work. A planar surface across the base of the device and perpendicular to the p-n junction, as shown in Figure 5, was obtained by lapping on 600-grit silicon carbide paper and polishing with 0.03 micron alumina.

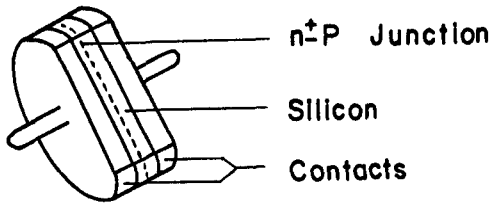

FIGURE 5. GEOMETRY OF LAPPED SILICON P-N JUNCTION DOSIMETER

The forward voltage-versus-distance profile at various constant current levels was obtained with the circuit shown in Figure 6 before and after exposure to fast neutron irradiation. A Southwestern Industrial Electronics Company Model R-1 voltmeter, shunted across an appropriate resistor, was used as an ammeter and a Keithley Model 610 electrometer was used for the voltage measurements.

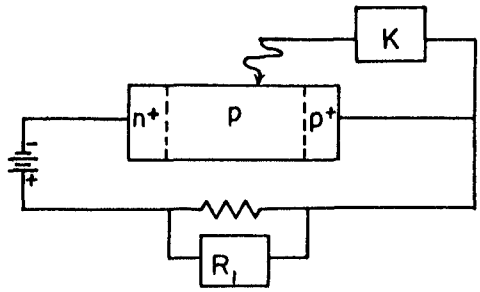

A-34734

FIGURE 6. CIRCUIT FOR OBTAINING VOLTAGE PROFILE OF SILICON P-N JUNCTION DOSIMETERS

In order to obtain a low resistance, ohmic contact to the surface of the silicon, a 2-mil diameter gallium-doped gold wire was bonded to the surface with a capacitor discharge unit at several points between the two contacts. After removing the bonded gold wire, a p^+ region remained, which gave reproducible ohmic contacts for the potentiometric voltage measurements. A fine tungsten point was used with micromanipulators to contact the gold-doped p^+ regions.

Representative curves of one of the diodes are shown in Figure 7. The negative voltage is plotted with the p^+ contact at zero potential. Curves for constant currents of 10^{-3}, 10^{-1}, and 1 ampere are given. For the two higher current values, the base region is flooded with current carriers and is conductivity modulated.

The theoretical junction voltages were calculated at different injection levels using the following formulas:

$$p\text{-}n^+, \quad J = 2qn_o\sqrt{\frac{D_a}{\tau}}\left(\exp\frac{qV_1}{kT} - 1\right) \tag{6}$$

$$p\text{-}p^+, \quad J = 2qp_o\sqrt{\frac{D_a}{\tau}}\left(\exp\frac{qV_2}{kT} - 1\right) , \tag{7}$$

where

D_a = ambipolar diffusion constant, $cm^2\ sec^{-1}$

J = current density, amperes cm^{-2}

τ = lifetime, seconds

q = electronic charge, coul

$p_o = 3 \times 10^{14}$, cm^{-3}

$n_o = 5 \times 10^5$, cm^{-3}

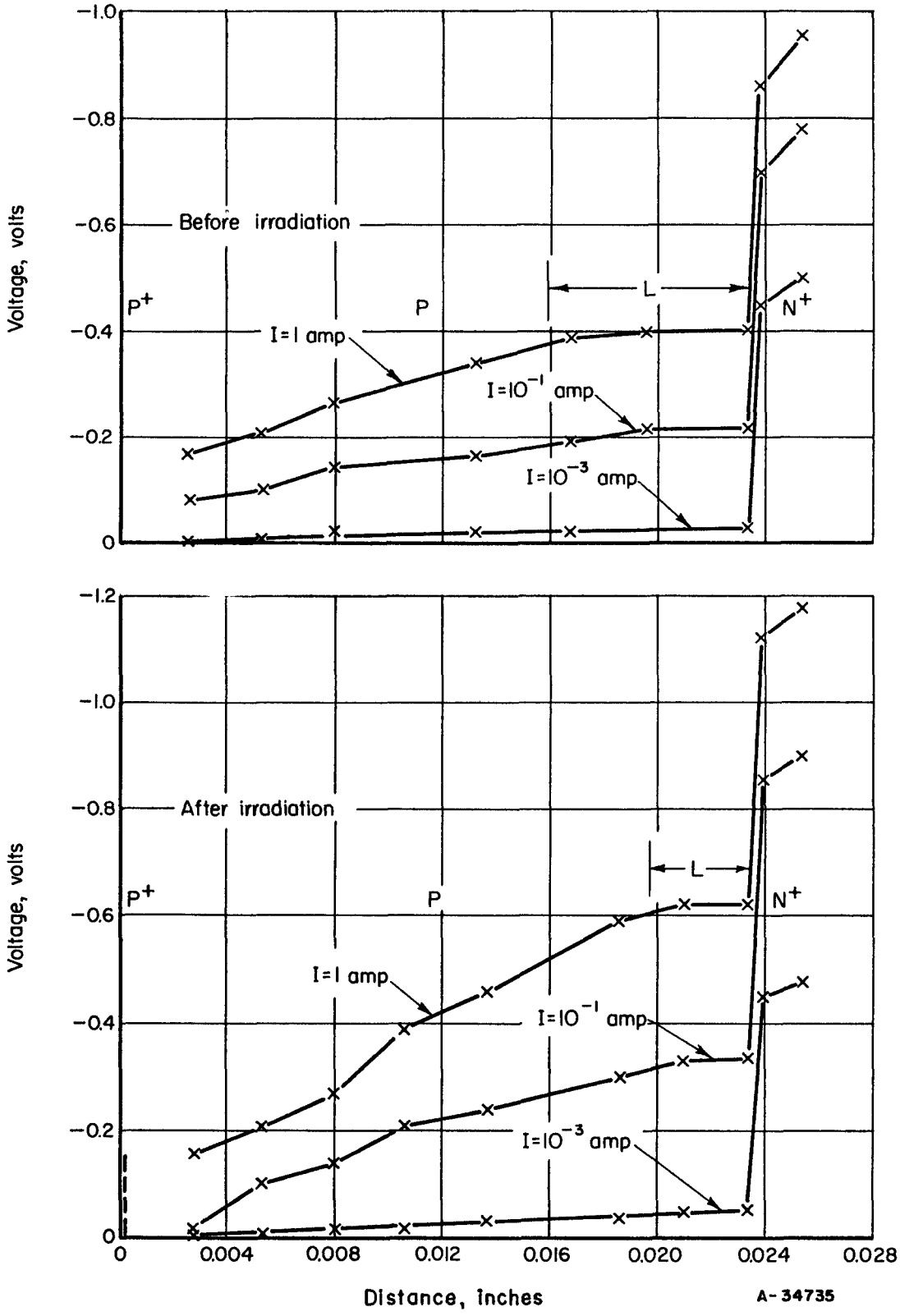

FIGURE 7. PREIRRADIATION AND POSTIRRADIATION VOLTAGE PROFILES OF EXPERIMENTAL SILICON P-N JUNCTION DOSIMETERS

In Table 4 the calculated values of the junction voltage for different current levels are compared to the values obtained by probing across the junction. The experimentally obtained values of the voltage across the p-p^+ junction agree very well with those obtained by the theoretical calculation. However, the voltages at the n^+-p junction are considerably lower than the calculated values. This probably means that the potential profile has been appreciably disturbed at the small degenerate regions used as contacts for the voltage probe. The slight increase in the junction voltage after irradiation as shown in Table 5, may be attributed to error in measurement, or inability to obtain the actual junction voltage. That the true junction voltage is unaffected by irradiation in the range of interest is also suggested by the fact that no change was observed in the junction capacity of the devices as a function of irradiation.

TABLE 4. CORRELATION OF THEORETICAL AND OBSERVED JUNCTION VOLTAGES BEFORE IRRADIATION

Junction	Current, amperes	Voltage, volts	
		Theoretical	Observed
n^+-p	10^{-3}	0.48	0.42
n^+-p	10^{-1}	0.60	0.48
n^+-p	1	0.66	0.46
p-p^+	10^{-1}	0.07	<0.08
p-p^+	1	0.13	<0.17

TABLE 5. N^+-P JUNCTION VOLTAGE, BEFORE AND AFTER IRRADIATION

Current, amperes	Voltage, volts	
	Before	After
10^{-3}	0.42	0.40
10^{-1}	0.48	0.53
1	0.46	0.50

For the lower current of 10^{-3} ampere (below the level of conductivity modulation), the resistance of the base region before irradiation can be calculated. A value of 45 ohms was obtained from the calculation, which is in excellent agreement with the resistance obtained from the Hall mobilities and carrier concentrations. The low initial slope of the voltage-distance curve proceeding into the base region from the n^+-p junction can be attributed to the injection of charge carriers into the base. Using the ambipolar diffusion constant (16.9 for silicon), diffusion lengths of .0078 and .0041 inch before and after irradiation, respectively, were calculated from the radiation induced change in lifetime. As shown in the figure, the calculated ambipolar diffusion lengths, (high level injection) for both pre- and post-irradiation conditions are very nearly equal to the length of the flat portions of the curves.

It can also be seen in Figure 7 that the slopes of the voltage-distance curves are different for different levels of forward current. The change in slope is less than the

change in current, which means that the resistance of the base region must be decreasing with increasing injection levels. This decrease in resistance with increasing current is to be expected, as conductivity modulation is dependent upon high level injection into the base region and is independent of base resistivity.

It can be concluded that nearly all of the increase in voltage at constant current with irradiation is due to the introduction of fast-neutron-induced recombination centers into the base region of the silicon p-n junction dosimeter.

REFERENCES

(1) Wertheim, G. K., Phys. Rev., 110 (6), p 1272-9 (June 15, 1958).

(2) Kinchen, G. H., and Pease, R. S., "The Displacement of Atoms in Solids by Radiation", Rept. Prog. in Phys., 18, p 1 (1955).

(3) Dienes, G. J., and Vineyard, G. H., Radiation Effects in Solids, Interscience Publishers, p 9-27 (1957).

(4) Loferski, J. J., and Rappaport, P., Phys. Rev., 98, p 1861 (1955).

(5) Wertheim, G. K., Phys. Rev., 111 (6), p 1800 (1958).

(6) Seitz, F., and Koehler, J. S., Solid State Physics, Vol. 2, Academic Press, p 407 (1956).

(7) Wertheim, G. K., Phys. Rev., 110, p 1272 (1958).

(8) Schweinler, H. C., J. Appl. Phys., 30 (8), p 1125 (1959).

(9) Cahn, J. H., J. Appl. Phys., 30 (8), p 1310 (1959).

(10) Etherington, H., Nuclear Eng. Handbook, McGraw-Hill, p 7 (1958).

(11) Gobeli, G. W., Phys. Rev., 112 (6), p 732 (1958).

(12) Sullivan, W. H., Trilinear Chart of Nuclides, USAEC, 2nd Edit. (1957).

PHASE II. DETERMINATION OF THE RESPONSE OF THE EXPERIMENTAL DOSIMETER TO RADIATION

by

H. C. Gorton and A. R. Zacaroli

SENSITIVITY OF EXPERIMENTAL SILICON RECTIFIER DOSIMETERS TO FAST NEUTRON IRRADIATION

The primary objective of the current program has been the development of a prototype fast neutron dosimeter sensitive in the same range as human tissue. As has been explained in a previous section of the report, the sensitivity of the silicon p-n junction dosimeter is determined by both material and design factors. Associated with the material is the radiation damage constant in silicon, which defines the degree of lifetime change with fast neutron flux. The predominant geometry factor affecting device sensitivity is the width of the base region of the device.

To evaluate the sensitivity of the silicon p-n junction dosimeter to fast neutron irradiation, 10 devices fabricated from Czochralski-pulled silicon using the "nickel-slow cooled" process were exposed to a fast neutron flux of 1240 rads in 10 increments of approximately 120 rads each in the Battelle Research Reactor. After each incremental exposure, the devices were removed from the reactor and the charge carrier lifetimes and the current-voltage characteristics were measured. Of the 10 devices, 8 had base widths of .020 inch, one had a base width of .025 inch, and one had a base width of .030 inch.

The current-voltage profiles were obtained with a Moseley Autograf flat-bed recorder, as shown in Figure 8. A motor-driven variable-voltage source facilitated the rapid and accurate recording of the current-voltage profiles. Lifetimes were measured by the open-circuit voltage decay method illustrated in the schematic diagram in Figure 9. This method consists of passing forward current through the device, suddenly opening the circuit, and observing the voltage decay as a function of time on a Tektronics 435 oscilloscope. The voltage decays as a linear function of time, and lifetime is calculated from the slope of the voltage-time curve by the expression

$$\tau = - \frac{kT}{q} \frac{\Delta t}{\Delta V} \quad , \tag{8}$$

where k is Boltzmann's constant, q is the charge of an electron, T is absolute temperature, V is the observed voltage, and t is the observed time.

From the relationship $\tau_f^{-1} = \tau_o^{-1} + \alpha\, nvt$, it can be seen that the reciprocal charge carrier lifetime in an irradiated device should be proportional to the fast neutron flux, the proportionality constant being the radiation damage constant of the material. Figure 10 is a plot of reciprocal lifetime versus fast neutron dose for the eight .020-inch base width devices. At each irradiation level the average and the extreme values of reciprocal lifetime are plotted. The slope of the curve drawn through the experimental

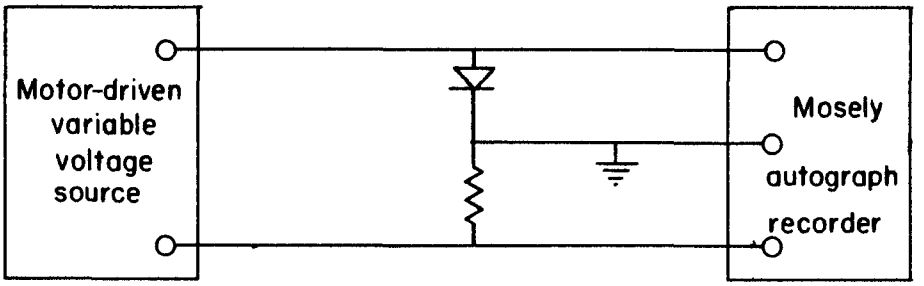

FIGURE 8. BLOCK DIAGRAM OF CIRCUIT FOR OBTAINING CURRENT-VOLTAGE PROFILES OF SILICON P-N JUNCTION DOSIMETER

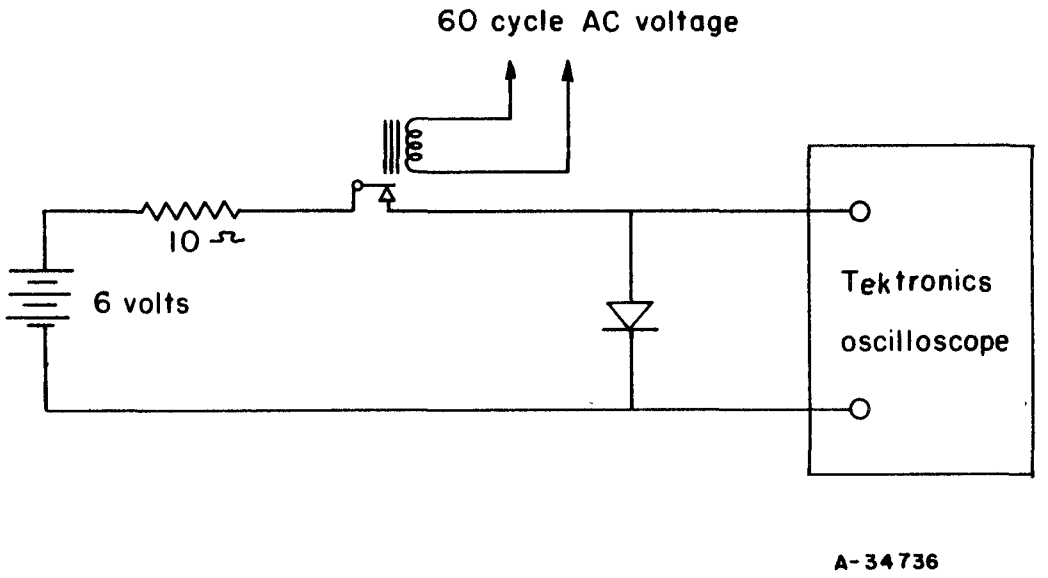

FIGURE 9. SCHEMATIC DIAGRAM OF CIRCUIT FOR OBTAINING LIFETIMES OF SILICON P-N JUNCTION DOSIMETER

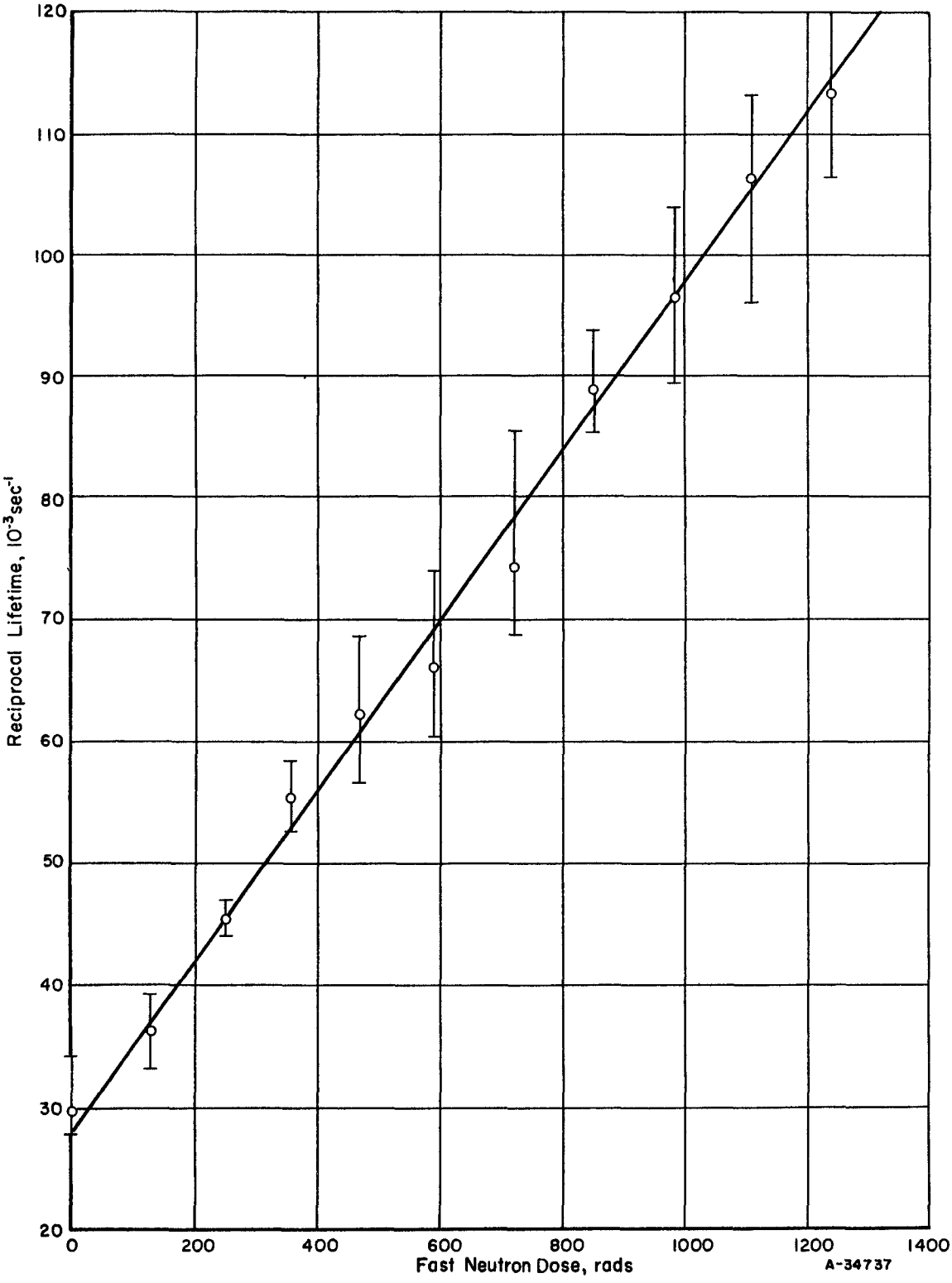

FIGURE 10. AVERAGE AND EXTREME VALUES OF RECIPROCAL LIFETIME VERSUS FAST NEUTRON IRRADIATION FOR EIGHT .020-INCH BASE WIDTH SILICON P-N JUNCTION DOSIMETERS

points represents a value of 65 rad^{-1} sec^{-1}. A typical family of current-voltage curves, with fast neutron irradiation as a parameter, is shown in Figure 11. The curve on the extreme right is the pre-irradiation curve, the curves shifting to the left with increasing irradiation. In Figure 12 is a plot of the normalized forward currents at constant voltages as a function of fast neutron irradiation with base width as a parameter. The curve for the 20-mil base width device is the normalized average current through each of eight units. The increase in sensitivity with increasing base width is very apparent. For example, at a fast neutron dose of 600 rads, the forward current is decreased by 35 per cent, 50 per cent, and 75 per cent for the .020-, .025-, and .030-inch base width devices, respectively.

It may be concluded from the above results that adequate sensitivity of the device to fast neutron irradiation in the dose range of interest has been achieved. It may be pointed out that the sensitivity of the device could be further increased by increasing the initial charge carrier lifetime and increasing the base width of the device. It also follows that a less sensitive device, suitable for measuring appreciably higher doses, could be made by degrading the initial lifetime and by decreasing the width of the base region.

SENSITIVITY TO GAMMA RADIATION

The ideal fast-neutron dosimeter would, of course, be insensitive to all other forms of radiation. It has been shown from theoretical considerations (see Table 2, page 11) that bulk silicon approaches this ideal for exposure to the radiation field of an enriched U^{235} reactor. Although the principal effect of radiation damage in the silicon p-n junction dosimeters is assumed to take place in the base region from interactions of fast neutrons with the bulk silicon, the actual effects of other forms of radiation on the electronic properties of the device had not been determined. To investigate such effects, a number of experimental silicon p-n junction dosimeters were exposed to gamma radiation in the Battelle Gamma Facility.

Six experimental devices which were exposed to gamma radiation had base widths of .010, .015, and .020 inch, and were processed from Czochralski crystals by the standard slow-cooled technique. Measurements of the forward current through the devices at constant voltage were obtained periodically during the irradiation. The assumption that transient ionization effects under conditions of high-level injection would be negligible was experimentally verified. The lifetime of injected charge carriers was determined before and after exposure to 1.8×10^6 reps of Co^{60} gammas.

Figure 13 shows the effect of gamma radiation up to 5.5×10^5 reps on the normalized forward current through each of the six dosimeters. For comparison purposes, the fast-neutron flux in the Battelle Research Reactor which corresponds to an equivalent number of reactor gammas is superimposed at the top of the graph. Thus, it may be seen, for example, that the change in forward current resulting from gamma irradiation associated with a fast-neutron exposure of 1000 rads in the Battelle Research Reactor would be less than 4 per cent in any of the six devices. It may also be observed from Figure 13, that the devices with wider base regions are correspondingly more sensitive to the gamma radiation. In order to clearly observe this trend, however, the gamma exposures were far in excess of the gamma flux in the exposure range of interest in the U^{235} fission spectrum.

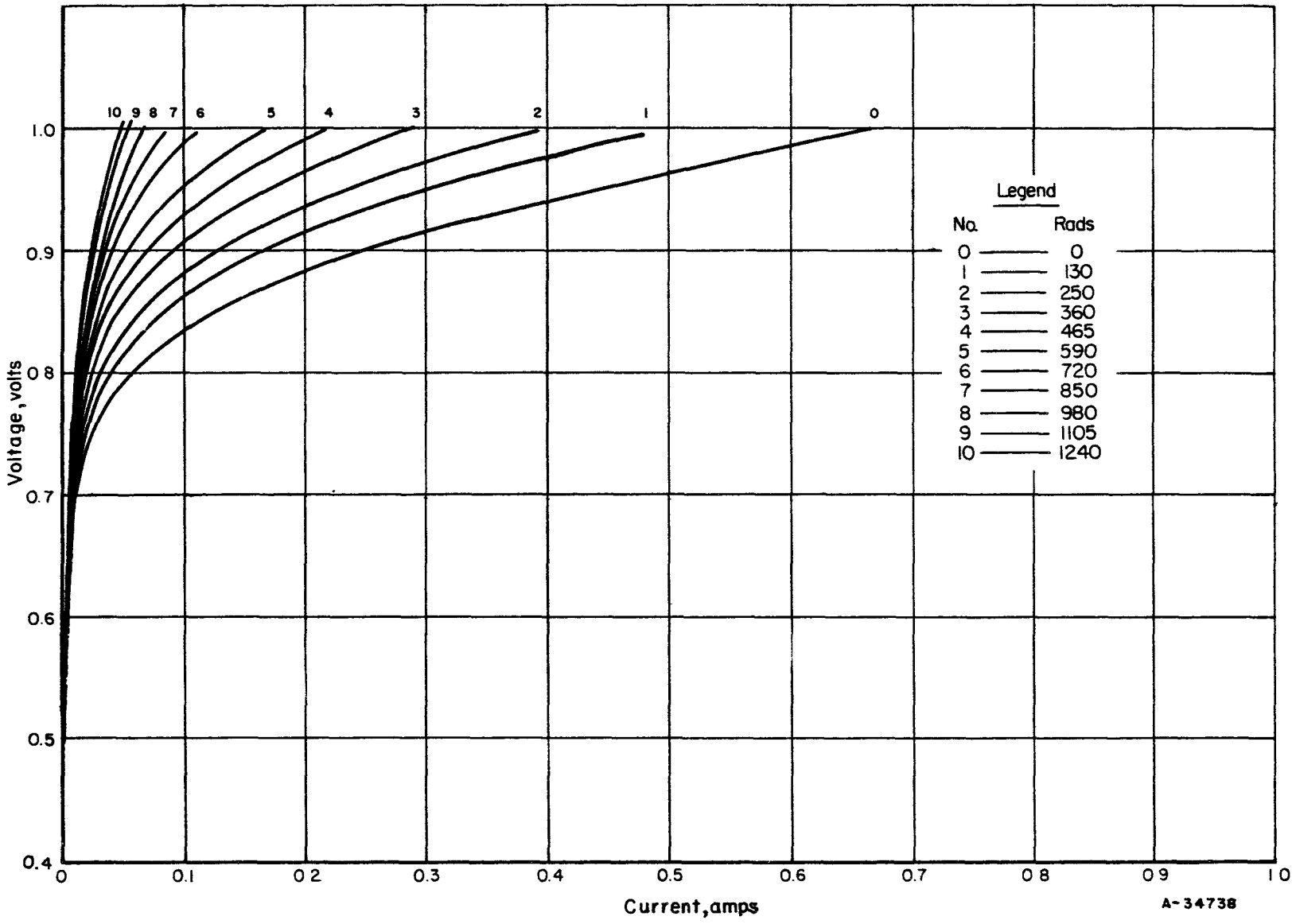

FIGURE 11. CURRENT-VOLTAGE PROFILES OF A .030-INCH BASE WIDTH SILICON P-N JUNCTION DOSIMETER

Fast neutron irradiation as a parameter.

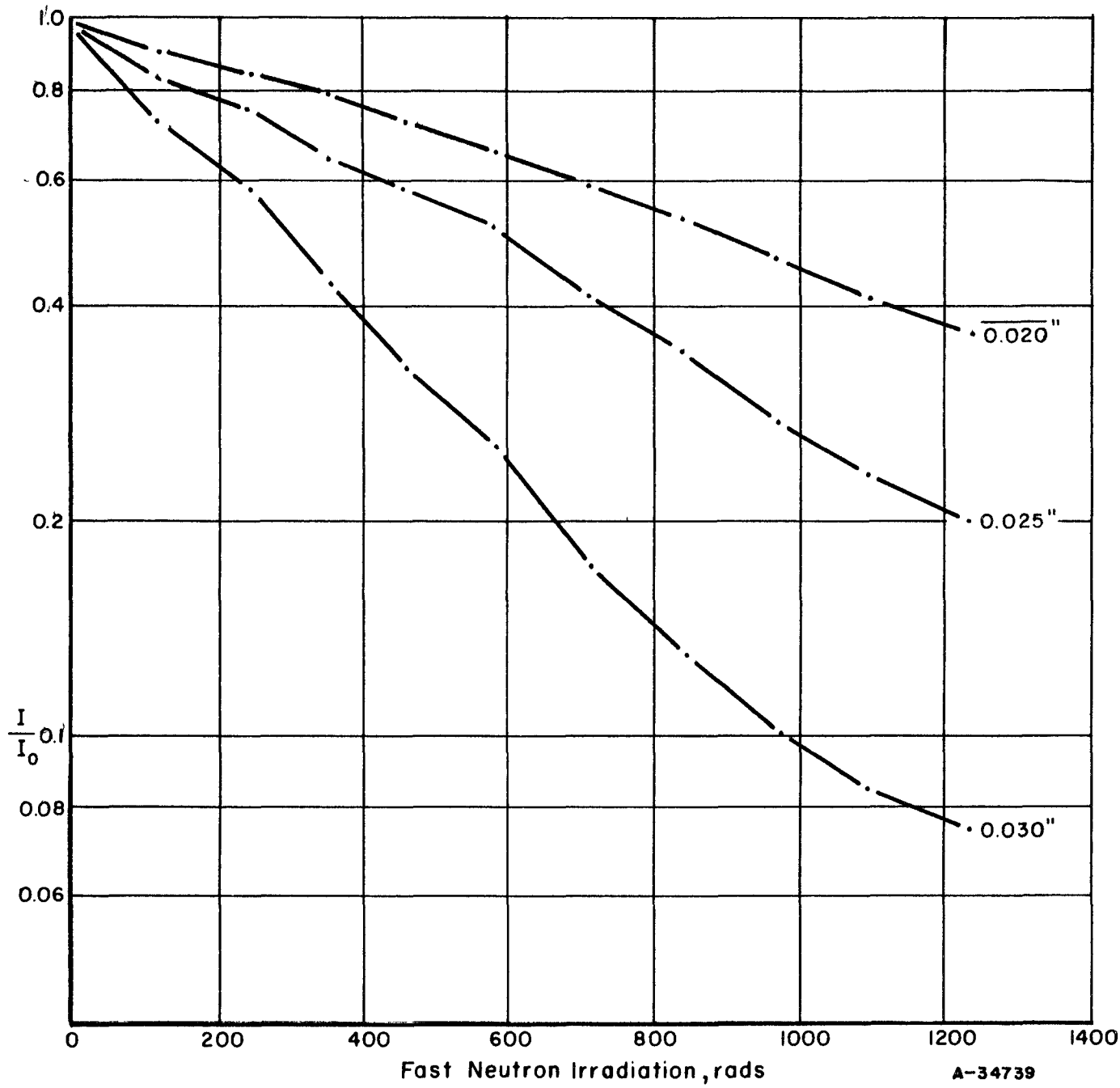

FIGURE 12. NORMALIZED FORWARD CURRENTS AT CONSTANT VOLTAGES FOR SILICON P-N JUNCTION DOSIMETERS

Base width as a parameter

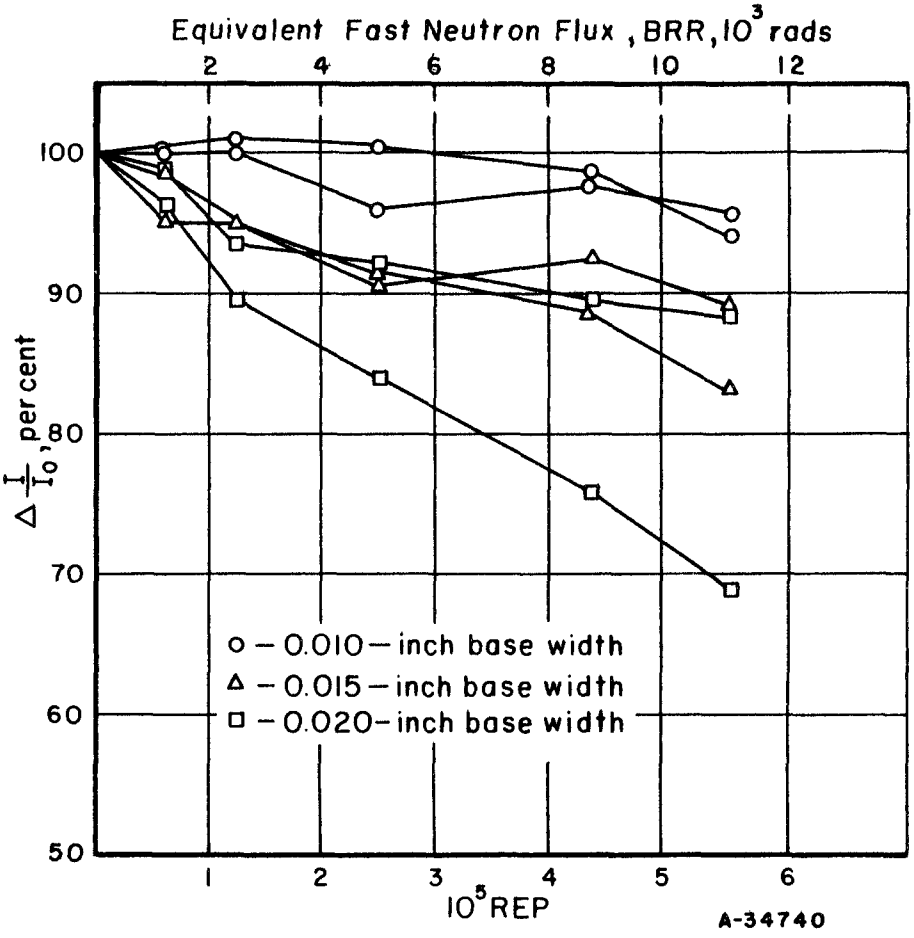

FIGURE 13. CHANGE IN NORMALIZED FORWARD CURRENT AS A FUNCTION OF EXPOSURE IN THE BATTELLE GAMMA FACILITY

Since the decrease in the forward current through the dosimeter at constant voltage results from the radiation-induced decrease in charge carrier lifetime in the device, one would expect appreciable changes in lifetime in the devices after an exposure of 10^6 reps to Co^{60} gammas. Pre- and post-irradiation lifetimes in the six devices exposed to the Battelle Gamma facility are shown in Table 6. As may be seen in Table 6, the expected decrease in lifetime, corresponding to the observed decrease in forward current at constant voltage, did not occur. Since the radiation-induced increase in resistance of the device under forward bias is a secondary effect, resulting from a decrease in charge carrier lifetime, and since a decrease in lifetime after exposure to 1.76×10^6 reps was not observed, it must be concluded that the observed increase in resistance is not associated with radiation damage in the base region of the device. Also, it will be shown in the next section that the exposure of a nominal .020-inch base width device to a fast-neutron dose of 1000 rads results in a decrease in forward current at constant voltage of about 55 per cent. Calculations of the relative damage introduction rates of fast neutrons and gamma rays in a reactor environment (see Table 2) show that the corresponding decrease in forward current from the equivalent gamma dose should be less than 0.2 per cent. The actual changes observed in the forward current of the two .020-inch base width devices exposed to the equivalent gamma irradiation in the cobalt source are 1 per cent and 4 per cent, and are assumed, therefore, to be anomalously high.

TABLE 6. LIFETIMES BEFORE AND AFTER EXPOSURE TO 1.75×10^6 REPS Co^{60} GAMMA IRRADIATION

Number	Base Width, inch	Initial Lifetime, microseconds	Final Lifetime, microseconds
1	.010	3.5	3.3
2	.010	3.8	3.3
3	.015	6.2	7.8
4	.015	7.0	7.3
5	.020	12.5	12.2
6	.020	17.7	16.6

Since changes in resistance outside the space-charge region do not affect the measured value of the injected charge carrier lifetime as obtained by the open-circuit voltage decay method, changes in the series resistance of the device resulting from gamma irradiation, for example at the ohmic contact-silicon interface, could account for the results observed. In any case, it is recommended that the effects of gamma irradiation on the device properties be studied further to ascertain whether the observed change in forward current was associated with an anomalous condition in the devices tested, or whether it may be associated with an inherent property of the dosimeter.

THE RATE DEPENDENCE OF FAST NEUTRON IRRADIATION ON THE SENSITIVITY OF SILICON P-N JUNCTION DOSIMETERS

Research efforts on the experimental silicon p-n junction dosimeters have been directed toward the development of a tactical device which is expected to be used for the evaluation of radiation damage from exposure to radioactive areas, where the dose rate

may be relatively low, as well as from exposure to nuclear detonations, where the dose rate is on the order of 2 x 10^{23} neutrons per kiloton. It is important, therefore, to determine the dose rate of fast neutron irradiation on the sensitivity of the devices. Accordingly, a number of experimental units were exposed to a fast neutron pulse at a rate of 2.5 x 10^4 rads sec^{-1} from the General Atomics TRIGA Reactor and were then compared to a number of similar units exposed to a fast neutron flux at a rate of 6 rads sec^{-1} from the Battelle Research Reactor.

Forty-eight p-n junction dosimeters were exposed to different total doses up to approximately 1500 rads in the General Atomic TRIGA Reactor. Eight of the devices were exposed at each of six positions from the reactor core. Each package of eight devices contained two each with base widths of 0.015, 0.020, 0.025, and 0.030 inch. One of each of the two devices of a given base width was processed by the standard technique and the other was processed by the technique involving the nickel-gettering process. Attenuation of the fast neutron flux was provided by the water moderator and large-area sulfur pellet dosimeters. Smaller sulfur pellet dosimeters were placed in each of the six p-n junction dosimeter packages to monitor the dose received by each group of devices. The activity of the small sulfur pellets, as obtained from Harry M. Murphy, Jr., Institute for Exploratory Research, USASRDL, is given in Table 7.

TABLE 7. SULFUR PELLET EVALUATION – TRIGA TRANSIENT 1048

Pellet	ICR, cpm	Fast Neutron Dose, n cm^{-2}		Tissue Rads
		E >2.5 Mev	E >0.63 Mev	
53	464.9	8.07 x 10^{10}	4.51 x 10^{11}	1492
59	324.7	5.64 x 10^{10}	3.19 x 10^{11}	1042
62	73.15	1.27 x 10^{10}	7.15 x 10^{10}	235
68	51.54	8.94 x 10^{9}	5.05 x 10^{10}	166
71	31.08	5.39 x 10^{9}	3.05 x 10^{10}	100
74	20.09	3.48 x 10^{9}	1.97 x 10^{10}	65

As a comparison with the high-dose-rate exposure in the TRIGA facility, four packages of eight silicon p-n junction dosimeters, identical to those exposed to TRIGA, were exposed in the Battelle Research Reactor to different total doses up to approximately 1000 rads at a reactor power level of 10 kilowatts. All of the p-n junction dosimeters were placed together in a polyethylene exposure tube and were placed in Core Position 84, 22 centimeters from the reactor core face. The different total doses were obtained by exposing the four packages for different lengths of time.

The total irradiation received by the devices was determined by counting the activity of gold-leaf dosimeters that were included in each of the packages. The gold dosimeters, which are sensitive to thermal and resonance neutrons, were calibrated by exposing both gold and aluminum dosimenters in the same location as the experimental units and comparing the induced radioactivity. The exposure, however, was at a reactor power of 200 kilowatts for 20 minutes in order to create sufficient activity in the aluminum for accurate evaluation.

The radiation received by each of the four sets of devices is recorded in Table 8.

TABLE 8. GOLD-FOIL EVALUATION – BRR COMPARISON RUN

Foil	Exposure Time, seconds	Fast Neutron Dose	
		total n cm^{-2}	Tissue Rads
7	312	6.77×10^{11}	1880
8	217	4.7×10^{11}	1309
9	76	1.65×10^{11}	459
10	21	4.5×10^{10}	125

Measurements of high-level lifetime in the devices before and after irradiation were made by the open-circuit voltage-decay method. As was shown in the preceding section, the preirradiation and postirradiation lifetimes of a material are related to the radiation dose through the expression

$$\frac{1}{\tau} - \frac{1}{\tau_o} = \alpha \, nvt \quad , \tag{9}$$

where the proportionally constant, α, is defined as the damage constant of the material. A comparison of the damage constants calculated for devices exposed to different amounts of radiation in the two reactors is shown in Figure 14. Each point represents the average for eight dosimeters of four different base widths and two processing procedures subjected to a given level of irradiation. The scatter in the damage constant among the eight samples at a given irradiation level is also shown. The increased scatter at low irradiation levels results from limitations in measuring lifetime. Since, as shown in Equation (9), the value of the damage constant is obtained from the difference between two measured values of lifetime, the percentage error in the damage constant increases as the difference between the preirradiation and postirradiation values of the lifetime decreases.

An expression relating the ratio of the error in determining the total dose to which the devices have been exposed to the error in measuring lifetime may be developed from Equation (9) as

$$\frac{\tau}{\Delta\tau} \frac{\Delta(nvt)}{nvt} = 1 + \frac{2}{\tau_o \, \alpha \, nvt} \quad . \; * \tag{10}$$

Since the error in measuring lifetime, $\frac{\Delta\tau}{\tau}$, is fixed at about 4 per cent, the percentage error in measuring the total dose received, $\frac{\Delta nvt}{nvt}$, may be seen to be inversely related to the initial lifetime, τ_o. Hence, it is pertinent to develop devices with as high an initial lifetime as possible.

The change in reciprocal lifetime averaged over the four base widths of the devices tested versus incident radiation in rads is plotted in Figure 15 for all the devices irradiated in the dose-rate-comparison experiments in the TRIGA and Battelle Research

*See Appendix A.

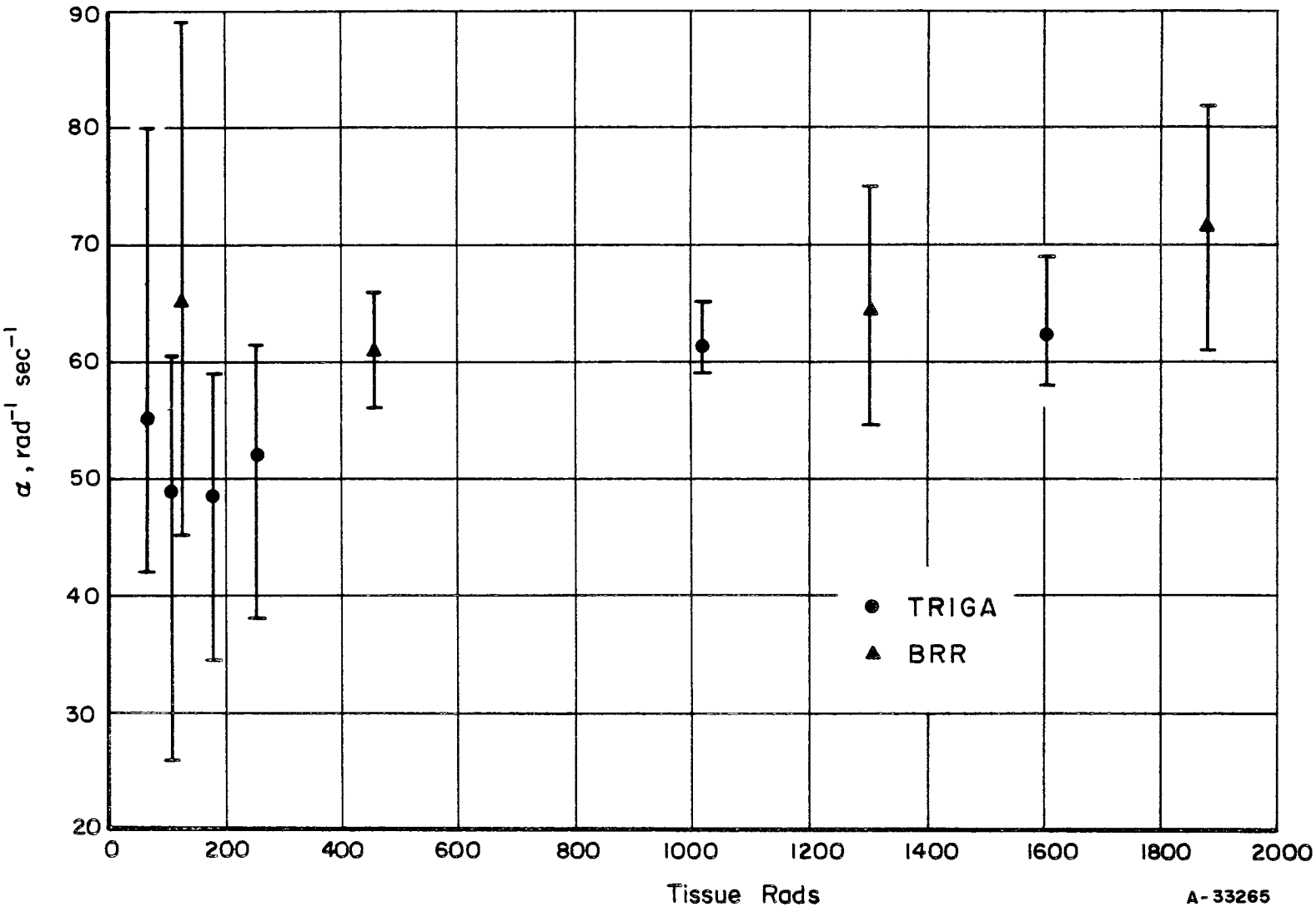

FIGURE 14. DAMAGE CONSTANT, α, AVERAGED OVER THE FOUR BASE WIDTHS TESTED

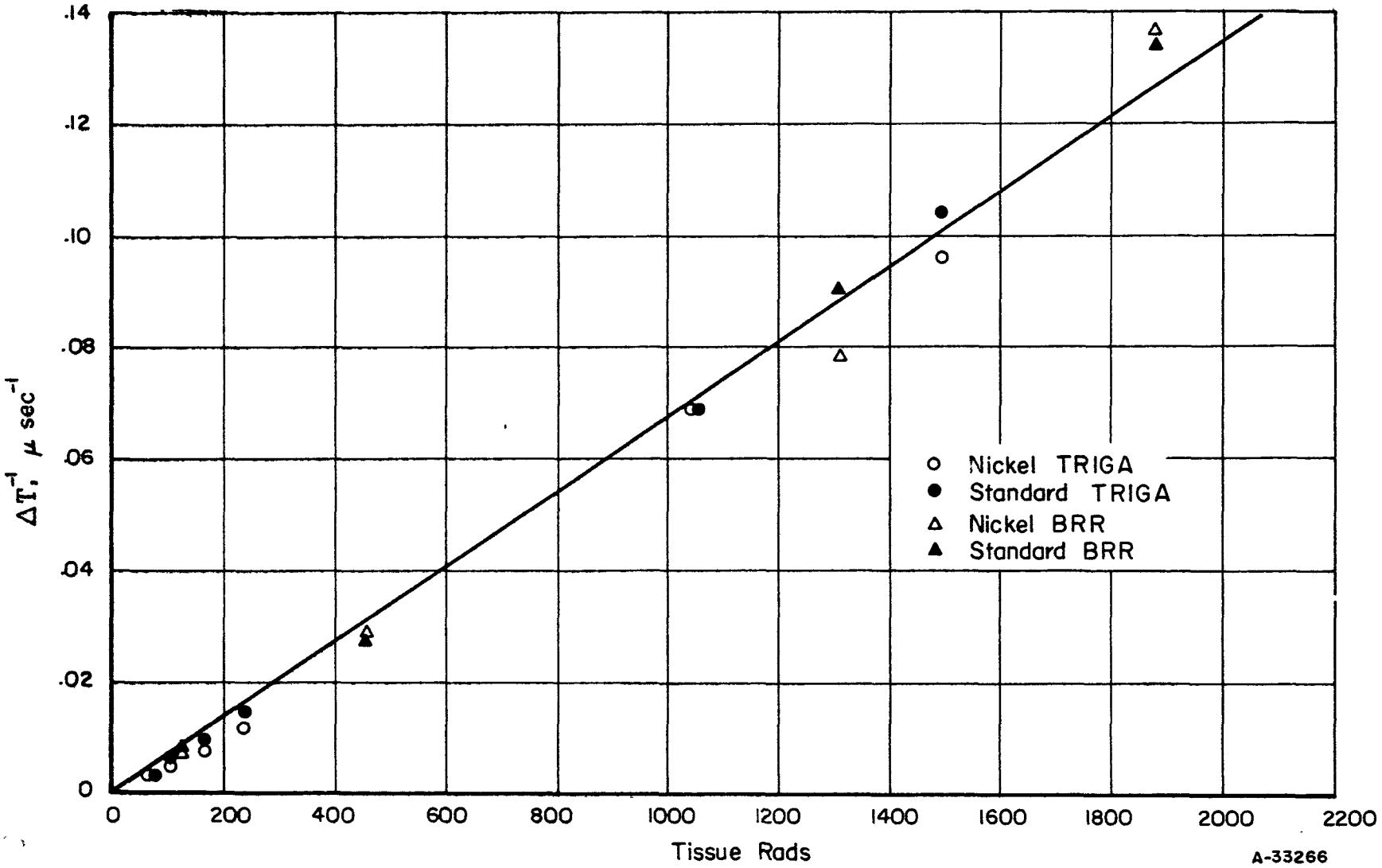

FIGURE 15. CHANGE IN RECIPROCAL LIFETIME AVERAGED OVER THE FOUR BASE WIDTHS TESTED

Reactors. The scatter about a straight-line fit of the data is encouragingly small, and it is observed that no significant difference in lifetime change resulted from the marked difference in dose rate between the two irradiations. It may also be noted, as is expected, that the addition of the nickel-gettering step in the processing procedure does not produce a significant change in the dependence of $\Delta\tau^{-1}$ on incident radiation. It may be noted further that the value of the damage constant is equal to the slope of the plot of $\Delta\tau^{-1}$ versus nvt, and the value obtained from the experimental data shown in Figure 15 is 67.6 rad^{-1} sec^{-1} (1.88×10^{-7} nvt^{-1} sec^{-1}).

Since fast-neutron irradiation of the silicon p-n junction dosimeters results in a change in the charge-carrier lifetimes in the material, any rate dependence of the effect of irradiation on the devices would be evidenced by a difference in the damage constant resulting from differences in the dose rate of the incident radiation. The dose rate to which the devices were exposed in the TRIGA facility was greater than 4000 times that to which the devices were exposed in the Battelle Research Reactor. Nevertheless, the difference in the two values of the damage constant averaged over all the devices exposed in each reactor was only 16 per cent, a value that is probably well within the experimental error in evaluating the dosimetry in the two reactors. It is concluded, therefore, that the sensitivity of the silicon p-n junction dosimeters to fast-neutron radiation is not rate dependent, at least up to 2.5×10^4 rads sec^{-1}.

TEMPERATURE DEPENDENCE OF READ-OUT CURRENT

The temperature dependence of the current through an ideal diode at constant applied voltage is of the form

$$I = A\, e^{\alpha/T} \tag{11}$$

Although the p-n junction dosimeter is a compound device comprising two junctions and an appreciably wide base region, it is reasonable to assume that the temperature dependence of the current maintains the same general relationship given above.[1] Therefore, experiments were carried out to investigate the significance of the expected change with temperature, and the possible effect of fast neutron radiation thereon.

Two 20 mil base width devices, whose initial forward currents at 0.800 volts applied potential differed by less than 10 per cent, were chosen for study. One of the two devices was exposed to 1240 rads fast neutron irradiation. Current-voltage profiles were then obtained from each device at several temperatures between -30 and 160°F. Figure 16 is a plot of the log of the forward current through the devices at 0.800 volts applied potential as a function of reciprocal temperature. The detailed forms of the curves obtained are not completely understood at the present time. For instance, in the preirradiation curve, an apparent discontinuity in the slope occurs at about 65°F; and in the postirradiation curve, the slope increased with increasing temperature. The continuous change of slope in the latter curve implies a radiation-induced change in a series resistance in the device with either increasing current or increasing temperature. Low temperature annealing effects are ruled out because of the reproducibility of the curve.

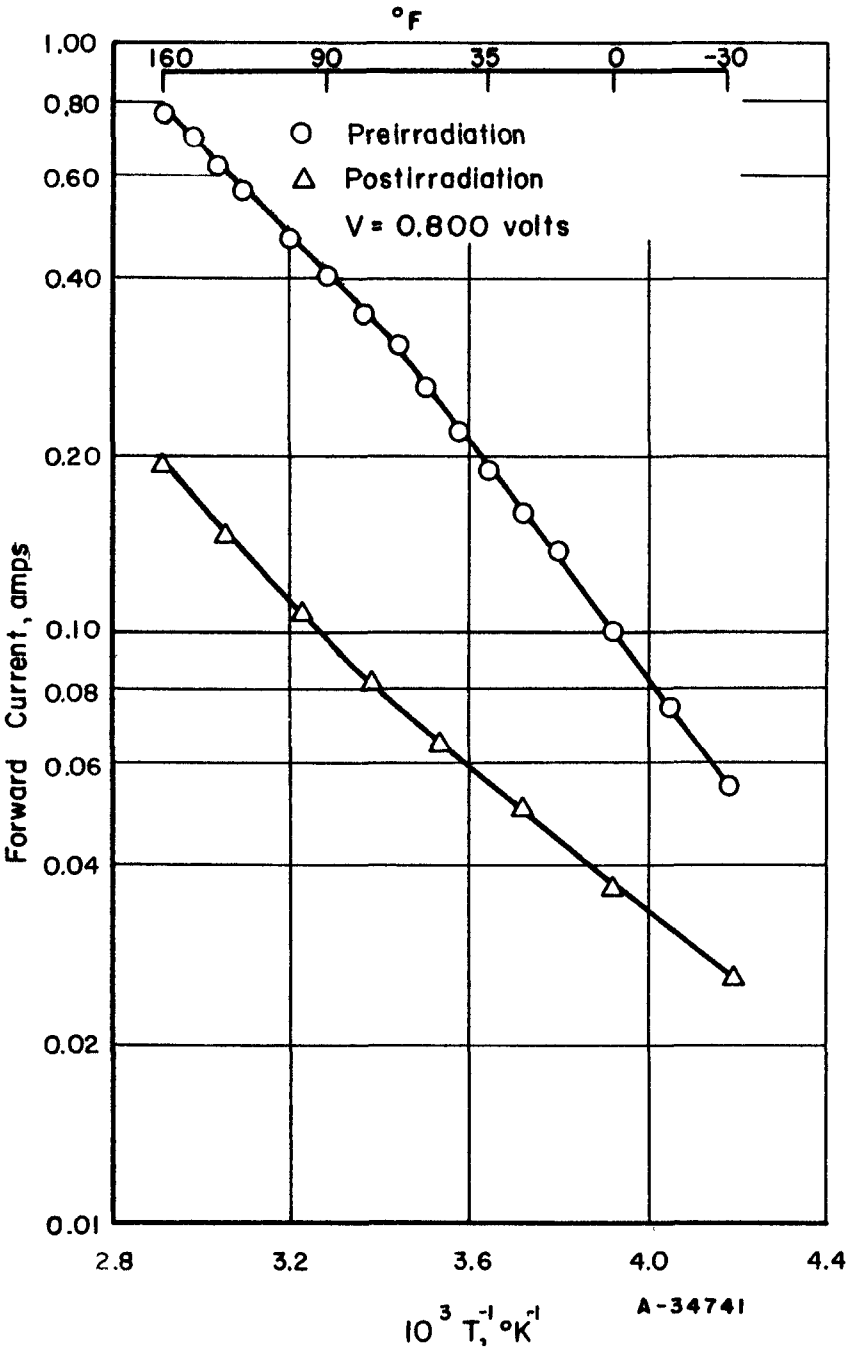

FIGURE 16. EFFECT OF AMBIENT TEMPERATURE ON FORWARD CURRENT IN .020-INCH BASE SILICON P-N JUNCTION DOSIMETERS BEFORE AND AFTER FAST NEUTRON EXPOSURE OF 1240 RADS

A rather strong temperature dependence of the current through the dosimeter at constant voltage is observed, the variation amounting to about 3 per cent per centigrade degree in the unirradiated device and about half that value in the irradiated device. Interpreted in terms of dose, this change corresponds to about 18 rads per centigrade degree in a nominal unirradiated 20 mil base width device. The fact that the temperature dependence of the current changes with irradiation seriously complicates the development of a compensating mechanism in the read-out circuit and may, therefore, impose limitations on the ambient read-out temperature.

ANNEALING STUDIES

It has been demonstrated that radiation-induced defects in silicon may be annealed out of the material at elevated temperatures.[2] If such an annealing effect were to take place within the expected ambient temperature to which the silicon p-n junction dosimeter would be subjected, the apparent radiation to which the device had previously been exposed would have been correspondingly decreased. Therefore, it is important to determine the minimum temperature at which annealing of radiation-induced defects takes place in the device. The possibility also exists that, under certain conditions of time and temperature, essentially all of the radiation-induced defects could be annealed out. The recovery and re-use of irradiated devices would then be possible. It is important therefore to determine the extent to which radiation-induced defects may anneal out at the maximum temperature to which the device could be subjected without permanently altering its electronic or physical properties. Reported in this section are the results of preliminary experiments which give some information on both minimum- and maximum-temperature annealing effects.

Three 20 mil base width devices with different initial lifetimes and current-voltage characteristics were chosen for study. These devices were taken from the 100 units that had been exposed to 1240 rads fast neutron irradiation. The three devices were annealed for 5 minutes at each of several temperatures between room temperature and 250°C. Then they were annealed for an additional 55 minutes and then 2-1/2 hours at the same temperature. Finally, they were annealed at 330°C for 3 minutes. After each anneal, the devices were cooled to room temperature and measurements of lifetime and current-voltage characteristics were obtained.

Figures 17 and 18 are graphical representations of the changes in lifetime and forward current at constant voltage, respectively, as a result of the temperature program just described. The per cent recovery of the initial preirradiation characteristics are plotted as a function of annealing temperature. As may be seen from the figures, two measurements were taken on each of the devices after the 5 minute anneal at 205°C. The first measurement was made immediately after returning the units to room temperature, and the second measurement was made 16 hours later. It is seen in the figures that there was some reversion of the forward current at constant voltage in all three devices, and of the lifetime in one of the three devices. The increased recovery of both lifetime and forward current from the prolonged anneal at 250°C is also apparent. An additional anneal for 2-1/2 hours at this temperature did not significantly change the lifetime and forward current from the values obtained after the 55 minute anneal. It is to be noted that no additional recovery of the initial characteristics was observed after

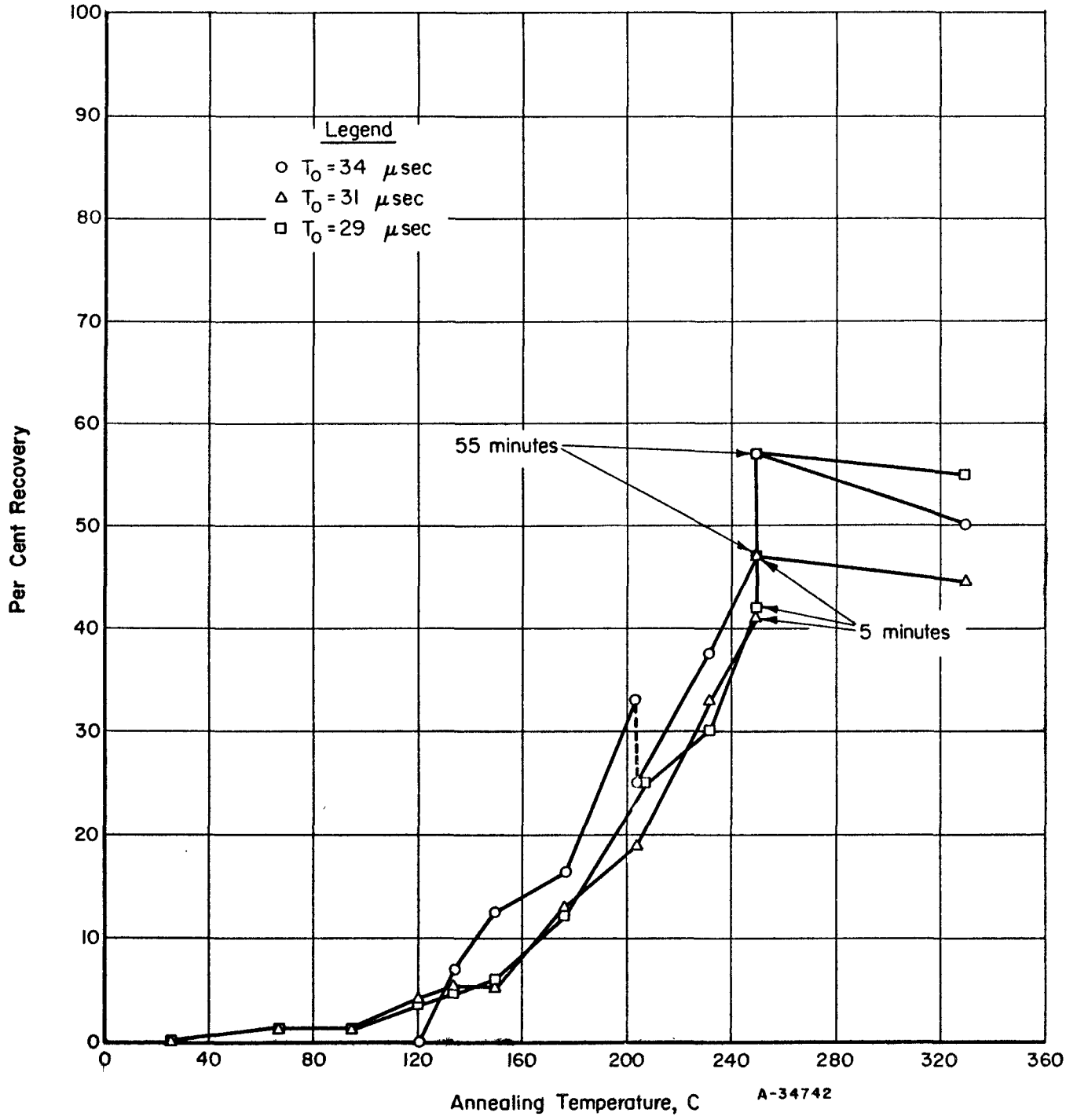

FIGURE 17. RECOVERY OF PREIRRADIATION LIFETIME AS A RESULT OF ANNEALING SILICON P-N JUNCTION DOSIMETERS EXPOSED TO 1240 RADS FAST NEUTRON IRRADIATION

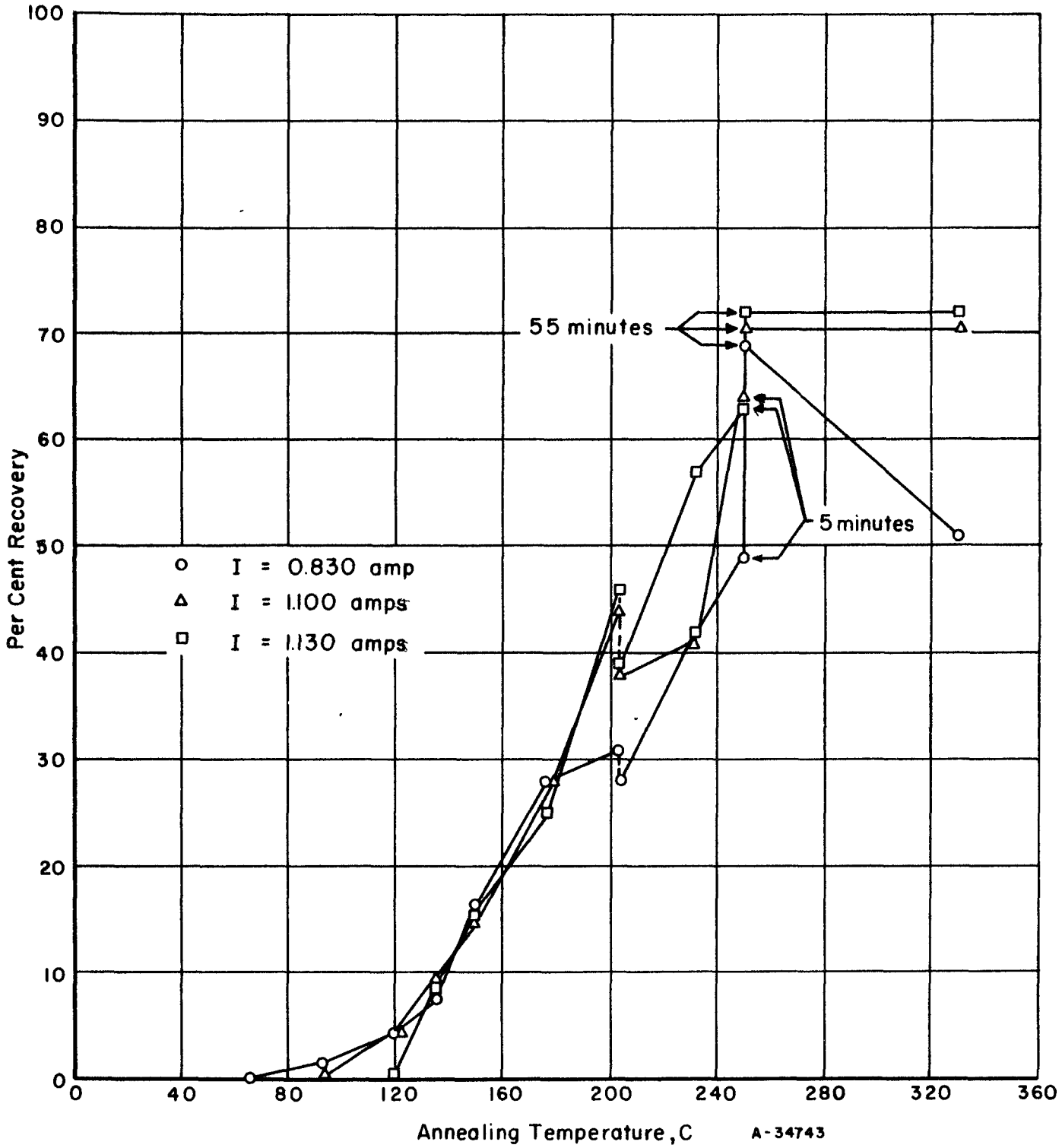

FIGURE 18. RECOVERY OF PREIRRADIATION FORWARD CURRENT AT V = 0.900 VOLTS AS A RESULT OF ANNEALING SILICON P-N JUNCTION DOSIMETERS EXPOSED TO 1240 RADS FAST NEUTRON IRRADIATION

heating the devices to 330°C for 3 minutes. In fact, a rather severe degradation in lifetime was observed in one device, and some decrease of the forward current at constant voltage was observed in all three devices.

The annealing of defects in bulk silicon is a complicated process, and is not completely understood at the present time. Moreover, the problem of understanding the mechanism is compounded when the silicon is processed into a device such as the one under study. Nevertheless, some conclusions can be drawn from the data at hand. In particular, no appreciable annealing effects were observed below 100°C, and it may be expected from the data of Bemski and Augustyniak[2] that damage effects would remain unchanged after much longer anneals at 100°C. Also, the fact that heating the devices to 250°C for 2-1/2 hours after the 60-minute anneal at the same temperature resulted in no additional recovery of initial characteristics, and that no improvements were seen after the short anneal to 330°C, suggests that a complete recovery of initial characteristics may not be possible within the temperature limits imposed by the physical properties of the device components.

REPRODUCIBILITY OF RADIATION EFFECTS

The need for uniformity from one device to another in the measured effects of radiation is obvious, the higher the degree of uniformity in the measured effects of radiation, the greater will be the accuracy of the observed radiation dose. Also, the achieving of similar initial characteristics would obviate the need to "tag" each device for appropriate compensating adjustments in the read-out circuit.

A study was made of the uniformity of the response to fast neutron irradiation of 100 devices processed from Czochralski-pulled crystals of silicon of a fixed resistivity. It is important to note, however, that although the resistivity of each slice of silicon was essentially the same, the slices were cut from several different ingots; the implication being that other characterizing parameters of the starting material, such as charge carrier lifetime, may not have been held constant.

In this experiment, 100 20 mil base width devices, fabricated by the "nickel-slow cooled" process, were selected from a total of 150 units on the basis of uniformity of charge carrier lifetime and current-voltage characteristics. The degree of uniformity of the initial characteristics of the 100 devices is shown in Figures 19 and 20. Figure 19 depicts the distribution in preirradiation lifetimes, and Figure 20 depicts the distribution of initial forward current through the devices at an applied potential of 0.850 volts. Fifty of these devices were exposed to a fast neutron flux of 720 rads and the other 50 to a fast neutron flux of 1240 rads in the Battelle Research Reactor. Measurements of the charge carrier lifetimes and current-voltage characteristics of the devices were obtained before and after irradiation.

As shown by Equation (9), page 33, the damage constant in silicon is defined by the ratio of the change in radiation-induced reciprocal lifetime to radiation dose. Theoretically, the damage constant has a single value for a given material, so any variation in the observed damage constant would be an indication of nonuniformity in the response of the device to fast neutron irradiation. Figure 21 shows the distribution of

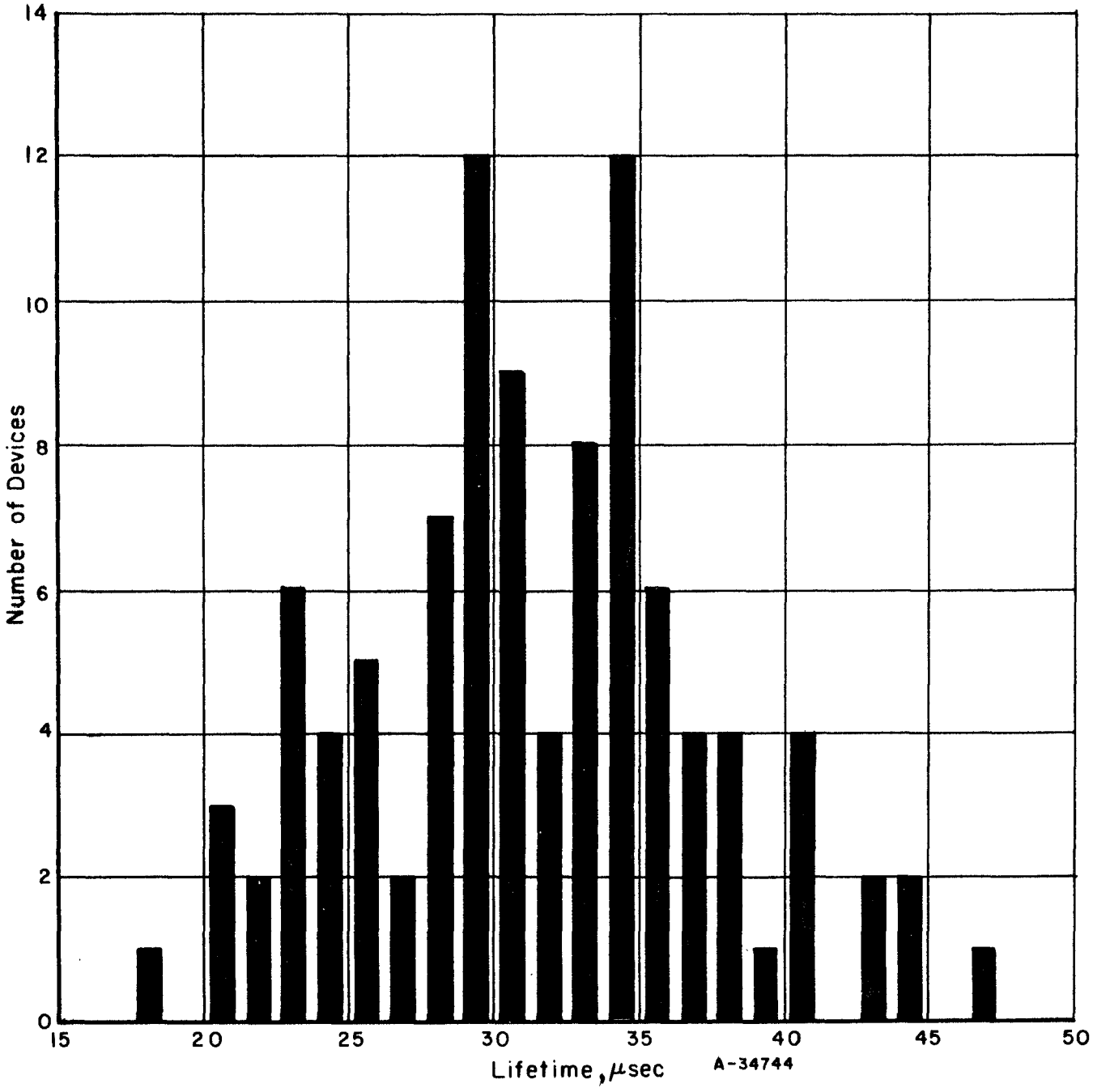

FIGURE 19. DISTRIBUTION IN PREIRRADIATION LIFETIME FOR 100 20-MIL-BASE SILICON P-N JUNCTION DOSIMETERS

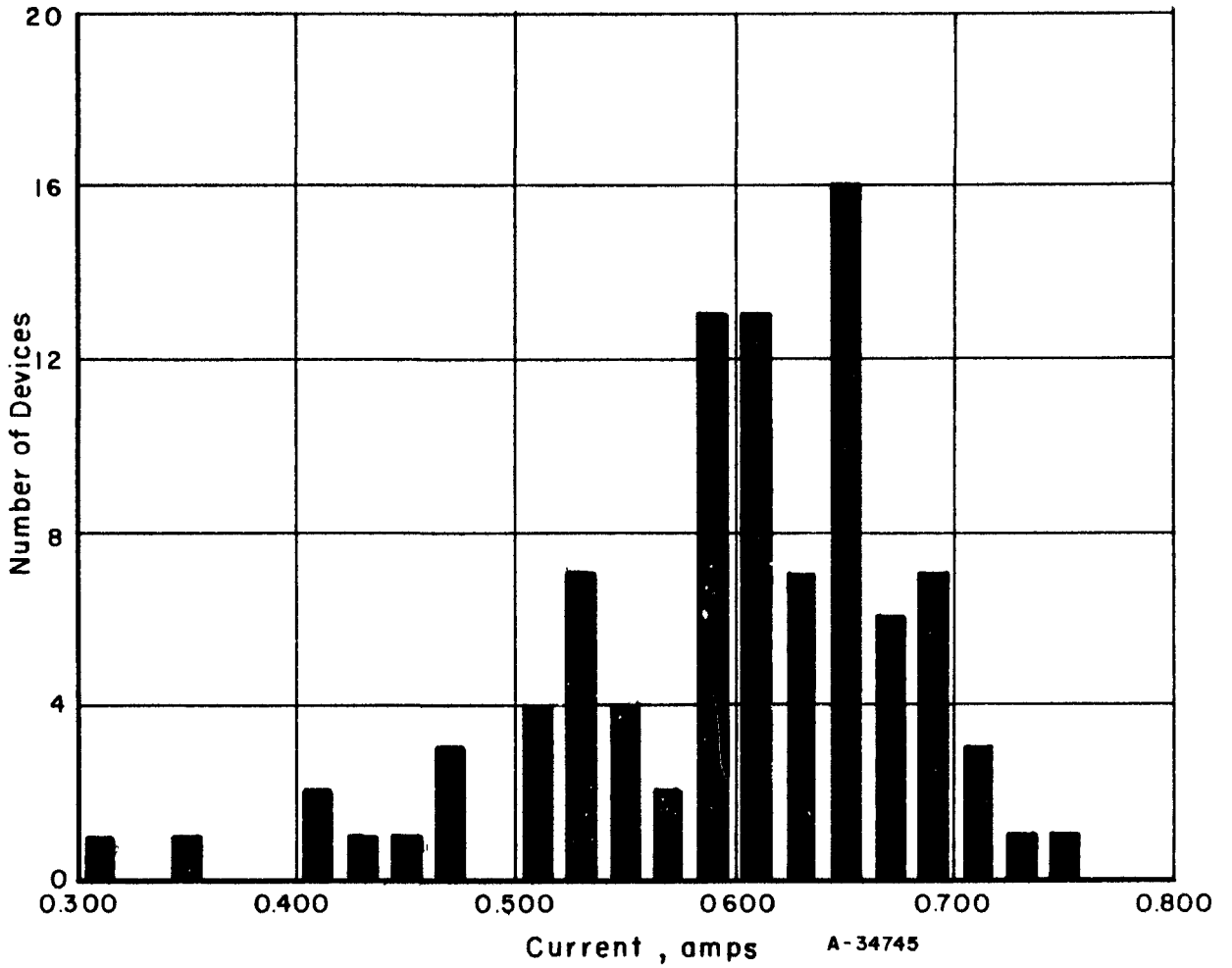

FIGURE 20. DISTRIBUTION IN PREIRRADIATION CURRENT AT V = 0.820 VOLTS FOR 100 20-MIL-BASE SILICON P-N JUNCTION DOSIMETERS

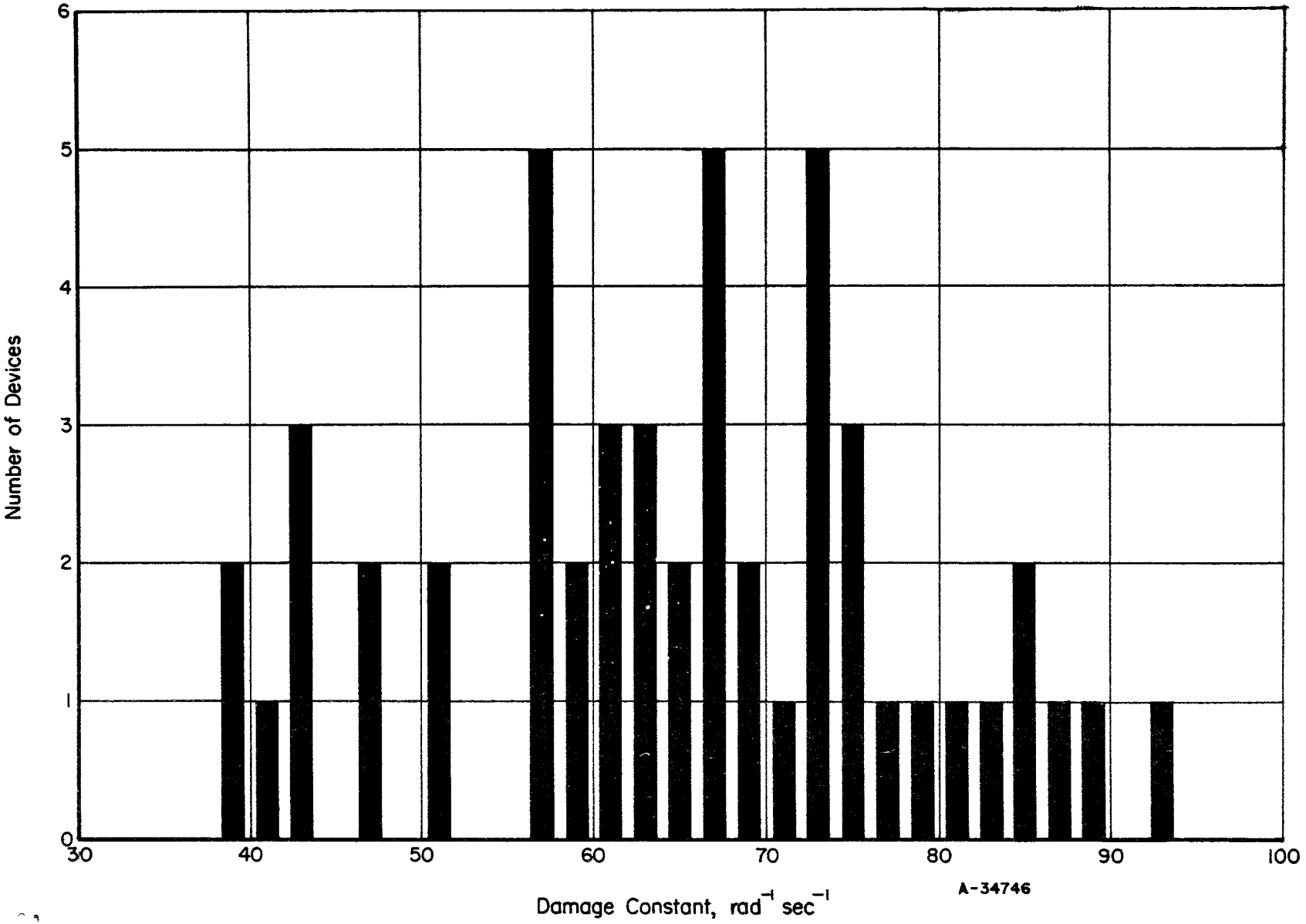

FIGURE 21. DISTRIBUTION IN DAMAGE CONSTANT FOR 50 DOSIMETERS EXPOSED TO A FAST-NEUTRON FLUX OF 712 RADS

the calculated values of the damage constant in the 50 devices exposed to 720 rads, and Figure 22 shows the distribution of the calculated values of the damage constant in the 50 devices exposed to 1240 rads. A comparison of Figures 21 and 22 shows no significant change in the damage constant as a function of radiation dose ($\bar{\alpha}_{720}$ = 65 rad^{-1} sec^{-1}, and $\bar{\alpha}_{1240}$ = 63 rad^{-1} sec^{-1}) which indicates that the calculated values of the damage constant appear not to be dependent on radiation dose.

The degree of uniformity in the forward current at constant voltage after exposure to 720 rads and 1240 rads is shown in Figures 23 and 24. In these figures the value of the current through each device is reported at that voltage which was required to pass 0.500 amp through the device prior to irradiation. This is not to be confused with Figure 20, which shows the distribution in initial current when the same voltage is applied to each device.

Several factors could contribute to the lack of uniformity of radiation response observed in the group of devices referred to above. One of the possible causes of this nonuniformity may be inferred from an analysis of the data depicted in Figure 25. Here the initial lifetime in each of the devices is plotted against the calculated damage constants after exposure to a fast neutron dose of 1240 rads. The data in the figure are grouped about the average value of 65 $rad^{-1}sec^{-1}$ in three boxes, each 20 $rad^{-1}sec^{-1}$ wide, to demonstrate the observed trend that the higher values of the damage constant appear to be associated with lower initial device lifetimes, and that the lower values of the damage constant appear to be associated with the higher initial device lifetimes. At least two possibilities may account for such a trend. One, of course, would be that the damage constant in silicon is reciprocally related to lifetime. Recent work has been reported showing that impurities in silicon, such as oxygen and phosphorus, may interact with radiation-induced vacancies to produce electron states in the forbidden band which may act as recombination centers and, hence, influence the charge carrier lifetime in the material[3, 4]. Since only postirradiation lifetime would be affected by such a mechanism, the calculated damage constant would be influenced by the impurity content of the silicon. In fact, Watkins states[3] that in high purity silicon most defects due to radiation are associated with impurities such as oxygen.

A second possibility is that the damage coefficient may indeed be a constant for a given material. Referring again to Equation (9), page 33, it may be seen that if the observed lifetime in the device were greater than the true lifetime by some factor, k_i, for each device, then the form of the equation would be

$$\frac{\alpha}{k_i} = \frac{\frac{1}{k_i \tau_o} - \frac{1}{k_i \tau_f}}{nvt} \quad . \tag{12}$$

Therefore, the apparent lifetime, $k_i \tau_f$, would be reciprocally related to the apparent damage constant, $\frac{\alpha}{k_i}$. As was stated above, this reciprocal relationship is observed in Figure 25, and may therefore indicate the influence of some factor in the device on the observed lifetime. The magnitude of the difference between initial and final lifetimes after 1240 rads fast neutron irradiation is such that the inherent measurement error* does not significantly influence the trend observed in Figure 25. In general, the spread observed in the current-voltage characteristics and in the calculated damage constant of

*See Appendix A.

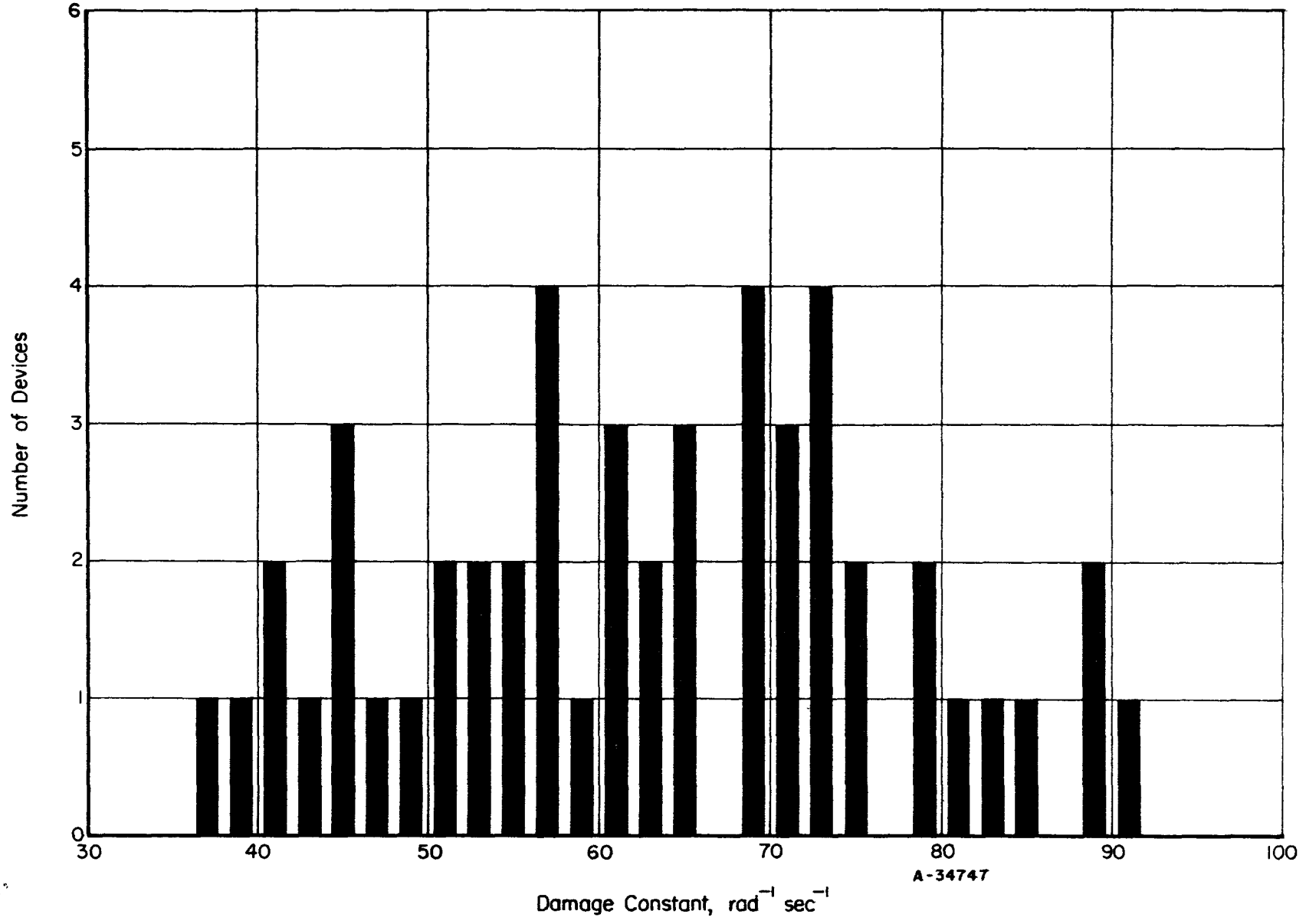

FIGURE 22. DISTRIBUTION IN DAMAGE CONSTANT FOR 50 DOSIMETERS EXPOSED TO A FAST-NEUTRON FLUX OF 1240 RADS

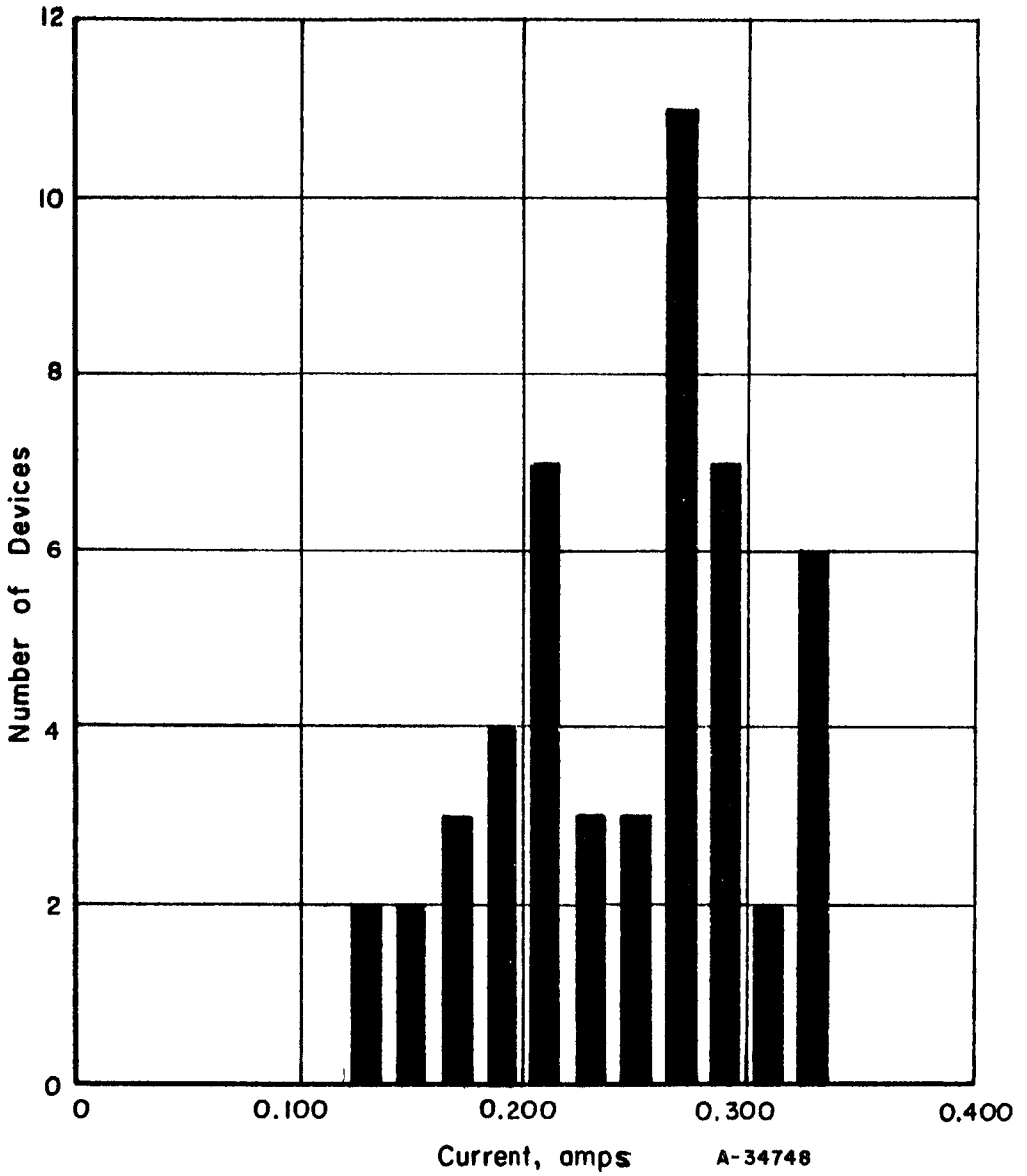

FIGURE 23. DISTRIBUTION IN FORWARD CURRENT AT CONSTANT VOLTAGES (I_o = 0.500 AMP) FOR 50 DOSIMETERS EXPOSED TO A FAST NEUTRON FLUX OF 720 RADS

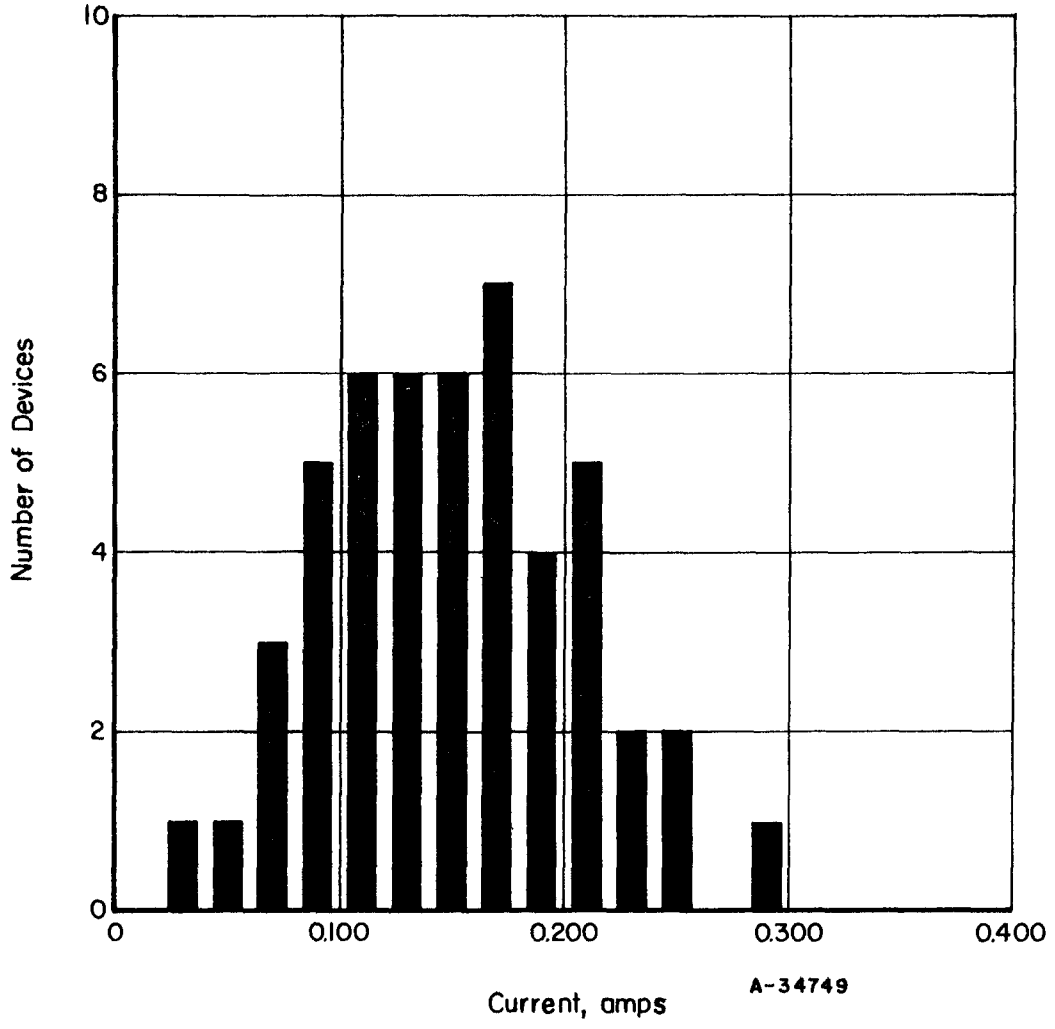

FIGURE 24. DISTRIBUTION IN FORWARD CURRENT AT CONSTANT VOLTAGES (I_O = 0.500 AMP) FOR 50 DOSIMETERS EXPOSED TO A FAST NEUTRON FLUX OF 1240 RADS

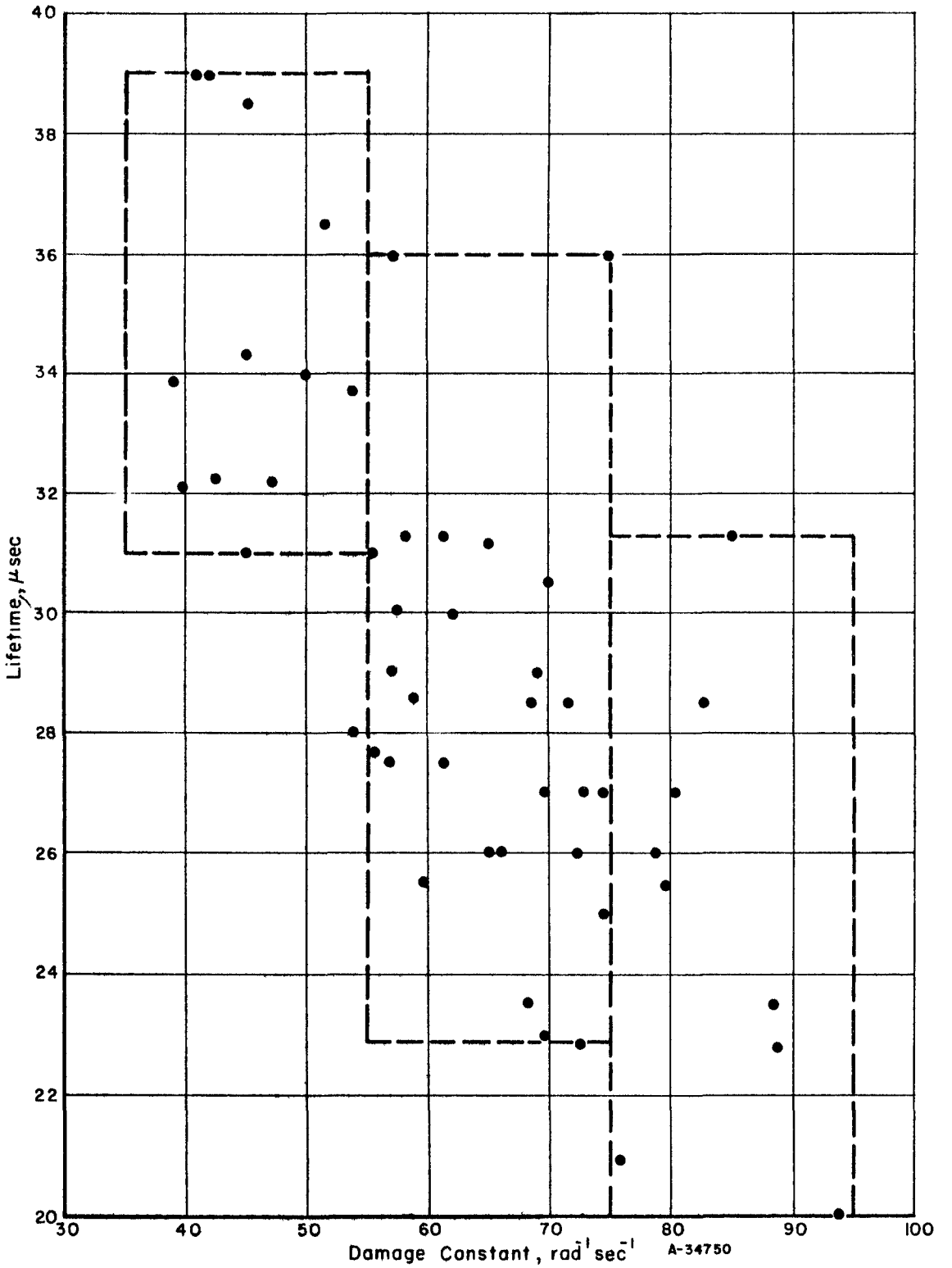

FIGURE 25. PREIRRADIATION LIFETIME VERSUS DAMAGE CONSTANT FOR 50 DOSIMETERS EXPOSED TO A FAST NEUTRON FLUX OF 1240 RADS

this group of devices after exposure to fast neutron irradiation may be associated with variables in the bulk silicon from which the devices were fabricated and/or from variables introduced into the device during the fabrication procedure. Investigation of these possible effects will be required to insure a high degree of reproducibility in the read-out of radiation damage effects.

REFERENCES

(1) Stafeev, V. I., "Effect of the Resistance of the Bulk of a Semiconductor on the Form of the Current-Voltage Characteristic of a Diode", J. Tech. Phys., 28 (8), 1631 (1958).

(2) Bemski, G., and Augustyniak, W. M., Phys. Rev., 108 (7), 645-8 (1957).

(3) Watkins, G. D., Invited Paper, Am. Phys. Soc. Meeting. Detroit (March, 1960).

(4) Sonder, E., and Templeton, L. C., Bull. Phys. Soc., 3 (5), 126 (March, 1960).

PHASE III. DESIGN AND DEVELOPMENT OF A PRACTICAL READ-OUT FACILITY

by

R. K. Crooks

In order to present a complete account in this report of the essential phases of the development of the dosimeter read-out circuitry, certain information which was developed throughout the project and which was described in previous quarterly reports, will be repeated where it can be of benefit.

The original concept of the read-out device for indicating the total irradiation exposure was a small self-contained assembly that would be associated with each p-n junction dosimeter in a complete compact dosimeter package. With such an arrangement, the read-out device, of necessity, would have to be immune to radiation effects. This requirement restricts the kind of components that can be used in the device, as well as its complexity. For instance, the use of transistors and diodes would be questionable. Vacuum tubes might be used; however, low-power consumption is a necessity and, therefore, their use would also be questionable.

It is evident that if a system were adopted in which each individual p-n junction dosimeter is "read out" on a common portable read-out device located in an area not subjected to radiation environment, the problems mentioned would be alleviated considerably and more refined measurements on the dosimeters would be possible. It was, therefore, decided early in the project that the read-out device for consideration at this time would not be restricted to the small self-contained assembly to be associated with each dosimeter, but might be of the common portable read-out device type mentioned. This decision simplified the read-out problem considerably and permitted the consideration of circuitry which would not otherwise have been considered.

Types of Read-Out Measurements

From the discussion in the earlier part of the report, it is evident that two parameters are sensitive to irradiation. These are the forward current at a fixed voltage and the charge carrier lifetime. The charge carrier lifetime is a sensitive and direct measurement of dosage. However, the circuitry required to measure lifetimes of the order of 5 to 50 microseconds is somewhat involved. On the other hand, the resistance of a rectifier under forward bias is a relatively simple, straightforward measurement, even though certain difficulties are present, which will be discussed later. After some consideration of the relative merits and complications of the two types of measurements, it was decided that the major emphasis in this contract would be toward the design of a d-c forward resistance read-out device, with a minor consideration being given to measurement of charge carrier lifetimes. The following describes the work on these two types of read-out devices.

Forward Current

It is evident from the data presented previously in this report that the forward current, or d-c resistance, of a rectifier measured at about 0.85 volts is a very sensitive indicator of radiation exposure. It is also evident from the data that, if the voltage at which the current or resistance is measured is not the same for each measurement, considerable error in the indicated irradiation exposure would result. It is essential, therefore, that the read-out circuit be so arranged that the same voltage be applied to the dosimeter for each measurement, both prior and subsequent to irradiation. This is a basic problem in the read-out instrumentation and one to which considerable thought has been given. It is quite possible to regulate the voltage to the desired accuracy through a conventional transistor-regulated voltage aupply. However, to achieve this degree of accuracy in the voltage applied to the dosimeter by a simple means presents a problem. The severity of the problem can be seen from data taken on a typical dosimeter, as shown in Table 9.

TABLE 9. D-C RESISTANCE VERSUS VOLTAGE

	D-C Resistance, ohms	
V, volts	Zero Rads	1359 Rads
0.90	1.63	2.77
0.85	2.78	4.85
0.80	5.15	8.90
0.75	10.00	17.50

From these data, it can be seen that a change of read-out voltage from 0.90 to 0.85 (about 5.5 per cent change) represents a change of about 1350 rads in the indicated radiation exposure. Assuming a linear relationship, this amounts to a constant error of about 250 rads per 1 per cent change in the read-out voltage. Thus, the read-out error in a measurement taken after an exposure of, say, 1350 rads would be approximately 250 rads, or about 18 per cent, even though the dosimeter measurement voltage was no more than 1 per cent different from the voltage at which the dosimeter was originally measured for calibration. A read-out accuracy of 10 to 20 per cent has been indicated in our conferences as being acceptable. From this, it is evident that it is necessary to regulate the applied voltage to the dosimeter to less than 1 per cent of a given specified value.

It was mentioned earlier that with a transistorized, self-regulating circuit it would be possible to supply the required voltage for measurement. Such a circuit is shown in the Third Quarterly Progress Report. It was decided, however, to concentrate our efforts at this time on the development of a simplified manually-adjusted read-out circuit, as discussed below. The proposed circuit shown in Figure 26 consists of a means for manually adjusting the test voltage impressed on the dosimeter to equal a predetermined voltage established by a second reference circuit. The measured current through the dosimeter is then an indication of the radiation exposure. Slight modifications are incorporated in the proposed circuit over that reported in the Third Quarterly Progress Report.

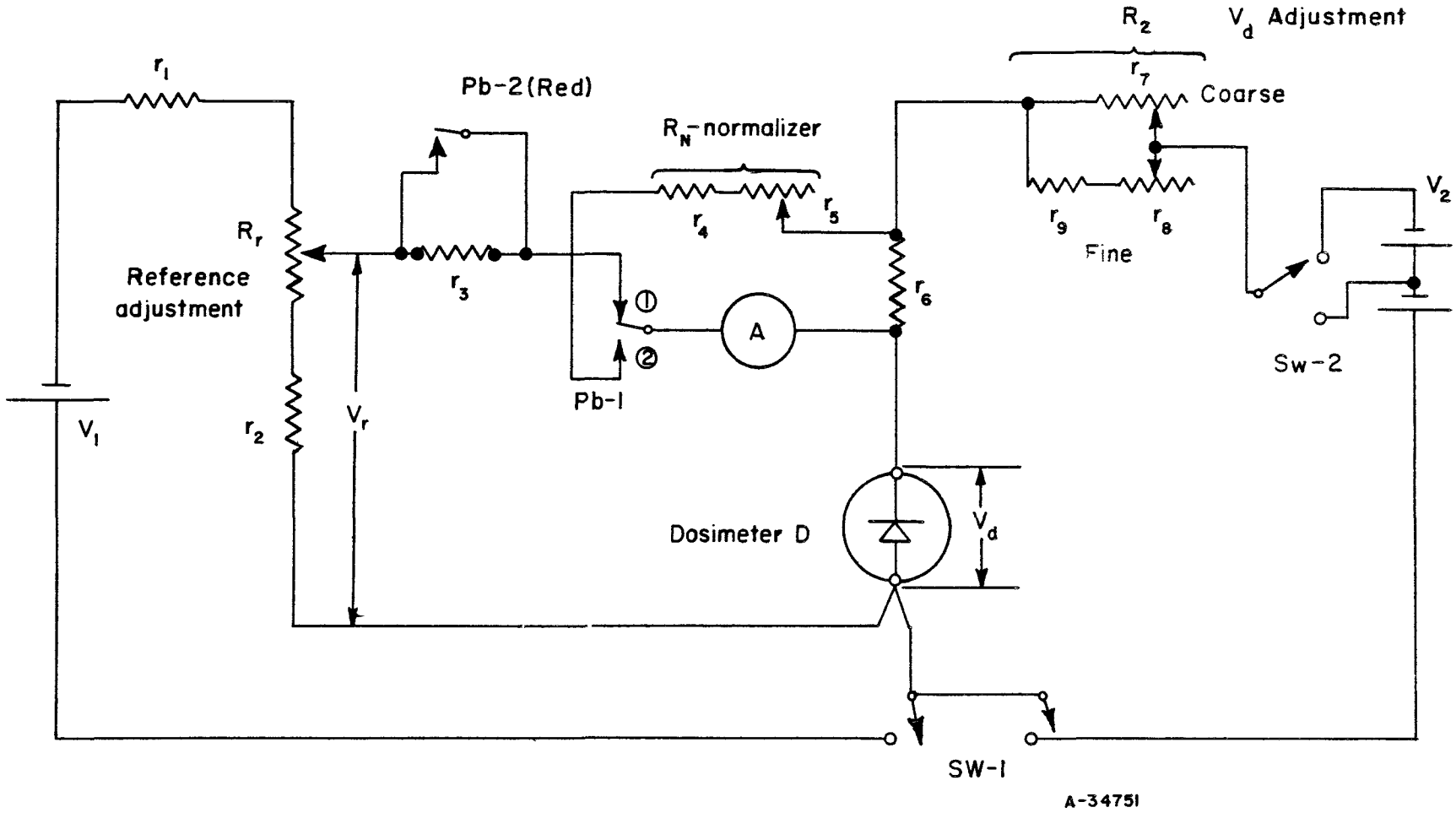

FIGURE 26. DOSIMETER READ-OUT CIRCUIT

Forward current, V_d=K.

The precise reference or test voltage, V_r, at which the forward current measurement of the dosimeter, D, is to be made is established by the mercury cell, V_1, and can be adjusted to the desired voltage by means of the potentiometer, R_r. The voltage, V_d, impressed across the dosimeter may be adjusted by means of the potentiometer network, R_2. With the push-button switch P_b-1 in position 1, the microammeter, A, indicates a current which is proportional to the difference between the voltage, V_d, across the dosimeter and the reference voltage, V_r. When R_2 is adjusted such that V_d is equal to V_r, the microammeter will read zero. At this point the dosimeter voltage is equal to that of the reference, V_r. With push-button P_b-1 in position 2, the microammeter then reads the current flowing through the dosimeter, the major part of the current being shunted around the microammeter by the resistance r_6. The resistance r_3 provides series current limiting in the microammeter circuit during the coarse adjustment of the dosimeter voltage. This resistor can be shorted by depressing P_b-2 after the dosimeter voltage has been adjusted approximately equal to the reference voltage. The potentiometer network, R_2, is actually two potentiometers, r_7 and r_8, arranged for coarse and fine adjustment of the voltage across the dosimeter.

From the data presented earlier in this report, taken on a number of dosimeters, it is evident that there is some variation in the preirradiation current. The adjustable resistance, R_N, is therefore provided to permit adjustment of the reading on the microammeter to full scale (100 per cent) for each individual dosimeter under the initial preirradiation condition. With this setting of R_N for each individual dosimeter, it is then possible to determine the percentage change in forward current due to subsequent irradiation exposure. It should be pointed out here that because of this variation in the individual dosimeters, it is necessary to "tag" each dosimeter in some manner that will permit the setting of the resistance R_N to the proper point corresponding to the initial dosimeter current reading. The switch Sw-2 is provided for operation of the meter on either high or low range, depending upon the degree of irradiation being measured. The low range is achieved by the use of only one of the mercury cells.

A laboratory model of the read-out device, shown in the photograph in Figure 27, was constructed in order to determine the practicability of the proposed circuit. Information on the major components used in the model are indicated below.

V_1-1 Mallory RM-4R Mercury Cell

V_2-2 Mallory RM-42R Mercury Cells

A-1 Simpson #1329, 0-100 microammeter

r_1-1 400 ohm 5 watt fixed resistor

r_2-1 700 ohm 5 watt fixed resistor

r_3-1 22,000 ohm 1 watt fixed resistor

r_4-1 1000 ohm 1 watt fixed resistor

r_5-1 WP-3000 ohm IRC wire wound control

r_6-1 1 ohm 5 watt fixed resistor

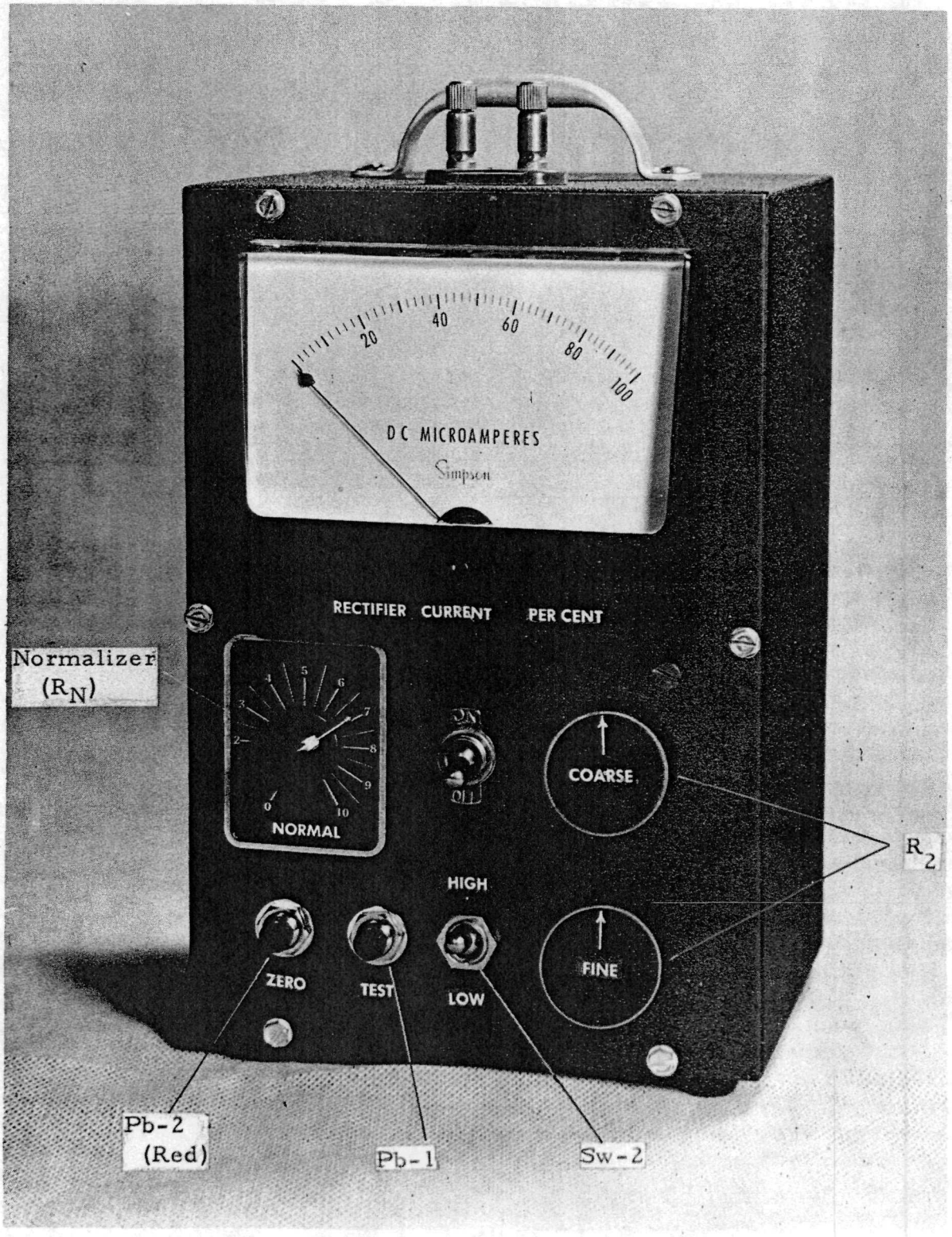

FIGURE 27. LABORATORY MODEL OF READ-OUT INSTRUMENT

r_7-1 M15DK 15 ohm Mallory wire wound control

r_8-1 WP-50 ohm IRC wire wound control

r_9-1 30 ohm 1 watt fixed resistor

R_r-1 WP-250 ohm IRC wire wound control.

All resistors are wire wound except r_3 and r_8 which are carbon composition.

Operating Procedure

Prior to the making of any measurements, the reference voltage V_r will have been set to some predetermined voltage, at which the measurements are to be made, by the adjustment of R_r. This adjustment is inaccessible from the outside of the meter case and, therefore, does not enter into the read-out procedure. It was mentioned earlier that the adjustable resistance R_N, Figure 26, is provided in order to establish an initial dosimeter current reading with which subsequent dosimeter current measurements could be compared. This resistance is labeled "Normalizer" in the photograph of Figure 27. In practice, each dosimeter would be tagged in a manner which would permit the setting of the Normalizer at the point on the indicator dial corresponding to the initial (pre-irradiation) current through the dosimeter. The calibration of this control setting over a range of dosimeter current for full scale meter reading is shown in Figure 28.

With the "Normalizer" set at the proper position, the dosimeter may be inserted in the test holder provided and the off-on switch placed in the "on" position. Since both push buttons, P_b-1 and P_b-2, are normally in position 1 (Figure 26), the meter will read an unbalanced current. This current is then reduced to near zero by adjustment of the coarse "Zero" control. When the meter is reduced to a low level, P_b-2 (red) may be depressed, thus increasing the sensitivity of the meter circuit. A finer adjustment, then, is achieved by further adjustment of the "fine" control. When the meter reading has been reduced to as near zero as possible, P_b-1 should be depressed, at the same time releasing P_b-2. The reading on the meter will then indicate the forward current through the irradiated dosimeter as a percentage of the initial current under preirradiation conditions. The percentage reduction in forward current then is related to the irradiation dose. This relationship between percentage reduction in forward current and the dose will need to be determined through further study of a large number of dosimeter samples.

No attempt has been made to miniaturize the laboratory version of this read-out circuit, since the main objective was to prove the practicability of this method of measurement. The resistors used throughout the meter are commercially available, non-precision resistors. In a final version of the read-out device, precision low temperature-coefficient resistors would be used. Mercury cells, for the reference and the main power source, were chosen for their long-life and constant-voltage characteristics and should provide a satisfactory source of energy for the final read-out device.

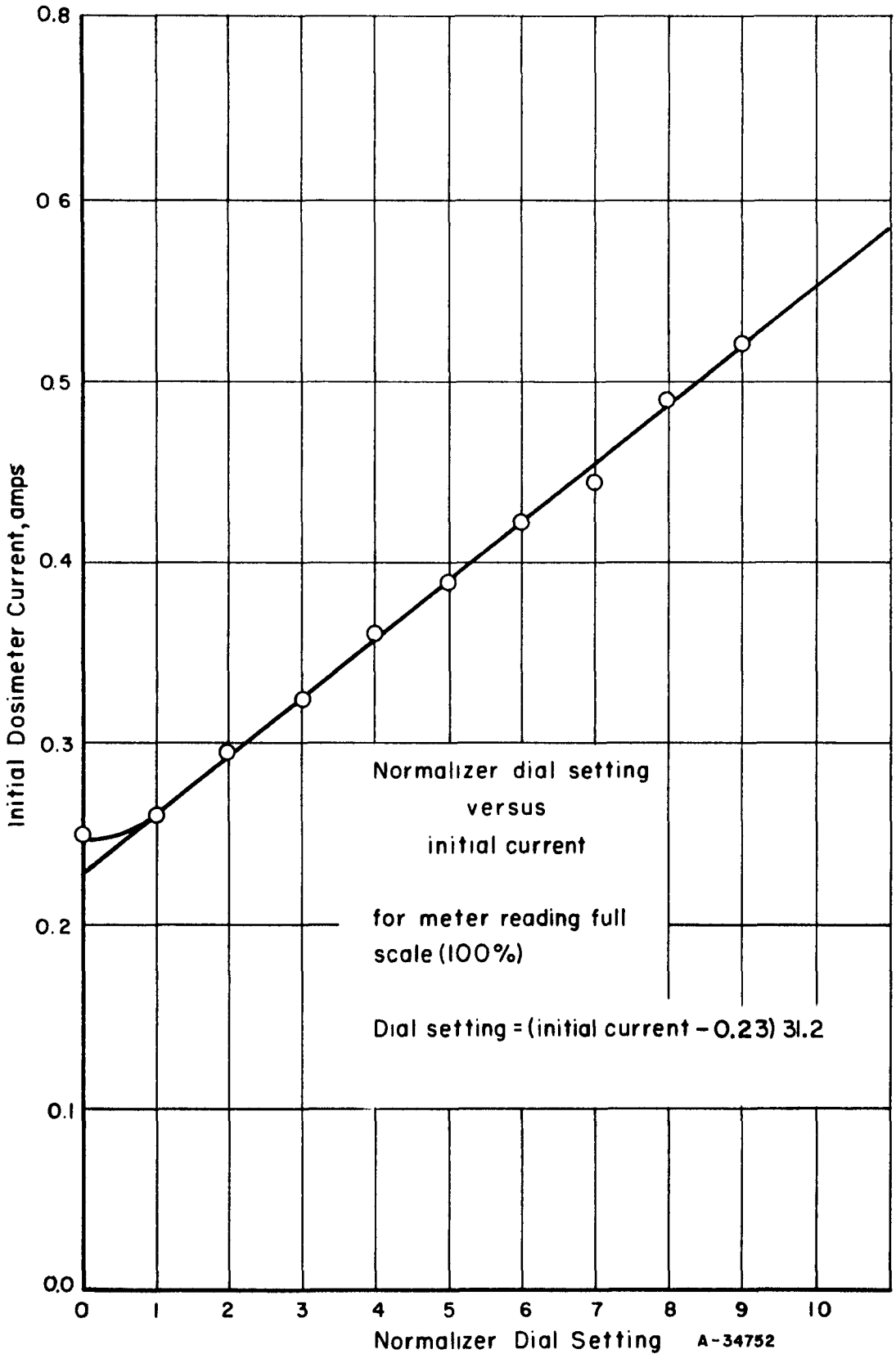

FIGURE 28. NORMALIZER DIAL SETTING (r_5 -FIGURE-28)

Read-Out Device Tests

A number of sample dosimeters were selected from the group measured by conventional means, as indicated by curve data, and were tested to determine the accuracy of the read-out instrument. The results of these tests are shown in Table 10. In each case the "Normalizer" was set at the point indicated by the calibration curve, Figure 28, for the initial (preirradiation) current of the dosimeter under test. The results of the tests, as tabulated below, show good agreement between the change in forward current (per cent of initial current) measured in the conventional manner and the change indicated by the read-out instrument. A maximum difference between the two measurements is 2.8 per cent, excluding device 7I which appears to be defective.

TABLE 10. READ-OUT DEVICE TESTS

All measurements taken at a dosimeter voltage of 0.825 volts.

	Conventional Measurement, amps			Read-Out Device	
Dosimeter	Initial – No Rads	Irradiated – 1242 Rads	% of Initial	Normalizer Setting	% of Initial
19A	0.500	Not irradiated	100	8.4	100
5I	0.450	0.125	27.8	5.6	28.5
6I	0.390	0.123	31.6	5.0	32.5
7I	0.310	0.040	12.9	2.2	13.9
8I	0.470	0.165	35.2	7.5	35.5
10I	0.380	0.125	33.0	4.7	32.5

Charge Carrier Lifetime

Although no great amount of effort has been put forth in this contract toward the detailed consideration of a means of measuring charge carrier lifetime as a read-out parameter, it is believed that the idea shows enough promise to warrant some mention and perhaps further consideration. The possible means of achieving this measurement was described in the Third Quarterly Report, and for completeness of this report, will be repeated here.

The characteristic decay of the voltage appearing across the p-n^+ junction of the dosimeter after an impressed voltage has been removed is shown in Figure 29. The slope of the linear portion of the characteristic over the time interval M, following the initial rapid decay, has been used as a measure of the charge carrier lifetime. The circuit proposed measures this slope and produces a read-out on an indicating meter that would be calibrated in lifetime.

A functional block diagram of the proposed lifetime read-out instrument is shown in Figure 30. A square-wave voltage of suitable amplitude with a period of about 400 microseconds is impressed on the dosimeter, as shown. The voltage-decay characteristic of the junction during each "off" time, as indicated on the diagram, is differentiated. However, the differentiator is activated by a delay circuit, so that it functions only

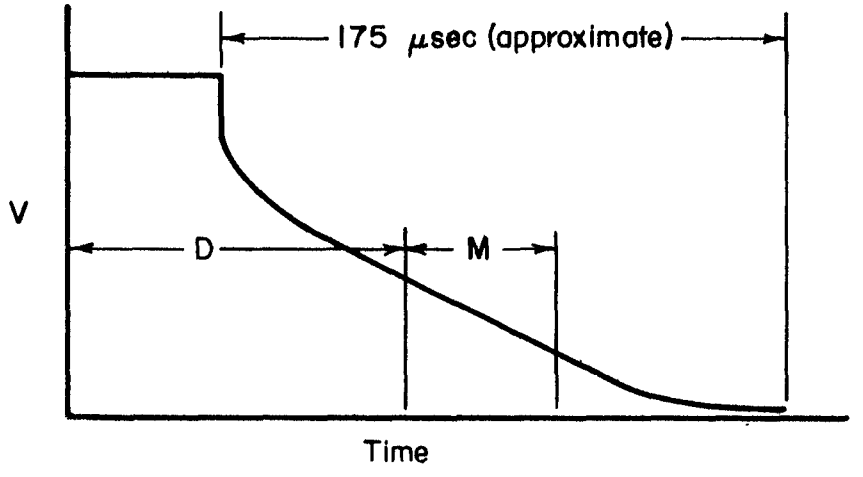

FIGURE 29. TYPICAL OPEN-CIRCUIT VOLTAGE-DECAY CHARACTERISTIC OF FORWARD-BIASED P-N JUNCTION DOSIMETER

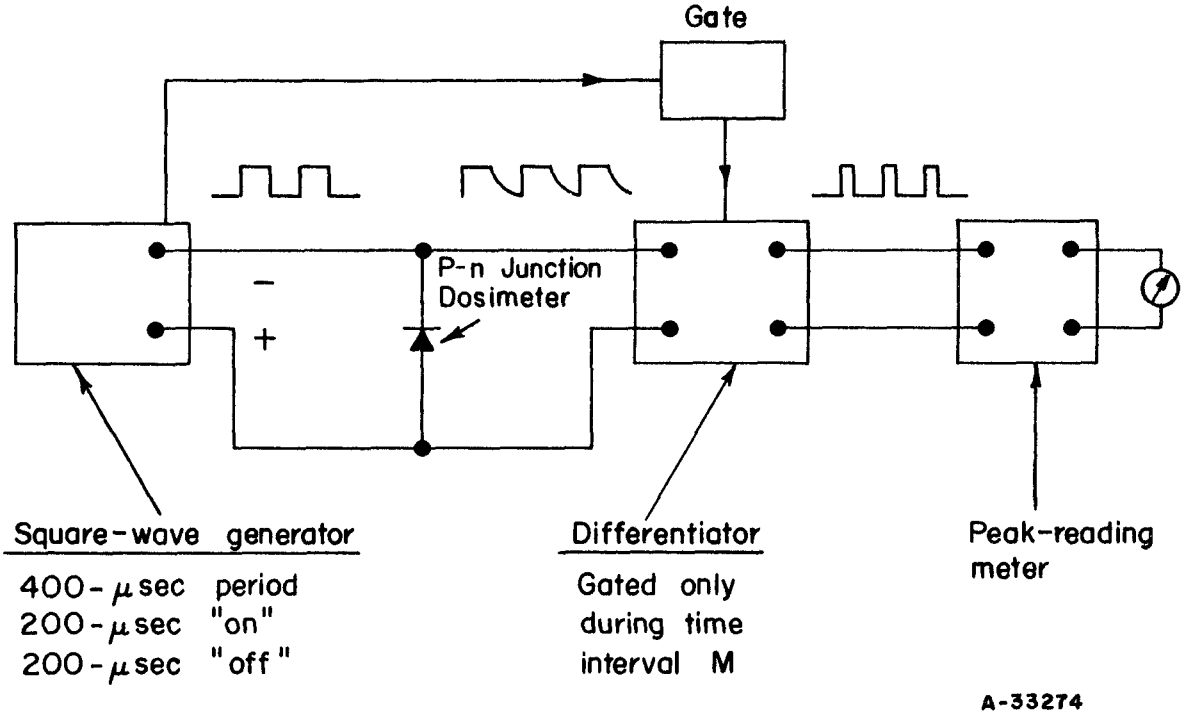

FIGURE 30. LIFETIME MEASURING READ-OUT CIRCUIT

after a time interval D and only during the interval M (Figure 29), which may be about 50 to 75 microseconds. Therefore, the output of the differentiator will be a series of pulses of constant duration, M, whose amplitude is proportional to the slope over the interval M and, hence, proportional to lifetime.

The accuracy to which the exposure can be read on such a system is limited mainly by the accuracy to which the peak value of the pulses can be read. This should be about 5 per cent over the range of exposures.

Although the detailed design of this circuit has not been worked out as yet, no great obstacles are anticipated, since all of the functions required can be accomplished with conventional circuitry. It is estimated that from six to ten transistors would be required to perform the functions indicated and that the instrument could be powered with several mercury cells.

Major Read-Out Problems

Irrespective of the type of read-out method finally adopted, a number of problems must be resolved. A relationship representing all dosimeters must be established between the percentage change in forward current, or lifetime, as the case may be, and radiation. To determine such a relationship, a statistical study of many samples will be required. The effect of temperature on the forward current of a dosimeter must be compensated for in some manner in the read-out device. It is not evident at this time how this might be accomplished conveniently. Since it is evident that there will be a difference in the initial forward current in the dosimeters, it is necessary to establish some means of "tagging" each dosimeter in order to take account of this difference in subsequent measurements. A possible means has been described in the Second Quarterly Report. It consists of incorporating a small adjustable resistor with each dosimeter, perhaps both on a small card. Initially, before radiation exposure, the resistance of the resistor could be adjusted to match that of the dosimeter at the specified test voltage. After exposure, the change in the resistance of the dosimeter from the initial value could be determined by a comparison measurement with the resistor. The resistor would, of necessity, be a radiation immune film-type that could be trimmed at the initial reading.

Conclusions

From the work in this contract, it is evident that a practical read-out device can be developed which will read the forward current at a specified constant voltage through a dosimeter to the desired degree of accuracy. The laboratory model of the read-out device, while not of the optimum design, nevertheless indicates that such a read-out device is practical and reliable. It is evident that the transistorized regulating circuit mentioned could also be developed into a simple read-out device requiring no manipulation on the part of the observer, since it would permit the direct reading of the percentage change in the dosimeter current and, therefore, might be more acceptable from an operator's viewpoint. In principle, the charge carrier-lifetime-measuring circuit is sound. However, it will be considerably more complicated than either of the other two circuits mentioned. It would, however, permit the measurement of a parameter which is more directly related to radiation dose than is the forward current.

Further work on this type of dosimeter should involve the selection of a read-out device based on one of the three methods mentioned and should include consideration of the solutions to the problem mentioned related to the characteristics of the device.

PHASE IV. DEVELOPMENT AND PROCESSING TECHNIQUES FOR THE FABRICATION OF SILICON P-N JUNCTION DOSIMETERS

by

O. J. Mengali

The silicon p-n junction dosimeters were fabricated using a "two-step" diffusion process. The processing steps described are presented in chronological order, starting with the silicon crystal wafering and continuing through to the final assembly of the complete device.

For the purpose of continuity, factors that are pertinent to each step of the process are incorporated under the particular step being discussed. At several points during processing, qualitative examinations may be performed on the silicon wafers to insure proper processing conditions; these include p-n junction depth determinations and surface conductivity.

The utilization of a wide-base silicon diffused rectifier as a sensitive fast-neutron dosimeter, requires that the high level injection lifetime of the device have a value commensurate with the device base width. Therefore, the retention of the minority carrier lifetime in processed silicon wafers must be maintained. Since high-temperature diffusion techniques seriously degrade the minority carrier lifetime in processed silicon, it is necessary to introduce lifetime retention treatments during processing to obtain adequate lifetimes in the device. Several methods have been used during the present state of development of the dosimeter; these include: (a) slow cooling of diffused wafers following the high-temperature diffusion cycles, (b) gettering of impurities which introduce recombination centers by the use of metallic nickel, and (c) the combination of both gettering and slow cooling.

Boron trichloride has been used exclusively as a boron diffusant source in the formation of the p-base region. Previous investigations have shown that B_2O_3, used as a diffusant source in the processing of diffused silicon rectifiers, introduces a high degree of scatter in the forward characteristic and results in low rectifier yield. Therefore, the use of B_2O_3 as a diffusant source is not recommended. Rather, BCl_3 is recommended as a diffusant source.

Equipment requirements for fabricating the dosimeter are not included in the process description, since most manufacturers of diffused silicon devices are familiar with and adequately equipped for such diffusion-type processes.

During the course of the project, several investigations were undertaken with the aim of establishing the necessary controls on initial material characteristics, geometry factors, and process conditions to obtain dosimeters having adequate lifetimes and reproducible forward current-voltage characteristics to give the maximum sensitivity to low neutron dose. The results of these investigations (see the Third Quarterly Report, February 14, 1960) were helpful in establishing device geometry (base width), and initial bulk silicon properties.

One large group of devices was made to determine the statistical variations due to processing. As a result, a large number of dosimeters were available for radiation

studies. Several process and material variations were introduced. The preliminary data on the devices prior to radiation are discussed following the detailed process description.

Diffusion of Phosphorus and Boron Into Silicon

In the fabrication of diffused-silicon p-n junction dosimeters having an n^+-p-p^+ structure, phosphorus from P_2O_5 is used to form the n^+ region. For the p^+ region, elemental boron from BCl_3 is used.

The surface solubility of P_2O_5 in SiO_2 provides essentially an infinite reservoir of phosphorus which diffuses into silicon according to established laws of diffusion. The solubility (several per cent of phosphorus in silicon) results in a high surface concentration of phosphorus (C_o = 10^{20} to 10^{21} atoms cm^{-3}). Similar conditions hold true in the case of boron. Under the conditions stated, the solution of the diffusion equation leads to the following relationship:

$$C = C_o \operatorname{erfc}\left[\frac{x}{(4Dt)^{1/2}}\right] , \qquad (13)$$

where

C = concentration at any depth in cm^{-3}

C_o = surface concentration in cm^{-3} ($x = 0$)

x = depth in cm

D = diffusion constant in $cm^2\ sec^{-1}$

t = time in sec

erfc = the complementary error function (1-erf).

The diffusion constant D, as a function of temperature, and the surface concentration C_o, for both phosphorus and boron have been determined.[1] The value of D, as a function of temperature, is given by

$$D = D_o \exp(E/RT) , \qquad (14)$$

where

D_o = 10.5 $cm^2\ sec^{-1}$ for both P and B

E = 85,000 cal

R = gas constant

T = absolute temperature.

With the above two expressions, it is possible to compute the depth of the p-n junction for any time and temperature. Figure 31 is a plot of the diffusion coefficients, for both phosphorus and boron, against the reciprocal absolute temperature.(1)

Figure 32 is a plot of the computed phosphorus concentration as a function of distance into silicon for phosphorus diffusion times of 16 and 32 hours at a temperature of 1230°C. These times and temperatures are normally used in the two-step diffusion process for fabricating diffused silicon diodes and power-type rectifiers. However, for the p-n junction dosimeter, the 16-hour period was used exclusively.

The dotted horizontal lines in Figure 32 represent the charge-carrier concentrations for the various resistivities in p-type silicon. The intersection of these lines with the phosphorus concentration curves represents the depth of the n^+-p junction for that resistivity material. At this point, the donor and acceptor concentrations are said to be equal.

Figure 33 is a similar plot for the boron concentration as a function of distance for a diffusion time of 2 hours at a temperature of 1150°C. Again, as in the case for phosphorus, the p-p^+ junction is at the intersection of the boron concentration curve and the dotted line corresponding to material of a given resistivity.

Several important factors are associated with the use of the curves given in Figures 32 and 33:

(1) The surface concentration of the diffusant must be maintained. If the diffusant is depleted at the surface, then the carrier-concentration curves shift to the left, resulting in a shallower junction, and possibly a nonplanar junction, which would lead to nonuniform injection of carriers.

(2) Lowering of the initial resistivity of the starting silicon results in decreased junction depths. Changes in bulk resistivity, by thermal conversion effects, can result in the formation of secondary rectifying junctions in the base region, thereby causing variations in the base width and adversely effecting conductivity modulation. Lowering the surface conductivity to a less degenerate condition also results in a higher contact resistance, thereby limiting the forward current through the device.

Details of Processing Steps

Figure 34 is a block diagram showing the chronological order of the steps in processing silicon wafers to the final, diffused silicon p-n junction dosimeter. The diagram is included to serve as a reference guide during the detailed description of the steps.

It will be noted that several alternative approaches in processing are shown. For example, the addition of a temperature program gettering step is alternatively added following Step 4, the phorphorus-diffusion step. This variation was included to maintain a reasonable charge-carrier lifetime in the completed dosimeter.

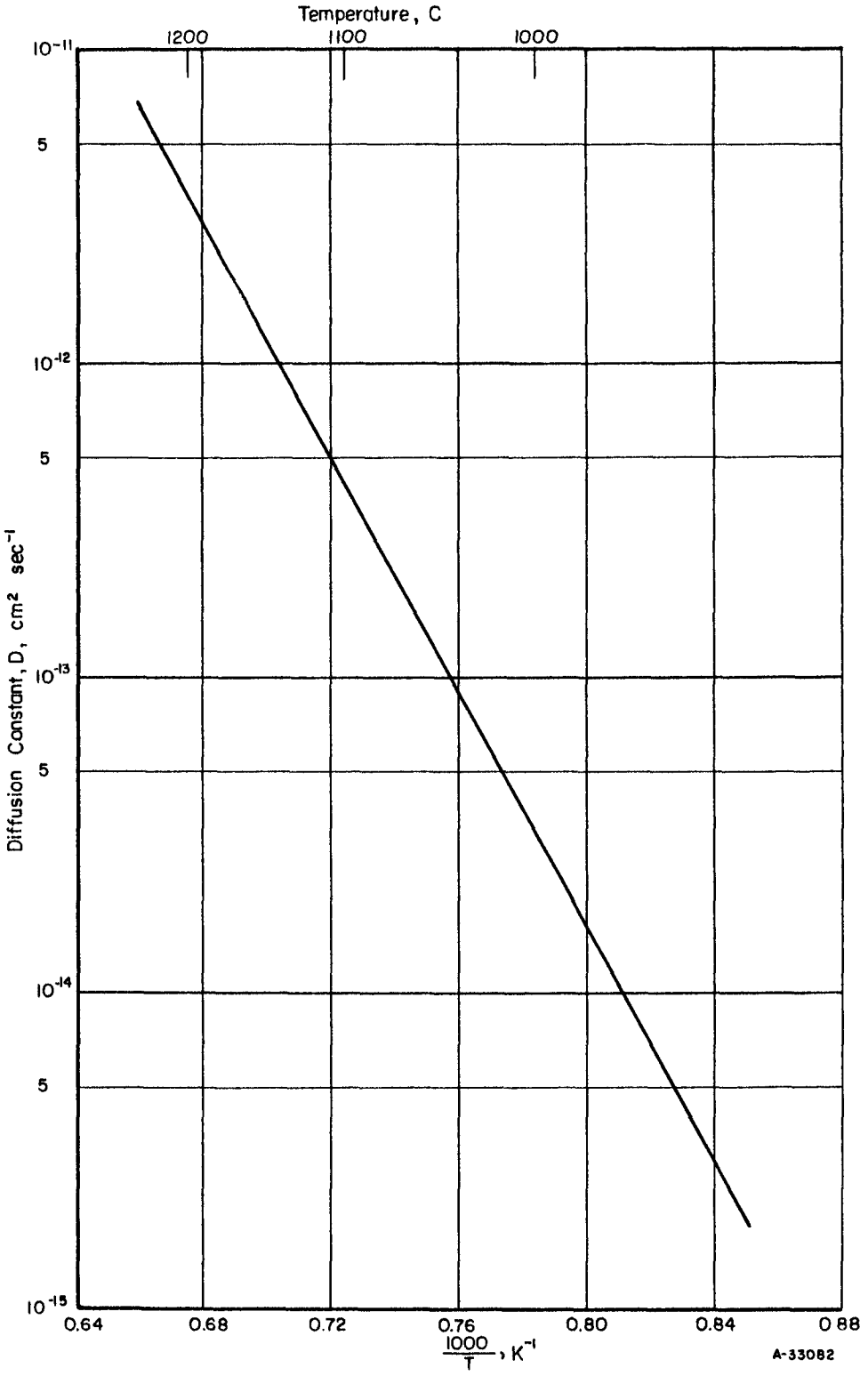

FIGURE 31. DIFFUSION COEFFICIENTS FOR BORON AND PHOSPHORUS IN SILICON AS A FUNCTION OF RECIPROCAL ABSOLUTE TEMPERATURE

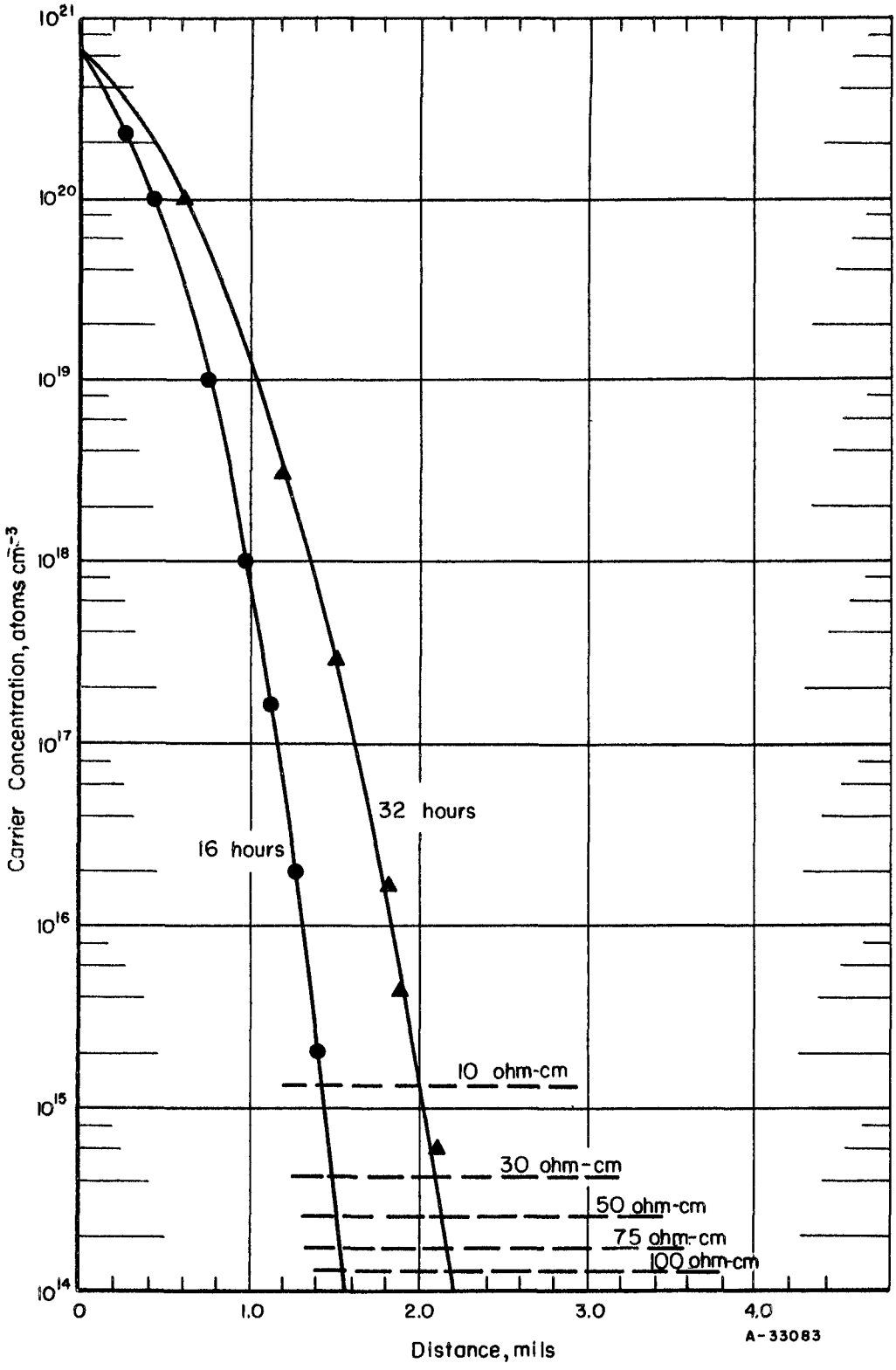

FIGURE 32. CARRIER CONCENTRATION AS A FUNCTION OF DISTANCE FOR PHOSPHORUS DIFFUSED INTO P-TYPE SILICON AT 1230°C

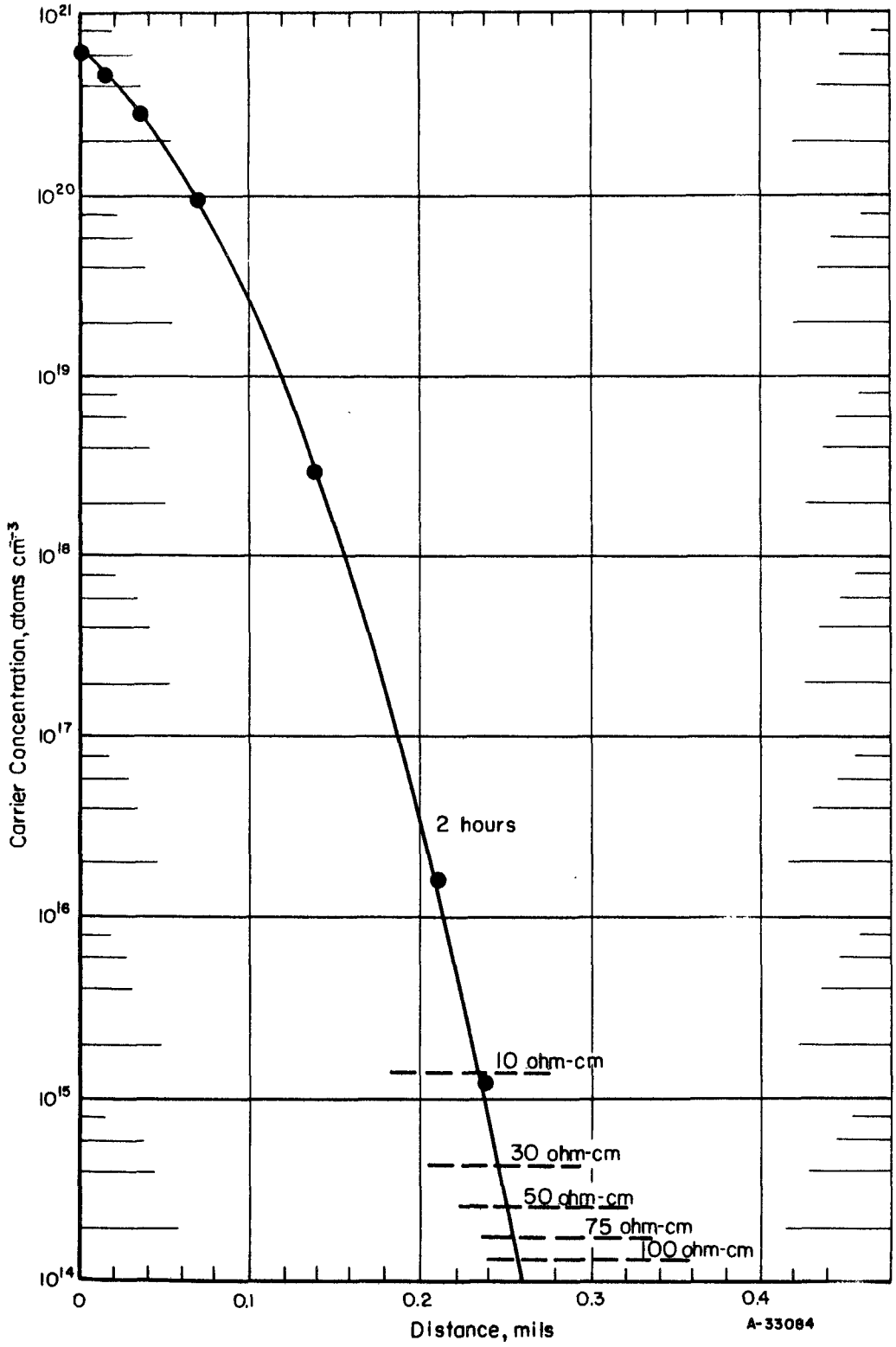

FIGURE 33. CARRIER CONCENTRATION AS A FUNCTION OF DISTANCE FOR BORON DIFFUSED INTO P-TYPE SILICON AT 1150°C

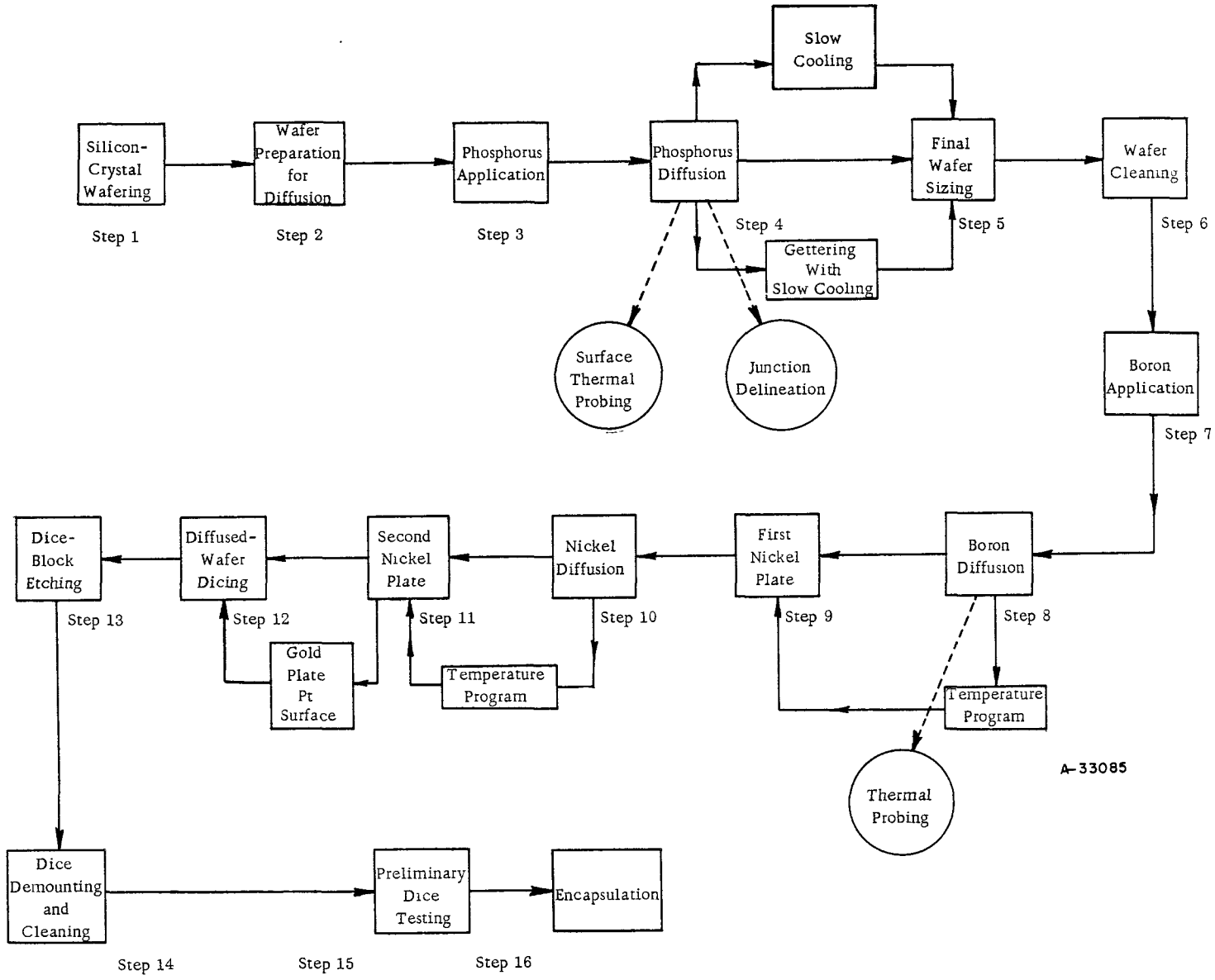

FIGURE 34. BLOCK DIAGRAM OF PROCESSING STEPS FOR SILICON P-N JUNCTION DOSIMETERS

Junction delineation and surface thermal probing are qualitative checks of the process and are incorporated under the phosphorus-diffusion step. Temperature programming was used following the phosphorus-, boron-, and nickel-diffusion steps. Surface thermal probing is again used as a qualitative check following boron diffusion.

Step 1. Silicon-Crystal Wafering

Silicon crystals, as purchased or grown by the user, are cut into wafers normal to the growth plane. Although crystal orientation has not been known to effect diffuse-junction rectifier characteristics, wafering the crystal along a known plane is recommended. Usually the (111) plane has been employed, but other orientations can be used. Anisotropic diffusion of impurities into silicon has not been observed.

Silicon-crystal wafering is accomplished with a diamond cutting saw. Cut-off machines for silicon and germanium are available from several sources. It is recommended for good cutting facilities be used to minimize cutting time, wafer breakage, and wafer "wedging". Subsequent mechanical operations become time consuming if excess wedging occurs.

The wafer thickness will depend largely on the thickness of device being fabricated. For the dosimeters, wafer thicknesses of .030 inch or greater are recommended.

Cutting, and subsequent mechanical operations, damage the silicon to depths of the order of 0.004 inch. It is usually necessary to remove this damaged layer by etching prior to processing. For the silicon dosimeters, this may not be necessary, since they are operated in the forward direction only. However, yield and uniformity of device characteristics can be influenced by mechanical damage. Damage can also contribute to nonplanar junction formation, which leads to nonuniform current injection. Therefore, it is recommended that the damaged layer be removed.

Step 2. Wafer Preparation for Diffusion

Silicon wafers, as sliced, are lapped flat on one surface only. A 600- to 800-grit surface finish is desired. This is accomplished with SiC lapping compounds and a lapping facility, such as "Lapmaster".* For polarity identification purposes, a small sandblasted depression is placed on the lapped surface near the edge of each silicon wafer. The size of the lapping equipment is governed by the production rate desired. After the lapping and identification code operation, the wafers are treated in the following manner:

(1) Rinse wafer in hot running tap water for 2.0 minutes

(2) Rinse in hot distilled water for 2.0 minutes

(3) Etch wafers in nitrite etch solution for 30 seconds

(4) Rinse in hot distilled water for 2.0 minutes

(5) Store wafers in C.P. acetone.

*Manufactured by The Crane Packing Company, Morton Grove, Illinois.

Storing of wafers in acetone is not necessary if processing is to proceed without delay. The composition and conditions for using the nitrite etch are given in Appendix B.

Step 3. Phosphorus Application

The two-step diffusion process as originally published has been modified by the addition of a phosphorus application step prior to the diffusion period. Several advantages have been realized by the introduction of this application step:

(a) Large numbers of silicon wafers can be processed in a normal day's operation, thereby allowing some flexibility in production of devices

(b) The phospho-silicate glass formed on the surface acts as a reservoir for the phosphorus during the diffusion period

(c) The thin glassy layer formed during the diffusion cycle serves as a protective mask against boron during its diffusion

(d) A more uniform phosphorus concentration is maintained at the diffusing surface, thereby aiding the formation of more planar and uniform p-n junctions.

The conditions and procedure used for the phosphorus application step are given below.

Conditions.

P_2O_5 temperature	200°C
Quantity of P_2O_5	2-3 grams
Application temperature	1150°C
P_2O_5 carrier gas	Argon or nitrogen
Carrier-gas flow rate	1500 cc/min
Application time	20 minutes

Procedure.

(1) Load the clean dry silicon wafers into a quartz carrier tray in the vertical position. (Do not allow wafers to mask one another.)

(2) Insert loaded tray from the open end of reaction tube and move it into the center of the furnace.

(3) Soak for 20 minutes and pull tray slowly into the cool, open exhaust end of furnace.

(4) Allow 10 to 20 minutes cooling time before removing from furnace.

(5) Transfer wafers into clean, dry petri dish.

The quantity of P_2O_5 suggested was found to be adequate for an 8-hour day.

The P_2O_5 source can be placed in the closed end of the reaction tube at the appropriate temperature if a separate furnace heater for the P_2O_5 is not available. Back diffusion of water vapor into the hot zone is allowed by the open exhaust end of the reaction tube. Water vapor enhances the phospho-silicate glass formation at the silicon-wafer diffusing surface. A visual examination of treated wafers will indicate the quality of the formation, using the color order of the reflected light from the surface. Occasionally, it is necessary to introduce water vapor into the system to insure the proper glass formation. This is accomplished by passing the carrier gas through a distilled-water bubbler maintained at 70°C.

The open end of the furnace tube is exhausted into a hooded duct. For the first several minutes, considerable P_2O_5 vapor will be discharged from the reaction tube. This is normal and is not an indication of faulty conditions.

Step 4. Phosphorus Diffusion

To minimize losses of elemental phosphorus from the dissociation of the phospho-silicate composition, oxidizing conditions are maintained during the diffusion cycle. This is accomplished by allowing the furnace tube ends to remain open to ambient atmosphere. Under an inert or reducing atmosphere, the glassy phospho-silicate layer will decompose at the high diffusion temperature and, as a result, a nonuniform concentration of diffusant occurs at the diffusing surface. Such a condition causes the formation of a quartz like surface layer which is difficult to remove in the cleaning step prior to nickel plating. Also, nonplanar junctions, as well as nondegenerate surfaces are obtained. The latter contributes to high contact resistance at the silicon-metal interface.

The diffusion cycle is performed as follows:

Conditions.

Diffusion temperature	1230°C
Diffusion time	16 or 32 hours
Atmosphere	Air

Procedure.

(1) Load silicon wafers, to which phosphorus has been applied, into a quartz carrier tray. (Precautions against masking are not necessary in this step.)

(2) Insert carrier tray into the uniform hot zone of the diffusion furnace.

(3) Diffuse for the time chosen (16 or 32 hours).

(4) Cool in furnace following the diffusion period.

(5) Remove tray from furnace and store diffused wafers in clean, dry petri dish.

The system described offers a simple means of processing a sizeable number of wafers simultaneously, thereby allowing some regulation of the production output. Diffusion times of 16 or 32 hours will yield junction depths given in Figure 32 of this report.

At this point of the process (see block diagram, Figure 34), several process modifications are introduced for obtaining the desired p-n junction characteristics. These modifications, as well as several process checks, are discussed in the following sections.

Excess-Charge-Carrier-Lifetime Retention. The degradation of the lifetime of excess charge carriers in the bulk silicon occurs when diffused silicon wafers are cooled rapidly from the high temperatures used in the diffusion process. The degradation is attributed to "freezing in" of thermal defects and recombination impurity levels. By such rapid-cooling procedures, initial bulk lifetimes of 100 microseconds can be degraded to values of the order of 0.1 microsecond. To preserve a reasonable charge-carrier lifetime, several techniques have been used in the preparation of diffused devices: (a) temperature programing (slow cooling) following any high-temperature treatment used in the process, (b) gettering[2] of impurities introducing recombination centers with materials, such as nickel, that do not alter the bulk conductivity, and (c) a combination of programing and gettering.

Normal furnace cooling has been found to be effective in maintaining a sufficient excess-charge carrier lifetime for devices having small base widths.* However, with devices having bases in excess of 0.01 inch wide lifetime retention treatments are necessary in the diffusion process to assure an effective base conductivity-modulation.

Temperature programing at a rate of 70°C/hour has been used with success after each of the phosphorus-, boron-, and nickel-diffusion steps (see Figure 34, process block diagram). Programing is accomplished with a temperature controller having a programing feature.

Gettering of recombination impurities by the use of nickel as a "gettering" agent has been only moderately successful with silicon wafers processed with normal furnace cooling following the diffusion cycles. Fast cooling of nickel-treated wafers revealed a serious degradation of the charge carrier lifetime in the device. However, incorporation of the nickel-gettering step in the slow cooling process resulted in less lifetime degradation than in the case of slow cooling alone.

Two methods have been used in preparing silicon wafers for the getting treatment:

(1) Silicon wafers cleaned and etched are plated with a .0004-inch layer of nickel using the electroless nickel-plating method. Wafers are then heat treated for 10 minutes at a temperature of 1000°C in an argon atmosphere. Following the heating period, the wafers are rapidly cooled to room temperature.

(2) Silicon wafers cleaned, etched, and plated in a similar manner as described above are soaked at 800°C for a period of two hours in a forming gas atmosphere. Again, as in the above, wafers are rapidly cooled to room temperature.

*The base width is defined as the region between the n^+-p junction and the p-p^+ base.

Following the use of either of the above gettering treatments, wafers are processed in the normal manner, as shown in the block diagram of the process. Method 1 above was found to be satisfactory in improving the minority carrier lifetime in the device. Gettering with slow cooling was more effective for silicon having a high oxygen content (pulled crystals). It was revealed that gettering with slow cooling was ineffective in maintaining an adequate lifetime for the devices processed from float-zoned silicon.

Junction Delineation. Junction delineation is included in the processing steps for the purpose of checking the quality of the phosphorus diffusion step. Several methods have been reported[3] for determining the junction depth for diffused devices. The correlation between the calculated values of junction depth given in Figure 32 and the measured depth can be ascertained. Although this method does not yield an absolute value of the p-n^+ junction depth, a reasonable check can be made. The procedure used to delineate the junction is given in Appendix B. The electrochemical deposition of copper onto the p-type diffused region is utilized. Usually, values of the calculated and measured junction depths agree within 10 per cent.

Surface Conductivity. Thermoelectric probing of phosphorus- and boron-diffused silicon wafers is used as a means for quickly determining the conductivity type and degree of degeneracy of the surface. However, only from experience can one use the thermal-probe method in determining the quality of the surface. High-conductivity surfaces are indicated by a strong thermoelectric effect as shown by the displacement on the galvanometer. As the conductivity decreases, the galvanometer movement diminishes. In many instances, zero displacement is noted. This condition indicates either an oxide surface (high resistance) or the approach of the surface conductivity toward an intrinsic value. A sketch of the thermal-probe equipment is shown in Figure 3 of Appendix B. The procedure used for surface thermal-probing evaluation of diffused wafers is as follows:

Procedure.

(1) Choose one or two wafers at random from processed group of wafers.

(2) Etch wafers in concentrated (48 per cent) HF for 2.0 minutes.

(3) Rinse in distilled water and dry.

(4) With the n^+ region up, lightly tap surface with hot probe maintaining cold probe in contact.

(5) Deflection of galvanometer denotes degree of surface conductivity and type.

Step 5. Final Wafer Sizing

Since the sensitivity of the dosimeter is related to the base width, final sizing should be as accurate as possible to maintain uniformity of base widths between processed wafers. Final sizing is accomplished on the as-sliced or unlapped surface. For

smaller quantities, hand lapping is adequate. A minimum of 0.003 inch is removed from the wafers to reach the original base material. The amount of removal will depend on the base width of the device and on the initial wafer thickness. A final surface having a 600-grit finish is desirable.

At this stage it is also recommended that a surface thermal-probe check be made. This will give assurance of adequate material removal from observation of the conductivity type of the base material.

Step 6. Wafer Cleaning

Following final lapping and before boron diffusion it is necessary to remove contaminants from the base surface.

(1) Rinse wafers thoroughly in hot, running tap water.

(2) Rinse in hot distilled water for 2.0 minutes.

(3) Rinse in hot ethyl alcohol for 1.0 minute.

(4) Rinse in hot Cellosolve* (95°C) for 2.0 minutes.

(5) Repeat Step (4) in fresh solution.

(6) Rinse in hot xylene** (95°C) for 3.0 minutes.

(7) Remove and air dry.

(8) Place into clean, dry petri dish.

Step 7. Boron Application

In the boron application step, elemental boron is deposited on the silicon wafer surface by the pyrolytic decomposition of BCl_3. This system has several advantages: (a) high surface concentrations of boron are achieved, (b) decomposition of the protective oxide coating at the n^+ surface is minimized, and (c) large quantities of wafers can be treated in a short time.

Conditions.

Application temperature	1150°C
Application time	20 minutes
Carrier gas	Dry nitrogen
Carrier flow rate	1000 cc/min
BCl_3 flow rate	1.5 cc/min

*Ethylene glycol monoethyl ether, manufactured by Carbide and Carbon Chemical Company, Technical Grade.
**CP grade.

Procedure.

(1) Load silicon wafers into quartz carrier tray in a vertical position. (Do not allow wafers to mask one another.)

(2) Increase carrier-gas flow rate to 3000 cc/min and insert carrier tray from open end of furnace and move to center of furnace.

(3) Allow 5 minutes for furnace temperature to stabilize at 1150°C. Decrease carrier gas flow rate to 100 cc/min.

(4) Meter into system a total of 1.5 cc of boron trichloride. (This quantity is adequate for 50 1-inch-diameter wafers.)

(5) Soak for 20 minutes at 1150°C.

(6) Increase carrier-gas flow rate to 3000 cc/min.

(7) Remove carrier tray to exhaust end of furnace to cool.

(8) After 10 minutes cooling, remove tray and transfer wafers into clean, dry petri dish.

For new furnace tubes, it is recommended that the system be "seasoned". Several dummy runs are recommended for seasoning the BCl_3 application furnace.

Good boron deposits appear as brownish-black layers. Occasionally some B_2O_3 formation occurs from the presence of water vapor. This deposit is not detrimental to the diffusion of boron.

Step 8. Boron Diffusion

The boron diffusion is carried out in similar manner to that described for phosphorus diffusion:

Conditions.

Diffusion temperature	1150°C
Diffusion time	2 hours
Atmosphere	Air

Procedure.

(1) Load boron-treated silicon wafers into a quartz carrier tray.

(2) Insert carrier tray into the uniform hot zone of furnace.

(3) Diffuse for 2.0 hours.

(4) Remove carrier tray to cool end of furnace and allow to cool before transferring wafers into clean, dry petri dish.

The diffused wafers are again slowly cooled (70°C/hour) in the manner previously discussed for lifetime retention.

For the diffusion time used, the boron concentration at the p-p^+ junctions for various initial bulk resistivities and the distances of the junction from the surface are shown in Figure 33.

Step 9. First Nickel Plate

A thin nickel-plated layer is applied to the diffused silicon wafers by the electroless plating technique. Other than the maintaining of degenerate diffused surfaces, the nickel-plating step is considered the most critical step in the process. The first nickel layer serves to improve the mechanical properties of the contact following a nickel diffusion period. Also, some nickel gettering of recombination impurities near the surface during the diffusion treatment has been reported.

The procedure presented below for applying the first nickel plate has been found to be adequate in removing oxide layers from the diffused wafers without altering the surface carrier concentration.

Procedure.

(1) Etch diffused wafers in concentrated (48 per cent) HF for 3.0 minutes.

(2) Rinse thoroughly in hot, running tap water for 1.0 minute.

(3) Nitrite etch for 30 seconds.

(4) Rinse in hot tap water for 1.0 minute.

(5) Rinse in hot distilled water (95°C) for 1.0 minute. (Two rinses are recommended.)

(6) Nickel plate for 2.0 minutes in electroless nickel-plating bath.

(7) Rinse in hot tap water for 1.0 minute.

(8) Rinse in hot distilled water for 30 seconds.

(9) Dry and store wafers in clean, dry petri dish.

The electroless nickel-plating bath composition is given in Appendix B. Wafers are carefully checked for nickel-plating adherence. Wafers demonstrating poor adherence of nickel by either peeling or flaking should be reprocessed in the manner described above, after removing the nickel plate with concentrated HNO_3. It is strongly recommended that separate receptacles be used for each wafer during cleaning and plating. Thorough removal of nitrite etch is not possible if more than one slice is processed in the same

rinse. The nitrite etch will, in time, complex the plating bath and cause poor plating on the wafers.

Step 10. Nickel Diffusion

To eliminate the possible oxidation of the nickel-plated layer during the diffusion cycle, a split furnace is used, whereby the furnace tube can be preflushed with an inert gas prior to inserting into the furnace. The conditions and procedure for the nickel diffusion process are given below.

Conditions.

Diffusion temperature	650°C
Atmosphere	Forming gas at 1000 cc/min ($N_2 + H_2$)
Diffusion time	1/2 hour
Cooling	Fast

Procedure.

(1) Load nickel-plated wafers into a quartz carrier tray and place into furnace tube.

(2) Flush tube for 5 minutes with forming gas at 1000 cc/minute.

(3) Place furnace tube into split furnace.

(4) Diffuse for 1/2 hour at 650°C with forming gas flowing at 1000 cc/min.

(5) Remove furnace tube and continue to flush until cool.

(6) Remove carrier tray from furnace tube and transfer wafer to clean, dry petri dish.

For charge-carrier-lifetime retention, slow cooling (70°/hour) to 400°C is required following Step 4 of the above procedure.

Step 11. Second Nickel Plate

The final or second nickel-plated layer is applied for soldering purposes. Several wafers can be plated in a common vessel without any adverse effects on the plating.

Procedure.

(1) Etch wafers in concentrated (48 per cent) HF acid for 30 seconds.

(2) Rinse in hot, running tap water for 1.0 minute.

(3) Rinse in hot distilled water for 1.0 minute (two separate rinses).

(4) Nickel plate for 4.0 minutes.

(5) Rinse in hot tap water followed by hot distilled water.

(6) Store plated wafers in Cellosolve to prevent surface oxidation of the nickel.

Identification Gold Plate. Following the second nickel-plating process, it is desirable to gold plate the p^+ base contact surface of processed wafers for polarity identification of the finished dice. The n^+ surface is distinguished from the p^+ base by the small depression coded near the edge of wafer, as previously described. The n^+ surface can be suitably masked with either low melting waxes or electroplate masking adhesive prior to plating.

Gold plating is accomplished by either the electroless gold-plating method or electroplating techniques. Both methods are standard techniques used throughout the solid state electronic industry.

Step 12. Diffused-Wafer Dicing

The silicon p-n junction dosimeters are ultrasonically machined to 0.120 inch in diameter. A "nest" of hypodermic, stainless steel tubing, having the proper inside diameter, soldered to the working tool is used for cutting the circular dice. Approximately 24 dice can be obtained from a wafer 3/4 inch in diameter for a closely-packed nest of cutting tubes.

Procedure.

(1) Heat a microscope slide, capable of accommodating two wafers, with a hot plate and apply a coating of wax.

(2) Place silicon wafer, n^+ region up, on molten wax and apply a coating on wafer.

(3) Place a thin cover glass (0.010 inch thick) over wafer and gently force out trapped air between cover glass and wax layer.

(4) Cool mounted wafers until wax hardens.

(5) Ultrasonically cut wafer into dice with the bundled cutting tubes. (Allow cutting to proceed into the microscope slide mounting.)

(6) Remove excess cutting compound with a spray of cold tap water.

(7) Rinse diced wafers with distilled water and dry with a warm air blast.

Note: Ganged sawing with diamond wheels can be used to prepare square type dice if ultrasonic equipment is not available. Wafer mounting for ganged sawing is similar to that described above. Mounting wax used is a 50-50 volume composition of Kel-F No. 200 and jewelers chasers cement.

Step 13. Dice-Block Etching

Etching of diced wafers is required to remove mechanical surface damage caused by the dicing operation. Also, block-etching allows the etch-back of the nickel contact near the p-n junction.

A two-step etch is used for block etching. The etchant compositions are given in Appendix B. The first etch is used to remove damaged silicon and to etch back the nickel contact. The second etch is used for polishing the surface at the p-n junction.

Procedure.

(1) Place mounted dice wafers into the aged modified CP_4 etchant for 3.0 minutes. Agitate solution gently to liberate gas from the silicon surface.

(2) Rinse in deionized water for 2.0 minutes.

(3) Etch with polish-etchant for 5.0 minutes.

(4) Remove from polish etchant and quickly rinse with deionized water. (This step should be carried out as quickly as possible.)

(5) Soak in H_2O_2 (30 per cent) for 10 minutes.

(6) Rinse in deionized water for 2.0 minutes and allow to air dry.

Note: Block etching may not be necessary if surface recombination does not present a problem with the charge carrier lifetime in the device. However, if etching is required, final etching on assembled unit can be used in place of the block etching if desired.

Step 14. Dice Demounting and Cleaning

Procedure.

(1) Dissolve mounting wax from dice with hot xylene (90°C) and transfer dice to a fine-mesh nickel or stainless steel basket.

(2) Rinse in hot xylene (90°C) for 5.0 minutes.

(3) Rinse in hot Cellosolve (95°C) for 3.0 minutes.

(4) Rinse in hot ethyl alcohol (75°C) for 2.0 minutes.

(5) Rinse in hot xylene (90°C) for 3.0 minutes.

(6) Dry dice with heated source and store in clean, dry vials.

Step 15. Preliminary p-n Junction Dosimeter Tests

Initial Lifetime. Initial high-level injection lifetime in the dosimeter dice is determined prior to assembly, using methanical pressure contacts to the individual dice. Sufficient carrier injection is obtained with pressure contacts to permit adequate lifetime measurements for dice selection purposes. The circuit used for performing the device lifetime measurement is described in Phase II of the report.

Forward Current-Voltage Characteristic. Mechanical pressure contacts are not suitable for measuring the forward voltage-current characteristics of conductivity-modulated rectifiers. Therefore, to evaluate the forward characteristic of the dosimeter, it is necessary to solder-assemble a representative number of units for measurement. The assembly technique used in applying contact pins to the dice is described in the following step of the process.

Step 16. Dosimeter p-n Junction Assembly

The p-n junction dosimeters are fabricated into axial "plug-in" units, as shown at the top of Figure 1 in Appendix B. A graphite multiple-jig fixture is used to solder-assemble several units simultaneously. For experimental research purposes, a jig fixture capable of accommodating nine units was constructed. For the large-scale production of dosimeters, a jig fixture capable of handling several hundred units can be readily used. Shown in Figure 2 of Appendix B are photographs of the disassembled and assembled sections of the graphite multiple jig.

Soldering of the completed assembly is carried out in a forming gas atmosphere (10 per cent H_2, 90 per cent N_2) to minimize the oxidation of the lead-tin solder and the dosimeter-dice nickel contact surfaces. Flux is also used to aid the initial wetting of the solder to the nickel contacts. The graphite-loaded jig is heated to the soldering temperature in an aluminum cavity mounted on a standard laboratory hot plate. The soldering temperature is maintained at 320°C. Preheated forming gas is continuously flushed through the cavity during soldering. The cavity is constructed in a manner to allow the application of a slight mechanical pressure to the individual assemblies during soldering. For large-scale production, hydrogen or forming-gas soldering furnaces are commercially available.

Assembly Material Specifications.

Contact Pins. Two sizes of contact pins are required. Pins are machined from pure nickel having the dimensions given in Figure 4 of Appendix B. The contact pins are referred to as the base or cathode pin, and the top or anode pin. Prior to use, pins

are thoroughly degreased in trichloroethylene and rinsed with ethyl alcohol. Pickling in a dilute solution of nitric acid for several minutes is used if pins are to be stored for prolonged periods.

Solder Composition. Circular solder preforms are prepared from a 95 per cent-5 per cent lead-tin composition having a melting point of 295°C. The thickness and diameters required are as follows:

Cathode preform – .003 inch thick and .120 inch in diameter

Anode preform – .008 inch thick and .120 inch in diameter.

Solder preforms are degreased in trichloroethylene, rinsed in ethyl alcohol, and stored in CP acetone.

Flux composition – A commercially available flux is used during soldering. The resin base Alpha No. 123* flux has been found to be satisfactory.

Soldering Procedure.

(1) Load graphite multiple-jig sections with cathode and anode pins.

Note: All parts to be handled either with tweezers or vacuum-chuck pick-up tool.

(2) Place one cathode solder-preform into each cathode pin recess.

(3) Place dosimeter dice, with p^+ surface (gold-plated base) down, into each cathode pin recess. (Completed dice are of the form shown in Figure 1 of Appendix B at bottom of photograph.)

(4) Place one anode solder-preform on n^+ region of dice.

(5) Apply a small quantity of flux to each anode-preform.

(6) Place loaded anode-pin section of jig into place.

(7) Insert into preheated furnace cavity for 3.0 minutes.

(8) Remove multiple jig from furnace and allow to cool for 1/2 minute.

(9) Place jig into a bath of isopropyl alcohol to cool.

The last step aids in removing flux residue and facilitates extracting soldered units.

*Manufactured by the Alpha Metal Company, Inc., Jersey City, New Jersey.

Packaging

The experimental axial "plug-in" type device, described in detail in the preceding section, does not offer any readily available solution to its encapsulation. However, the design of the device has not been finalized. For sealing of the unit against corrosive atmospheres, it may be necessary to alter the present dosimeter design.

It is suggested that molded plastics, low-temperature glasses, and capsule contaniers be investigated as a possible means for protecting the present plug-in unit.

Surface effects are not a serious problem, since the device is operated in the forward bias condition. Surface recombination effects on high-level lifetime in these devices have not been encountered for devices having base widths up to .035 inch in thickness. If the base widths of the dosimeters are increased to .045 inch for the purpose of increasing the sensitivity of the device for low neutron dose rates then, it may be advisable to ascertain the effects of surface recombination prior to redesigning the unit for protective encapsulation.

Process Evaluation Studies

For the realization of a practical neutron dosimeter, capable of being produced in large quantities with uniform initial characteristics, a statistical evaluation of the processing and material variation effects was considered necessary. As a result, a large number of dosimeters were prepared with the following primary objectives:

(1) To determine the degree of dosimeter uniformity and yield with controlled processing conditions and fixed initial material characteristics

(2) To evaluate the consistency of radiation-induced changes in the charge carrier lifetimes among devices having similar initial characteristics.

For an adequate statistical study of irradiated devices, it is apparent that a representative number of devices with uniformly high initial lifetimes and uniform forward voltage-current characteristics would be necessary. Several material- and process-variations were introduced into the statistical process study to assure a high yield of usable devices and simultaneously to gain additional information pertaining to material- and process-variation effects on the initial high-level lifetime in the device.

Material Variation Studies

Included in the material variation studies were two types of grown silicon crystals. these included:

(a) Float-zoned silicon, characterized by a low oxygen content and a high dislocation density

(b) Czochralski (pulled) silicon, characterized by high oxygen content and a low dislocation density.

Process Variation Studies

The process variations were directed toward the evaluation of techniques for maintaining a high lifetime in processed silicon wafers for both types of silicon listed above. These included:

(a) Nickel-gettering treatment with the addition of slow cooling following the diffusion cycles (method 1 used for the gettering treatment as described on page 72 of the process description).

(b) Slow cooling (70°C per hour) following each of the diffusion cycles.

(c) Nickel-gettering treatment with rapid cooling following each of the diffusion cycles.

As a result of the above process- and material-variations, a total of six groups of dosimeters were prepared. The device base width used for all groups was maintained at .020 inch. This base width was chosen on the basis of early results that indicated adequate sensitivity to low neutron dose exposures for .020-inch base width devices. All silicon wafers of each group were processed simultaneously to minimize variations introduced within each step of the process.

Table 11 summarizes the initial bulk properties of each of the two types of silicon crystals used in preparing the above dosimeters. The bulk lifetime values were furnished by the material supplier. The absolute value of the oxygen content and dislocation density are unknown; however, their values should be within the limits normally found in each type of crystal.

TABLE 11. INITIAL BULK PROPERTIES OF SILICON SINGLE-CRYSTAL WAFERS

	Resistivity, ohm-cm	Lifetime[(a)], microseconds	Crystal Orientation	Oxygen Content	Dislocation Density
Float Zoned	22-27	50	<111>	Low	High
Czochralski (pulled)	22-27	30	<111>	High	Low

(a) Lifetime values are estimates furnished by the material supplier. These values could not be checked in our laboratory, since adequate lifetime samples could not be cut from the wafers.

Table 12 is a tabulation of the preliminary results obtained for nine dice randomly chosen for assembly from each group. A code legend is included at the bottom of the table for ease of identification and type treatment used. Listed in the second column are the number of silicon wafers processed through the boron diffusion step. To fulfill the requirements for the number of experimental units needed for study and evaluation, it was not necessary to process all wafers to the dosimeter dice stage; therefore, only several wafers of each group were completed to the dice stage to meet the requirements for radiation studies. The total number of dice prepared from each group is given in the third column of the table.

TABLE 12. PRELIMINARY P-N JUNCTION DOSIMETER DEVICE CHARACTERISTICS

Group	No. of Wafers Processed	No. of Dice Prepared	Average Initial Lifetime, microseconds	Mean Deviation of Lifetime, microseconds	Average Forward Voltage Drop at 1.0125 Amperes, volts	Mean Deviation of Forward Voltage Drop, volts	Remarks
DD3-20FZ-NSC	50	343	15.6	8.2	0.99	0.07	Inconsistent forward voltage-current characteristics. A 30 per cent yield of units having a lifetime of 20 microseconds or greater.
DD3-20FZ-SSC	50	250	7.9	2.0	1.46	0.22	High forward resistance.
DD3-20FZ-NFC	5	115	--	--	--	--	Severe lifetime degradation-lifetime immeasurable.
DD3-20CP-NSC	50	295	27.9	8.2	0.93	0.09	All dice assembled for this group. 87 per cent yield of devices having a lifetime value greater than 20 microseconds.
DD3-20CP-SSC	50	345	9.0	1.5	0.98	0.04	Acceptable forward characteristics, and fair degree of uniformity of device lifetime.
DD3-20CP-NFC	5	119	--	--	--	--	Severe lifetime degradation. Lifetime immeasurable.

(a) Group Code Legend

DD3 – Dosimeter device; third process run.
20 – Base width in mils.
FZ – Float-zoned silicon.
CP – Czochralski (pulled) silicon.
N – Nickel getter treated.
SC – Slow cooled.
FC – Fast cooled.
S – Standard process.

Listed in the fourth and fifth columns of the table are the average initial lifetimes and mean deviations calculated from the measurement of nine assembled units from each group. Similar calculations of the average forward voltage drop and the mean deviations from the average (measured at the current specified) are also given.

Measurement of the charge carrier lifetimes in the p-n junction dosimeters prepared by the fast cooled nickel gettered method could not be performed because of their low values. The forward voltage drops in the devices in this group were extremely high, and therefore, are not given in the table.

From the preliminary data taken on the 9 devices, only group DD3-20CP-NSC (high oxygen-low dislocation content silicon) was considered adequate for assembling the remainder of the dice into plug-in units for radiation studies. An 87 per cent yield of the devices in this group was obtained with initial lifetime values greater than 20 microseconds. However, some degree of scatter in the lifetime was observed, as indicated by the deviation values. The measured voltage drop indicated that effective conductivity modulation was achieved.

Although the results obtained with the devices prepared from each of the groups shown in Table 12 were somewhat inferior to past results, the data are sufficient to allow several tentative conclusions to be drawn:

(1) Nickel gettering with rapid cooling is ineffective as a technique for lifetime retention in processed wafers for both the pulled and float-zoned type silicon crystals.

(2) Nickel gettering with the added slow cooling is more effective in lifetime retention for high oxygen content silicon. A similar result was found for devices prepared earlier in the program that were processed in the same manner. The role of oxygen as related to device lifetime is not well understood; therefore, it is suggested that future investigations be directed toward determining the mechanism by which oxygen aids in the anihilation of recombination centers. The solution to the latter could be of prime importance in the development of a practical reproducible dosimeter. These studies would, however, be basic in nature and may or may not be appropriate in a device-oriented program.

(3) The effectiveness of nickel gettering is again demonstrated as a lifetime retention method by the noted differences between the two float-zoned groups with and without nickel treatment. However, it is necessary to employ slow cooling to achieve higher lifetime values with the nickel treatment.

(4) The initial lifetime values obtained on devices prepared with the standard slow cooling method from Czochralski (pulled) type silicon (Group DD3-20CP-SSC) are lower than expected. This result cannot be explained in view of previous results obtained with slow cooling (see Third Quarterly Report, February 14, 1960).

(5) The degree of lifetime scatter is greater for the nickel-treated groups than the slow-cooled groups for both types of silicon. It is indicated

that higher lifetime retention by nickel treatment becomes more sensitive to processing and initial bulk silicon properties.

The observation made in (5) above is considered of prime importance in the fabrication of dosimeters with uniform characteristics. As a result, an inquiry to the material supplier was made regarding how the silicon wafers were furnished. The silicon wafers were purchased on the basis of a narrow resistivity range. This necessitated the cutting of wafers in the proper resistivity range. Unfortunately, the bulk lifetime furnished by the supplier was an estimated, rather than a measured value. It is apparent that a variation of bulk lifetime, oxygen concentration, and dislocation density would be present among wafers in both types of silicon. On the basis of these probable variations, it is concluded that the scatter introduced into the device lifetime, for the nickel-treated groups, is related to the uncertainty of the initial material characteristics. For future investigations a more stringent control should be applied to the initial silicon bulk properties prior to processing.

HCG:OJM:ARZ:RKC:JMS:CSP/mmk

APPENDIX A

DERIVATION OF ERROR EQUATION

APPENDIX A

DERIVATION OF ERROR EQUATION

by

(A. R. Zacaroli

$$\frac{1}{\tau_f} = \frac{1}{\tau_o} + \alpha\, nvt \quad . \tag{A-1}$$

$$\alpha\, nvt = \frac{1}{\tau_f} - \frac{1}{\tau_o} \quad . \tag{A-2}$$

$$\alpha\, \Delta\, nvt = \Delta \left(\frac{1}{\tau_f} - \frac{1}{\tau_o} \right) \quad . \tag{A-3}$$

$$\alpha\, \Delta\, nvt = \Delta\, \frac{1}{\tau_f} - \Delta\, \frac{1}{\tau_o} \quad . \tag{A-4}$$

If $\Delta\tau \ll \tau$,

$$\Delta\, \frac{1}{\tau} \approx - \frac{1}{\tau}\, \frac{\Delta\tau}{\tau} \quad . \tag{A-5}$$

From Equations (A-2), (A-4), and (A-5),

$$\frac{\Delta\, nvt}{nvt} = \frac{- \dfrac{1}{\tau_f}\, \dfrac{\Delta\tau_f}{\tau_f} + \dfrac{1}{\tau_o}\, \dfrac{\Delta\tau_o}{\tau_o}}{\dfrac{1}{\tau_f} - \dfrac{1}{\tau_o}} \quad . \tag{A-6}$$

Let Δ nvt represent the error in determining dose and $\Delta\tau$ represent the error in measuring τ. Also, assume that the relative error in measuring τ is constant in magnitude; i. e.,

$$\left| \frac{\Delta\tau_f}{\tau_f} \right| = \left| \frac{\Delta\tau_o}{\tau_o} \right| = \left| \frac{\Delta\tau}{\tau} \right| \quad . \tag{A-7}$$

Then

$$\frac{\Delta\, nvt}{nvt} = \pm \left[\frac{\dfrac{1}{\tau_f} \pm \dfrac{1}{\tau_o}}{\dfrac{1}{\tau_f} - \dfrac{1}{\tau_o}} \right] \frac{\Delta\tau}{\tau} \quad . \tag{A-8}$$

The maximum relative error in determining nvt will be

$$\frac{\Delta\, nvt}{nvt} = \pm \left[\frac{\dfrac{1}{\tau_f} + \dfrac{1}{\tau_o}}{\dfrac{1}{\tau_f} - \dfrac{1}{\tau_o}} \right] \frac{\Delta\tau}{\tau} \quad . \tag{A-9}$$

Rewriting Equation (A-9):

$$\frac{\Delta \text{ nvt}}{\text{nvt}} = \pm \left[1 + \frac{2 \frac{1}{\tau_o}}{\frac{1}{\tau_f} - \frac{1}{\tau_o}} \right] \frac{\Delta \tau}{\tau} \quad . \tag{A-10}$$

From Equations (A-2) and (A-10):

$$\frac{\Delta \text{ nvt}}{\text{nvt}} = \pm \left[1 + \frac{2}{\tau_o \, \alpha \, \text{nvt}} \right] \frac{\Delta \tau}{\tau} \quad . \tag{A-11}$$

Rewriting Equation (A-11):

$$\frac{\tau}{\Delta \tau} \frac{\Delta \text{ nvt}}{\text{nvt}} = \pm \left[1 + \frac{2}{\tau_o \, \alpha \, \text{nvt}} \right] \quad . \tag{A-12}$$

APPENDIX B

MISCELLANEOUS FABRICATION DETAILS

APPENDIX B

NITRITE-ETCH COMPOSITION

100 g NaOH

150 g $NaNO_2$

1000 cc distilled water

Temperature, 95°C

Storage temperature, 25°C

Use water bath for maintaining etch-solution temperature.

Replace etch solution when a considerable precipitation is noted.

Pyrex-type beakers are used for etch-solution container.

JUNCTION DELINEATION

Procedure

(1) Apply a thin coating of clear shellac to a heated (90°C) microscope slide.

(2) Place a diffused wafer (with thickness known) on melted cement with the *n* region up.

(3) Coat surface of silicon wafer and allow cement to harden.

(4) Lap a 20° to 30° bevel on mounted wafer with 600-grit SiC with 20° to 30° lapping block.

(5) Rinse with distilled water.

(6) Place into etch-plating bath for 10 seconds. Remove and rinse.

(7) Repeat (6) until copper plating is visible to eye.

(8) Determine depth of *n* region with calibrated eyepiece on low-power microscope.

Plating-Bath Composition

20 cc conc. HF (48%)	Dissolve copper in HNO_3
10 cc conc. HNO_3	Add water and HF
20 cc distilled water	Temperature, 25°C
300 mg copper	

NICKEL-BATH COMPOSITION

30 g/liter $NiCl_2 \cdot 6H_2O$

10 g/liter $NaH_2PO_2 \cdot H_2O$

50 g/liter NH_4Cl

100 g/liter $Na_3C_6H_5O_7 \cdot H_2O$

NH_4OH to give a pH of 9.0. This can be conveniently controlled by maintaining a blue color. Green-solution color denotes a low pH. Add NH_4OH as required. Temperature, 95 ± 2°C.

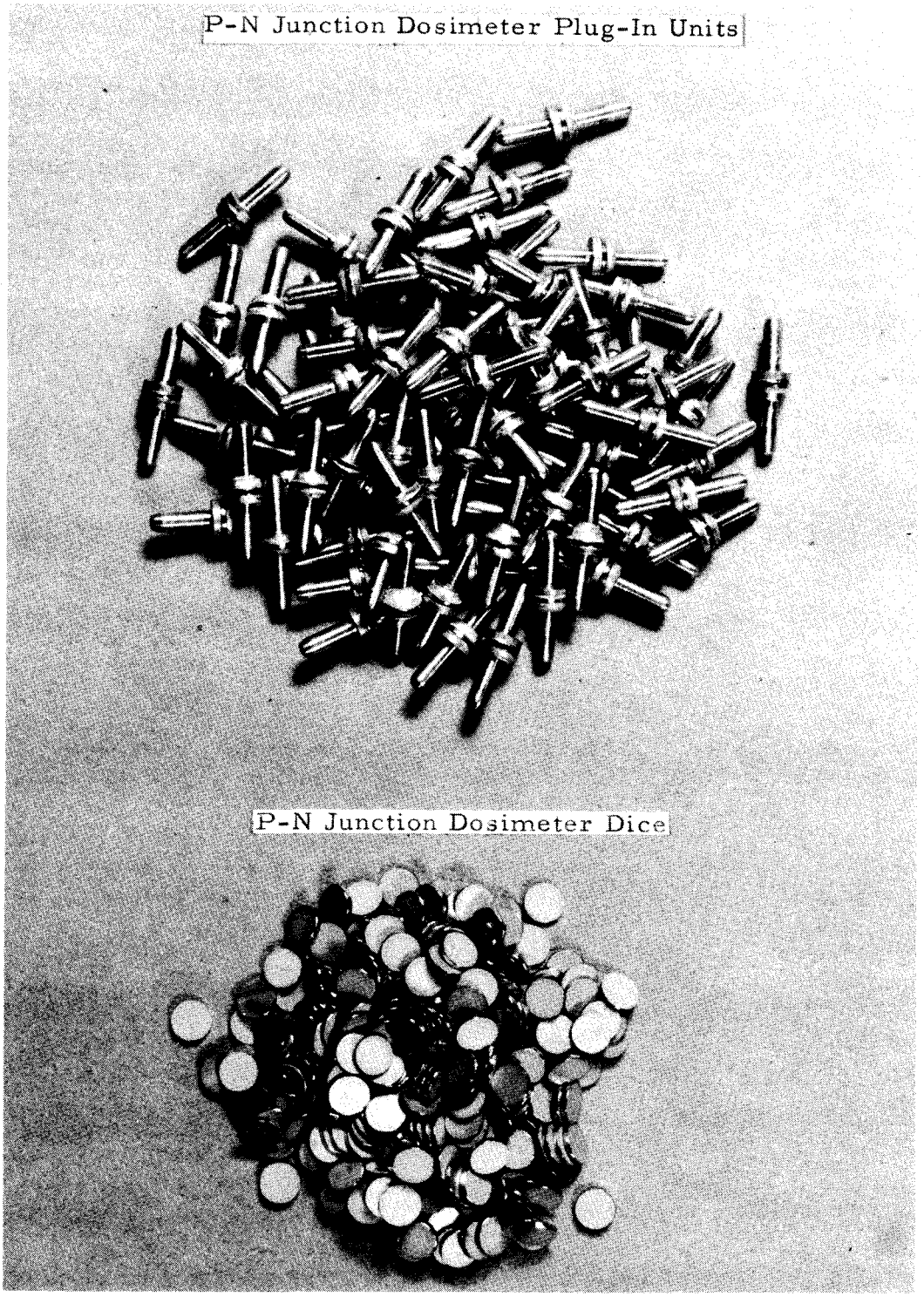

FIGURE B-1. UNASSEMBLED AND ASSEMBLED SILICON P-N JUNCTION DOSIMETERS

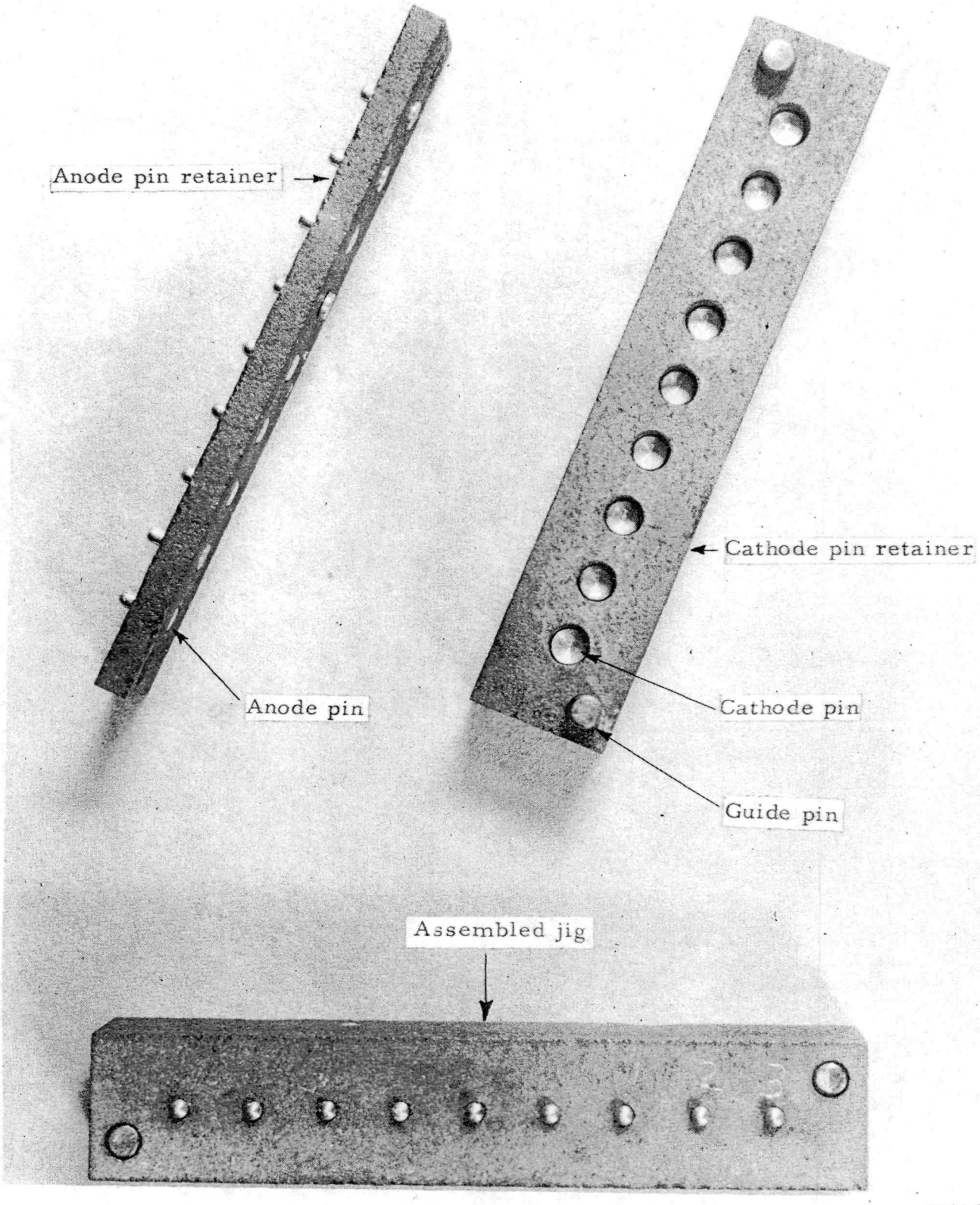

N68603

FIGURE B-2. GRAPHITE MULTIPLE SOLDER ASSEMBLY JIG

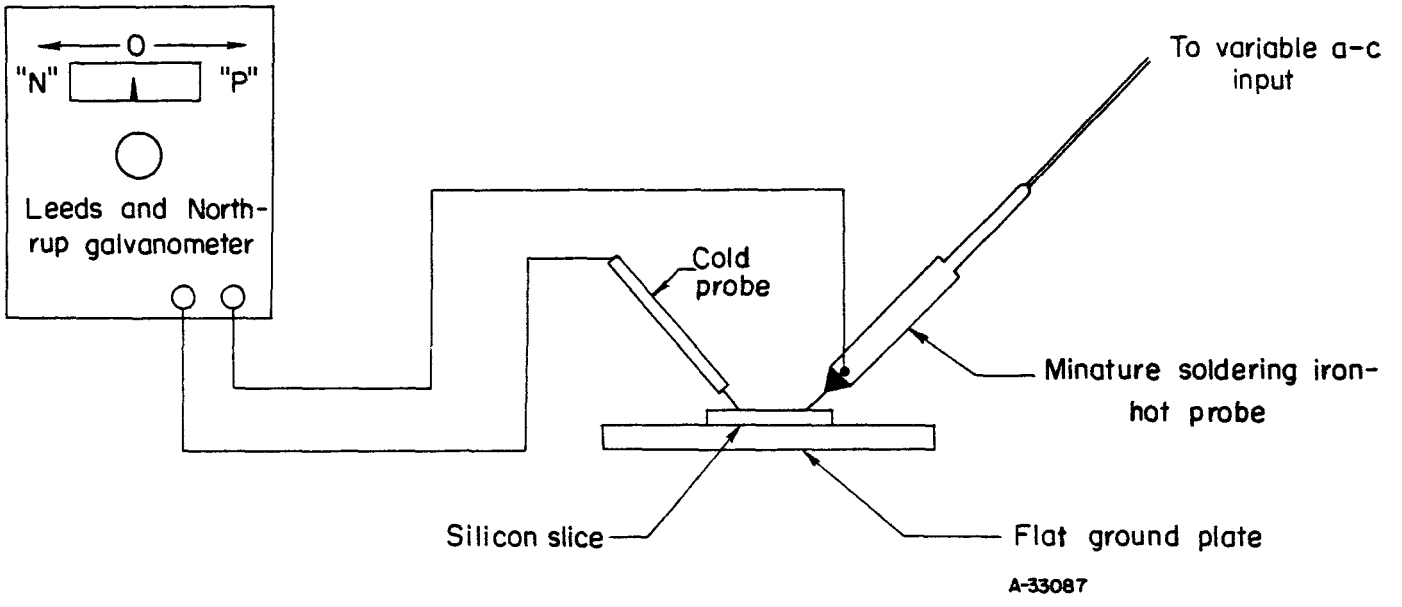

FIGURE B-3. THERMOELECTRIC-PROBE APPARATUS

Dimension Specfications For Pin Assemblies

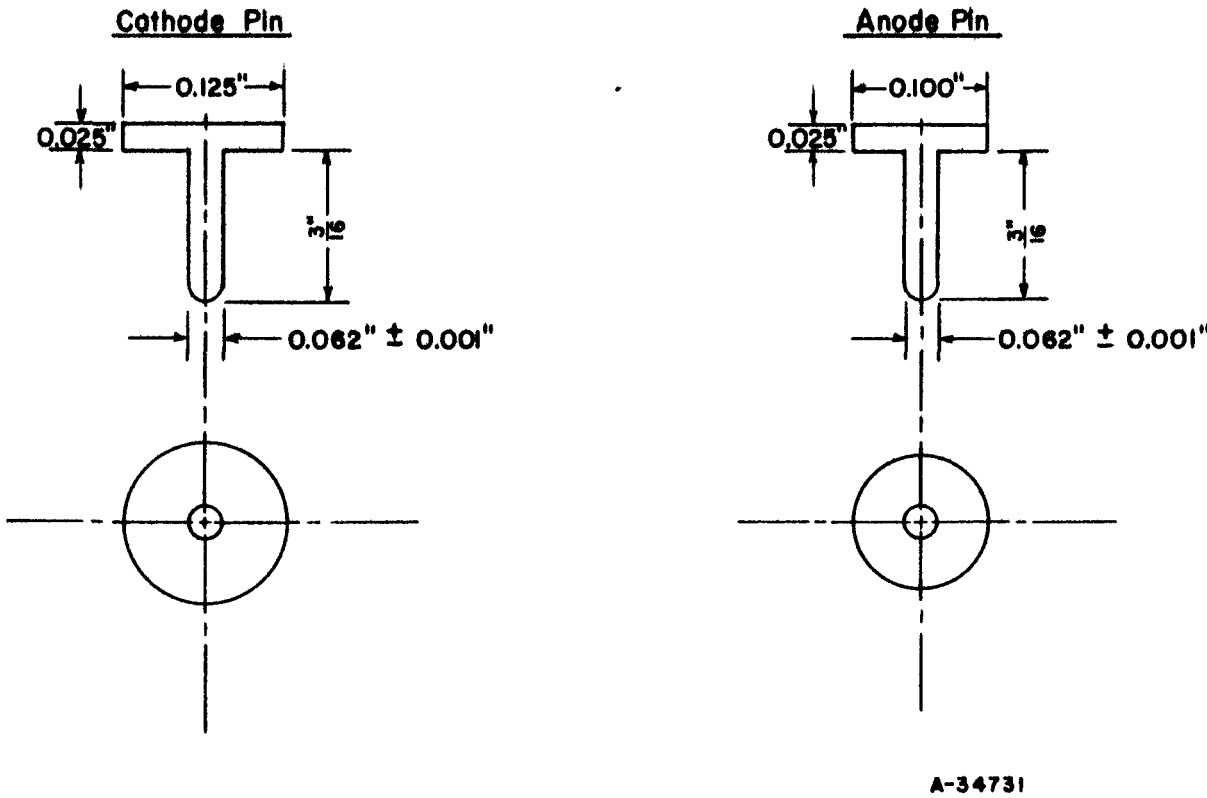

FIGURE B-4. DIMENSION SPECIFICATIONS FOR PIN ASSEMBLIES

BLOCK-ETCHANT COMPOSITIONS

Modified CP4 Etch

5 parts HNO_3(conc.)

3 parts HF (48%)

5 parts glacial acetic acid

Quantity, 500 cc

Temperature, 25°C

Age for 1/2 hour before using.

Polish Etch

1 part HNO_3 (conc.)

1 part HF (48%)

2 parts H_3PO_4 (conc.)

1/2 part glacial acetic acid

Temperature, 25°C

Quantity, 450 cc

No agitation of polish etch required during etching of silicon dice.

REFERENCES

(1) Fuller, C. S., and Ditzenberger, J. A., J. Appl. Phys., 25, 1439 (1954).

(2) Silverman, S. J., and Singleton, J. B., J. Electrochem. Soc., 105, 591 (1958).

(3) Turner, D. R., J. Electrochem. Soc., 106 (8), 701 (August, 1959).

(4) Veloric, H. S., and Smith, K. D., J. Electrochem. Soc., 104 (4) (April, 1957).

Data for this report are recorded in Battelle Memorial Institute Laboratory Record Book No. 13603, pages 1-100.

OJM/CSP:jvo

APPENDIX C

BIBLIOGRAPHY OF RADIATION DAMAGE IN SILICON, AND PERTINENT ELECTRONIC PROPERTIES OF SILICON P-N JUNCTIONS

APPENDIX C

BIBLIOGRAPHY OF RADIATION DAMAGE IN SILICON, AND PERTINENT ELECTRONIC PROPERTIES OF SILICON P-N JUNCTIONS

Radiation Damage

Cleland, J. W., and Crawford, J. H., "Thermal Neutron Radiation Effects in Semiconductors", Bull. Phys. Soc., II, 5 (3), 196 (1960).

Sonder, E., and Templeton, L. C., "Effect of Dissolved Oxygen on Radiation Damage in n-type Silicon", Bull. Phys. Soc., II, 5 (3), 196 (1960).

Ramdas, A. K., and Fan, H. Y., "Infrared Absorption in Irradiated Silicon, Oxygen-Dependent", Bull. Phys. Soc., II, 5 (3), 197 (1960).

Fan, H. Y., and Ramdas, A. K., "Infrared Absorption in Irradiated Silicon, Oxygen-Dependent", Bull. Phys. Soc., II, 5 (3), 197 (1960).

Watkins, G. D., and Corbett, J. W., "Indentification of the A Center in Irradiated Silicon. I. Spin Resonance", Bull. Phys. Soc., II, 5 (3), 197 (1960).

Corbett, J. W., Watkins, G. D., and McDonald, R. S., "Identification of the A Center in Irradiated Silicon, II. Infrared", Bull. Phys. Soc., II, 5 (3), 197 (1960).

Van Putten, Jr., J. D., and Vander Velde, J. C., "Solid-State Detector for Penetrating and Minimum Ionizing Particles", Bull. Phys. Soc., II, 5 (3), 197 (1960).

Bohan, W. A., Maxey, J. D., and Pecoraro, R. P., "Some Effects of Pulse Irradiation on Semiconductor Devices", Proc. Inst. Elec. Engrs., B, 15, 361-7 (1960), paper 3124E.

Vapaille, A., "Measurement of the Lifetime of Carriers Produced in Silicon By Electron Bombardment", C. R. Acad. Sci. (Paris), 249 (5), 648-50 (1959).

Wertheim, G. K., and Buchanan, D. N. E., "Electron Bombardment Damage in Oxygen-Free Silicon", J. Appl. Phys., 30 (8), 1232-4 (1959).

Wertheim, G. K., "Recombination Properties of Bombardment Defects in Semiconductors", J. Appl. Phys., 30 (8), 1166-74 (1959).

Loferski, J. J., and Rappaport, P., "Displacement Thresholds in Semiconductors", J. Appl. Phys., 30 (8), 1296-9 (1959).

Gossick, B. R., "Disordered Regions in Semiconductors Bombarded by Fast Neutrons", J. Appl. Phys., 30 (8), 1214-8 (1959).

Cahn, J. H., "Irradiation Damage in Germanium and Silicon Due to Electrons and Gamma Rays", J. Appl. Phys., 30 (8), 1310-6 (1959).

Sonder, E., "Magnetic and Electric Properties of Reactor-Irradiated Silicon", J. Appl. Phys., 30 (8), 1186-94 (1959).

Beck, R. W., Paskell, E., and Peet, C. S., "Some Effects of Fast Neutron Irradiation on Carrier Lifetimes in Silicon", J. Appl. Phys., 30 (9), 1487-9 (1959).

Brooks, H., "Radiation Effects in Materials", J. Appl. Phys., 30 (8), 1118-24 (1959).

Brown, W. L., Augustyniak, W. M., and Waite, T. R., "Annealing of Radiation Defects in Semiconductors", J. Appl. Phys., 30 (8), 1258-68 (1959).

Klein, C. N., "Radiation-Induced Energy Levels in Silicon", J. Appl. Phys., 30 (8), 1222-31 (1959).

Oen, O. S., and Holmes, D. K., "Cross-Sections for Atomic Displacements in Solids by Gamma Rays", J. Appl. Phys., 30 (8), 1289-95 (1959).

Schweinler, H. C., "Some Consequences of Thermal Neutron Capture in Silicon and Germanium", J. Appl. Phys., 30 (8), 1125-6 (1959).

Fan, H. Y., and Ramdas, H. K., "Infrared Absorption in Neutron Irradiated Silicon", J. Phys. Chem. Solids, 8, 272-4 (1959).

Buras, B., and O'Connor, D., "The Neutron-Phonon Interaction in Solids", Nukleonika, 4 (2), 119-40 (1959).

Gonser, N., "Concerning the Spike Formation in Radiation Damage by Charged Particles", Nukleonika, 1 (5), 182-3 (1959).

Rupprecht, G., and Klein, L. C., "Energy Levels in Neutron-Irradiated n-type Silicon", Phys. Rev., 116 (2), 342-3 (1959).

Wertheim, G. K., "Temperature-Dependent Defect Production in Bombardment of Semiconductors", Phys. Rev., 115 (3), 568-9 (1959).

Hill, D. E., "Electron Bombardment of Silicon", Phys. Rev., 114 (6), 1414-60 (1959).

Smoluchowski, R., "Radiation Effects in Solids", Radiation Research, Suppl No. 1, 26-52 (1959), Proceedings of the International Congress of Radiation Research, edited by D. E. Smith.

Bolteks, B. I., Plachenos, B. T., and Semenov, E. V., "On the Coefficient of Absorption of Co^{60} X-rays in Semiconductors", Dokl. Akad. Nauk, SSRR, 123 (1), 72-5 (1958).

Takeya, K., and Nakamura, K., "Current Amplification by Electron Bombardment in the Semiconductor Barrier Layer," J. Phys. Soc. 13 (2), 223 (Japan) (1958).

Fan, H. Y., and Lark-Horovitz, K., "Irradiation of Semiconductors", Semiconductors and Phosphors, Interscience Publishers, Inc., New York, 113-38 (1958).

Etherington, H., Nuclear Engineering Handbook, McGraw-Hill (1958).

Trice, J. B., "Measuring Reactor Spectra with Thresholds and Resonances", Nucleonics, 16 (7), 81-3 (1958).

Wertheim, G. K., "Electron-Bombardment Damage in Silicon", Phys. Rev., 110 (6), 1272-9 (1958).

Spitzer, W. G., and Fan, H. Y., "Effect of Neutron Irradiation on Infrared Absorption in Silicon", Phys. Rev., 109 (3), 1011-12 (1958).

Chynoweth, A. G., "Ionization Rates for Electrons and Holes in Silicon", Phys. Rev., 109 (5), 1537-40 (1958).

Wertheim, G. K., "Neutron-Bombardment Damage in Silicon", Phys. Rev., 111 (6), 1500-5 (1958).

Keesom, P. H., and Seidel, G., "Superfluid Helium Inside Neutron-Irradiated Silicon", Phys. Rev., 111 (2), 422-4 (1958).

Loferski, J. J., and Rappaport, P., "Radiation Damage in Ge and Si Detected by Carrier Lifetime Changes: Damage Thresholds", Phys. Rev., 111 (2), 432-9 (1958).

Gobeli, G. W., Alpha-Particle Irradiation of Ge at 4.2°K", Phys. Rev., 112 (6), 732-9 (1958).

Messenger, G. C., and Spratt, J. P., "The Effects of Neutron Irradiation on Germanium and Silicon", Proc. Inst. Radio Engrs., 46 (6), 1038-44 (1958).

Wagner, E. B., and Hurst, G. S., "Advances in the Standard Proportional Counter Method of Fast Neutron Dosimetry", Rev. Sci. Inst., 29 (2), 153-8 (1958).

Easley, J. W., "Comparison of Neutron Damage in Germanium and Silicon Transistors", Third Radiation Effects Symposium, USAF, V (1958).

Fainshtein, S. M., and Lysogorov, O. S., "The Effect of Ionic Bombardment on the Current-Voltage Characteristics of Silicon Point-Contact Diodes", Zh. Tekh. Fiz., 28 (3), 493-7 (1958).

Vyatskin, A. Xa., and Makhov, A. F., "Retardation of Electrons in Certain Metals and Semiconductors", Zh. Tekh. Fiz., 28 (4), 740-7 (1958).

Yurkoo, B. Ya., "The Penetration of Electrons into Germanium and Silicon (and Indium and Antimony)", Zh. Tekh. Fiz., 28 (6), 1159-64 (1958).

Gionola, V. F., "Damage to Silicon Produced by Bombardment with Helium Ions", J. Appl. Phys., 28 (8), 868-73 (1957).

Wittels, M. C., "Expansions in Reactor Irradiated Germanium and Silicon", J. Appl. Phys., 28 (8), 921 (1957).

Dienes, G. J., and Vineyard, G. H., "Radiation Effects in Solids", Interscience Publishers, New York (1957).

Gorton, R., "Effects of Irradiation Upon Diodes of the Silicon Junction Type", Nature (London), 179, 864 (1957).

Chynoweth, A. G., and McKay, K. G., "Threshold Energy for Electron-Hole Pair-Production by Electrons in Silicon", Phys. Rev., 188 (1), 29-34 (1957).

Wertheim, G. K., "Energy Levels in Electron-Bombarded Silicon", Phys. Rev., 125 (6), 1730-5 (1957).

Truell, R., Teutonico, L. J., and Levy, P. W., "Detection of Directional Neutron Damage in Silicon by Means of Ultrasonic Double Refraction Measurements", Phys. Rev., 105 (6), 1723-9 (1957).

Keisfer, G. L., and Stewart, H. V., "The Effects of Nuclear Radiation on Selected Semiconductor Devices", Proc. Inst. Radio Engrs., 45 (7), 931-7 (1957).

Xavier, M. A., "Correlation of Theoretical and Experimental Behavior of Silicon Junction Diodes During Neutron and Gamma Irradiation", Proceedings of the Second Conference on Nuclear Radiation Effects on Semiconductor Devices, Materials, and Circuits. (1957).

Patskevich, V. M., and Vavilov, V. S., and Smirnov, L. S., "Energy of Ionization by Electrons in Silicon Crystals", Zh. éksper. teor. Fiz., 33 [3(9)], 804-5 (1957).

Blout, E. I., "Energy Levels in Irradiated Germanium", Phys. Rev., 113, 995-98 (1957).

Sullivan, W. H., "Trilinear Chart of Nuclides", USAEC, 2nd. Edit. (1957).

Seitz, F., and Koehler, J. S., "Displacement of Atoms During Irradiation", Solid State Physics, Academic Press, Inc., New York, 2, 307-444 (1956).

Cottrell, A. H., "The Effects of Irradiation on the Physical Properties of Solids", Brit. J. Appl. Phys., Suppl. (5) (the physics of nuclear reactors), S43-S49, S49-S53 (1956).

Nelms, A. T., "Energy Loss and Range of Electrons and Positrons", Circ. Nat. Bur. Stand. (577), 1-30 (1956).

Aigrain, P., "The Effect of Radiations on Semiconductors", Action of High-Energy Radiations on Solids (Action des Rayonnements de Grande Energie sur les Solides), Gauthier-Villars, 81-8 (1956).

Miller, W., Bewig, K., and Salzberg, B., "Note on the Reduction of Carrier Lifetime in P-N Junction Diodes by Electron Bombardment", J. Appl. Phys., 27 (12), 1524-7 (1956).

Gobeli, G. W., "Range-Energy Relation for Low-Energy Alpha Particles in Si, Ge, and Insb", Phys. Rev., 103 (2), 275-8 (1956).

Cleland, J. W., Crawford, J. H., and Holmes, D. K., "Effects of Gamma Radiation on Germanium", Phys. Rev., 102 (3), 722-24 (1956).

Koch, L., "Semiconductors and Nuclear Radiation", Onde e'lect., 35, 977-80 (1955).

Rappaport, P., "Thresholds for Electron Bombardment Induced Lattice Displacements in Si and Ge", Phys. Rev., 100 (4), 1261 (1955).

Loferski, J. J., and Rappaport, P., "Electron Voltaic Study of Electron Bombardment Damage and Its Thresholds in Ge and Si", Phys. Rev., 98 (6), 1861-3 (1955).

Kinchen, G. H., and Pease, R. S., "The Displacement of Atoms in Solids by Radiation", Rept. Prog. in Phys., 18, 1 (1955).

Zakharov, A. I., "The Action of Radiation on the Physical Properties and Structure of a Solid Body", Uspekhi Fiz. Nauk, 57 (4), 525-76 (1955).

Rappaport, P., "Minority Carrier Lifetime in Semiconductors as a Sensitive Indicator of Radiation Damage", Phys. Rev., 94, 1409-10 (1954).

Electronic Properties

Waldner, M., and Sivo, L., "Lifetime Preservation in Diffused Silicon", J. Electrochem. Soc., 298-301, 107 (4) (1960).

Mackintosh, I. M., "Diffusion of Phosphorous in Silicon", The Electrochemical Society Spring Meeting, May 1-5, 1960, Chicago, Illinois.

Green, M., "Space Charge in Semiconductors Resulting from Low Level Injection", J. Appl. Phys., 30 (5), 744-7 (1959).

Jenny, D. A., and Wysocki, J. S., "Temperature Dependence and Lifetime in Semiconductor Junctions", J. Appl. Phys., 30 (11), 1692-8 (1959).

Evans, D. M., "The Measurement of the Temperature Dependence of the Mobility and Effective Lifetime of Minority Carriers in the Base Region of Silicon Transistors", J. Electronics and Control., 6 (3), 204-8 (1959).

Ziegler, G., and Zerbst, M., "On the Influence of Annealing on the Charge Carrier Lifetime in Silicon", Z. Naturforsch, 14a (1), 93-4 (1959).

Frosch, C. J., "Silicon Diffusion Technology", Transistor Technology, III, Chap. 3B, 90-9, D. Van Nostrand Company, Inc., Princeton, New Jersey (1958).

Prince, M. B., "Diffused P-N Junction Silicon Rectifiers", Transistor Technology, II, Chap, 9A, 245-65, D. Van Nostrand Company, Inc., Princeton, New Jersey (1958).

Fuller, C. S., and Dolesden, F. A., "Interactions Between Oxygen and Acceptor Elements in Silicon", J. Appl. Phys., 29 (8), 1264-5 (1958).

Jonscher, A. K., "Analysis of Current Flow in a Planar Junction Diode at a High Forward Bias", J. Electronics and Control, 5 (1), 1-14 (1958).

Blakemore, J. S., "Lifetime in p-type Silicon", Phys. Rev., 110 (6), 1301-8 (1958).

Shockley, W., "Electrons, Holes, and Traps", Proc. Inst. Radio Engrs., 46 (6), 973-90 (1958).

Moll, J. L., "The Evolution of the Theory for the Voltage-Current Characteristic of P-N Junctions", Proc. Inst. Radio Engrs., 46 (6), 1076-82 (1958).

Hoerni, J. A., "Carrier Mobilities at Low Injection Levels", Proc. Inst. Radio Engrs., 46 (2), 502 (1958).

Sandiford, D. J., "Temperature Dependence of Carrier Lifetime in Silicon", Proc. Phys. Soc., 71, Part 6, 1002-6 (1958).

Putley, E. H., "The Temperature Variation of the Concentration of Impurity Carriers in Silicon", Proc. Phys. Soc., 72, Part 5, 917-20 (1958).

Schonhofer, A., "The Temperature Dependence of Energy Losses in the Band Model of Solids", Z. Phys., 150 (1), 67-73 (1958).

Stafeev, V. I., "The Effect of the Bulk Resistance of the Semiconductor on the Form of the Current-Voltage Characteristic of a Diode", Zh. tekh. Fiz., 28 (8), 1631-41 (1958).

Tuchkesich, V. M., and Chelnokov, V. E., "Current-Voltage Characteristics of Diffused Silicon P-N Junctions", Zh. tekh. Fiz., 28 (10), 2115-23 (1958).

Vul, B. M., and Segal, B. T., "Theory of the P-N Junctions in Semiconductors", Zh. tekh. Fiz., 28 (4), 681-8 (1958).

Fomin, N. V., "High (Electric) Fields in the Theory of the Electrical Conductivity of Semiconductors", Zh. tekh. Fiz., 28 (4), 783-6 (1958).

Givargizov, E. I., and Pokrovskii, Ya. E., "The Effect of Thermal Treatment on the Electrical Properties of Silicon", Zh. tekh. Fiz., 28 (5), 974-6 (1958).

Veloric, H. S., and Prince, M. B., "High Voltage Conductivity-Modulated Silicon Rectifier", Bell Syst. Tech. Jr., 36 (4), 975-1004 (1957).

Logan, R. A. and Peters, J. A., "Diffusion of Oxygen in Silicon", J. Appl. Phys., 28 (7), 819-20 (1957).

Fuller, C. S., and Logan, R. A., "Effect of Heat Treatment Upon the Electrical Properties of Silicon Cyrstals", J. Appl. Phys., 28 (12), 1427-36 (1957).

Fletcher, N. H., "General Semiconductor Junction Relations", J. Electronics, 2 (6), 609-10 (1957).

Nijland, L. M., and van der Pauw, L. J., "The Effect of Heat Treatment on the Bulk Lifetime of Excess Charge Carriers in Silicon", J. Electronics and Control, 3 (4), 391-5 (1957).

Misawa, T., "Impedance of Bulk Semiconductor in Junction Diode", J. Phys. Soc., (Japan), 12 (8), 882-90 (1957).

Roberts, D. H., Stephens, P. H., and Hunt, P. H., "Effect of Oxygen on the Carrier Lifetime in Silicon", Nature (London), 180, 665-6 (1957).

Hrostowski, H. J., and Kaiser, R. H., "Infrared Absorption of Oxygen in Silicon", Phys. Rev., 107 (4), 966-72 (1957).

Ross, B., and Madigan, J. R., "Thermal Generation of Recombination Centers in Silicon", Phys. Rev., 108 (6), 1428-33 (1957).

Bemski, G., and Augustyniak, W. M., "Annealing of Electron Bombardment Damage in Silicon Crystals", Phys. Rev., 108 (3), 645-8 (1957).

Chih-Tang Sah, Noyce, R. N., and Shockley, W., "Carrier Generation and Recombination in P-N Junctions and P-N Junction Characteristics, Proc. Inst. Radio Engrs., 45 (9), 1228-43 (1957).

Davies, L. W., "Low-High Conductivity Junctions in Semiconductors", Proc. Phys. Soc., B, 70, Part 9, 885-9 (1957).

Saby, J. S., "Junction Rectifier Theory", Semiconducting Meeting Report, 39-48, Publication of the Physical Society, 153 (1957).

Ribout, M. S., "The Temperature Dependence of Minority Carrier Lifetime in p-type Germanium and Silicon", Semiconductor Meeting Report, 33-7, Publication of the Physical Society, 153 (1957).

Deigen, M. F., Dykman, I. M., and Tolpygo, K. B., "All-Union Conference on the Theory of Semiconductors", Zh. tekh. Fiz., 27 (7), 1628-42 (1957).

Ioffe, A. F., "Further Development of the Theory of Semiconductors", Zh. tekh. Fiz., 27 (6), 1153-60 (1957).

Prince, M. B., "Diffused P-N Junction Silicon Rectifiers", Bell Syst. Tech. J., 35 (3), 661-684 (1956).

Gortner, W., "Ambipolar Carrier Transport Through the Base Region of a Junction Transistor", J. Appl. Phys., 27 (10), 1252 (1956).

Kaiser, W., Keck, P. H., and Lange, C. F., "Infrared Absorption and Oxygen Content in Silicon and Germanium", Phys. Rev., 101 (4), 1264-8 (1956).

Longini, R. L., "Temperature-Dependent Factor in Carrier Lifetime", Phys. Rev., 102 (2), 584-5 (1956).

Gubanov, A. I., and Makovskii, L. L., "On the Reasoning in the Paper of K. B. Tolpygo and I. G. Zaslavskaya, 'Ambipolar Diffusion in Semiconductors at Large Currents'", Zh. tekh. Fiz., 26 (9), 2126-7 (1956).

Tolpygo, K. B., "Remarks on the Letter of Gubonov and Makovskii on the Reasoning in the Paper of Tolpygo and Zaslavskaya, 'Ambipolar Diffusion in Semiconductors at Large Currents'", Zh. tekh. Fiz., 26 (9), 2127-8 (1956).

Rashba, E. I., and Tolpygo, K. B., "Forward Current-Voltage Characteristics of a Planar Rectifier at Large Currents", Zh. tekh. Fiz., 26 (7), 1419-27 (1956).

Tolpygo, K. B., and Zaslavskaya, I. G., "Ambipolar Diffusion in Semiconductors at Large Currents". Zh. tekh. Fiz., 25 (6), 955-77 (1955).

Prince, M. B., "Drift Mobilities in Semiconductors, II. Silicon", Phys. Rev., 93 (6), 1204-6 (1954).

Von RoosBroeck, W., "Theory of the Flow of Electrons and Holes in Germanium and Other Semiconductors", Bell Syst. Tech. J., 24, 560-607 (1950).

Shockley, W., "The Theory of P-N Junction Transistors", Bell Syst. Tech. J., 28, 435-489 (1949).

Zerbst, M., and Heywang, W., "On the Temperature Dependence of the Charge Carrier Lifetime in High Purity Silicon", Semiconductors and Phosphors, Interscience Publishers, Inc., New York, 392-8 (1958).

ERRATA

Second Progress Report, page 23, paragraph 2, line 13; "1000 barns" should read "4000 barns", and all subsequent values of thermal neutron damage in the section on Damage from the Transmutation of Boron should be increased correspondingly by a factor of 4.

Page 23, paragraph 3, line 8; "5.5×10^{9}" should read "5.5×10^{4}".